Upcycling Mixed Plastic Waste into Composites and Fuel

A thesis

Presented in Partial Fulfillment of the Requirements for the

Degree of Master of Science

with a

Major in Environmental Science

in the

College of Graduate Studies

University of Idaho

by

Lucky I. Ewurum

Approved by:

Major Professor: Armando G. McDonald Ph.D.

Committee Members: Lili Cai, Ph.D.; Kristopher V. Waynant, Ph.D.

Department Administrator: Lee Vierling, Ph.D.

December 2021

Abstract

The growing concern with regards to the amount of mixed plastic waste (MPW) especially in municipal solid wastes (MSW) and with the significant quantity ending up in the landfill has led to search for more sustainable mode of disposal. MPW are the non-recyclable fraction after sorting and it is comprised of single use items, such as packaging and generally plastics with resin codes between 2-5. Mechanical and chemical recycling can divert these wastes especially MPW containing some paper fibers from the landfill. This study evaluated the mechanical, thermal, and rheological properties MPW in combination with fibers derived from residual hop bines and coupling agents to form composite materials and secondly the thermal deconstruction (pyrolysis) of MPW into liquid fuel.

MPW were used to formulate composites. To improve the interfacial bonding between MPW and fibers, maleated polyolefin (MAPE) and glycidyl methacrylate polyolefin were evaluated as coupling agents, while dicumyl peroxide (DCP) was evaluated as a long chain branching and grafting agent in the formulations. The use of the coupling agents, especially MAPE, was observed to increase interaction between the polymer matrix and fiber leading to a better performance in tensile strength. The addition of DCP to the MPW formulations slightly reduced its tensile strength probably due to polymer chain scission. The addition of hops fiber improved the tensile modulus of the composites relative to MPW.

For chemical recycling, the homogenized MPW was pyrolyzed (with and without Zeolite Y catalyst) between 500 to 600 °C in a tube reactor. Liquid products were trapped and characterized using a combination of GCMS and ESI-MS. The physical and chemical characteristics of the solid char product were also characterized by FTIR spectroscopy. Pyrolysis products were mainly straight chain hydrocarbons, while catalytic pyrolysis products were short-branched hydrocarbons and aromatics. These results clearly show that catalytic pyrolysis was successful in producing a liquid fuel comparable to gasoline.

Acknowledgments

I will love to appreciate Dr. Armando G. McDonald who literally made all these possible. For the privilege to learn and work under his tutelage. Also, to my committee members Dr Lili Cai, Dr. Kristopher V. Waynant for their supervision.

I also acknowledge the support from (1) National Science Foundation grant number 1827364; (2) M.J. Murdock Charitable Trust for the purchase of the twin-screw extruder; (3) Margaret Zee for collecting the hop bines and (4) USDA-CSREES grant 2007-34158-17640 for support in the purchase of the DSC.

Dedication

A big thanks to my bloods, Nnaemeka Ewurum and Anthony Ewurum. To Farid Sotoudehnia who stood right by me from day one in the lab and outside, I really appreciate all your gestures and babysitting. A big shout out to my friend Gurkeerat Kukal and Courage Alorbu.

Table of Contents

Abstract ii

Acknowledgments iii

Dedication iv

List of Tables viii

List of Figures ix

List of Abbreviations and Symbols xi

Chapter 1: Overview and Research Objectives 1

1.1 Overview 1

1.1.1 Waste generation and characterization 2

1.1.2 Municipal solid waste (MSW) 2

1.1.3 Plastic solid waste (PSW) 3

1.1.4 Plastics in Municipal Wastes 4

1.2 Environmental Impact of plastic waste 7

1.2.1 Terrestrial Environment 8

1.2.2 Marine Environment 8

1.3 MSW management 9

1.3.1 Reduction and Reuse 10

1.3.2 Recycling 10

1.3.3 Energy recovery 11

1.4 Pyrolysis 11

1.4.1 Catalytic Pyrolysis 12

1.5 Factors influencing pyrolysis reaction 14

1.5.1 Temperature 14

1.5.2 Reactor type 14

1.5.3 Pressure and resident time 15

1.5.4 Presence of catalyst 15
1.6 Mechanical recycling of MPW to composite materials 16
1.7 Hops fiber (HF) 17
1.8 MPW composite processing techniques 18
1.8.1 Extrusion 18
1.8.2 Injection molding 19
1.9 Interfacial adhesion in MPW composite 20
1.10 Thermal Properties 21
1.11 Rheology 22
1.11.1 Dynamic rheology 22
1.11.2 Capillary Rheology 23
1.12 Thesis research objectives 24
Chapter 2: Mechanical recycling of MPW 25
2.1 Materials 25
2.2 Method 25
2.2.1 Hop fiber lignin and carbohydrate analysis 25
2.2.2 Compounding 26
2.2.3 Fourier-Transform Infrared Spectroscopy (FTIR) 26
2.2.4 Thermal analysis 27
2.2.5 Rheology 27
2.2.6 Tensile Testing 28
2.2.7 Water soak test 28
2.3 Results 29
2.3.1 Hops fiber (HF) 29
2.3.2 Mixed plastic waste analysis and compounding 29
2.3.3 Thermal analysis 30
2.3.4 Rheology 32

2.3.5 Viscoelastic properties 36

2.3.6 Tensile Properties 38

2.3.7 Water absorption tests 39

Chapter 3: Chemical upcycling through thermal deconstruction of MPW and fiber into wax-oil and its upgrading: pilot-scale investigation. 42

3.1 Characterization of the MPW 42

3.2 Thermal and catalytic pyrolysis experiments 42

3.3 Characterization of pyrolysis products 43

3.4 Results and Discussion 44

3.4.1 MPW characterization 44

3.4.2 Pyrolysis experiments 47

3.4.3 Characterization of pyrolysis products 48

Chapter 4: Conclusion and future recommendation 61

4.1 Conclusion 61

4.2 Future recommendation 62

Chapter 5: References 63

List of Tables

Table 1.1 Thermal and mechanical properties of polymer 4
Table 1.2 Properties of hops stem fiber compared to cotton and hemp [99] 17

Table 2.1 Thermal data (Ts, Tm, Tc and Xc) for the various MPW formulations determined by TMA and DSC 32
Table 2.2 Complex viscosity (η*) of the formulations at 1, 25 and 60 Hz and power law fit model equation 34
Table 2.3 Power law fit equation and R^2 values of formulations which confirms correlation 35
Table 2. 4 Storage modulus of formulations at 30 ^oC 37
Table 2.5 Tensile properties of MPW formulations 38
Table 2.6 WA (%) and diffusion coefficient of composite formulations 40

Table 3.1 Activation energy (*E*) and R^2 values of MPW and MPW+catalyst at various conversion factors (10-90%) 46
Table 3.2 Percentage composition of compounds found in thermal and catalytic pyrolysis.. 49
Table 3.3 Identified compounds and amount in the wax-oil product of thermal pyrolysis of MPW at 500, 550 and 600^0C 51
Table 3.4 Identified compounds and amounts in gasoline and the liquid product of catalytic pyrolysis of MPW 54
Table 3.5 Weight (M_w) and number average molar mass (M_n) and monomer/oligomer ratio of MPW pyrolysis oil 58

List of Figures

Figure 1. 1 Components of MSW according to EPA [11]. 3
Figure 1. 2 Forms of PE [24]. 6
Figure 1. 3 Structure of PP [30]. 6
Figure 1. 4 Structure of PET [35]. 7
Figure 1. 5 Different types of pyrolysis reactors [60]. 15
Figure 1. 6 Some properties of hops stem fiber compared to cotton and hemp [98]. 17
Figure 1. 7 Flow diagram of MPW composite production [40]. 18
Figure 1. 8 Schematics of the processing zones in a Coperion twin-screw extruder [49]. 19
Figure 1. 9 Schematics of a simple injection mold [51] 20
Figure 1. 10 A schematic showing a DSC thermogram [126]. 22
Figure 1. 11 Showing parallel plate geometry [132]. 23
Figure 1. 12 Schematic of a capillary rheometer [134]. 23

Figure 2. 1 Shredded MPW to extruded rod 26
Figure 2. 2 Tensile dog-bone specimens 28
Figure 2. 3 DSC thermograms showing (a) cooling and (b) heating cycle of MPW formulations with MAPE, GMPE and DCP and (c) cooling and (d) heating cycles of MPW formulations with HF and MAPE, GMPE and DCP. 31
Figure 2. 4 TMA thermograms of the various MPW formulations (a) without hops fiber and (b) with hops fiber 31
Figure 2. 5 Complex viscosity with respect to frequency of MPW formulations in logarithmic scale and power law fitted 33
Figure 2. 6 Flow curves MPW formulations with-out HF (a) and MPW formulations with HF (b) showing true shear viscosity vs true shear rate and power law fitted model. 35
Figure 2. 7 DMA thermogram of formulations showing storage modulus (E') vs Temperature. 37
Figure 2. 8 Water soak of formulations with respect to time. a): without HF, b): with HF ... 41

Figure 3.1 Schematic of the pyrolysis tube reactor [173] 43

Figure 3.2 TGA and DTG thermogram of (a) MPW and (b) MPW+catalyst at different heating rates 45
Figure 3.3 Plots of log heating rate (β) versus 1/K of a) MPW, b) MPW+catalyst..... 46
Figure 3.4 Products yield of thermal and catalytic pyrolysis..... 47
Figure 3.5 GCMS chromatograms of thermal pyrolysis of MPW at (a) 500^0C, (b) 550^0C, (c) 600^0C, (d) catalytic pyrolysis of MPW at 600^0C, and (e) regular gasoline 50
Figure 3.6 Positive-ion ESI-MS spectra of products of MPW pyrolysis at (a) 500°C, (b) 550°C, (c) 600°C, and (d) catalytic pyrolysis at 600°C..... 59
Figure 3.7 FTIR spectra of (a) extruded MPW, MPW pyrolysis char at (b) 500^0C, (c) 550^0C, (d) 600^0C, and (e) catalytic pyrolysis at 600^0C..... 60

List of Abbreviations and Symbols

Abbreviations

ASTM	American Society of the International Association for Testing and Materials
ATR	Attenuated total reflection
BPA	Bisphenol A
DCP	Dicumyl peroxide
DDT	Dichlorodiphenyltrichloroethane
DMA	Dynamic mechanical analysis
DMT	Dimethyl terephthalate
DSC	Differential scanning calorimetry
DTG	Derivative thermogravimetry
EMTS	Energy at max tensile stress
EPA	Environmental protection agency
ESIMS	Electrospray ionization mass spectrometry
FC	Fixed carbon
FCC	Fluidized catalytic cracking
FTIR	Fourier-Transform Infrared Spectroscopy
GCMS	Gas chromatography–mass spectrometry
GMPE	Glycidyl methacrylate polyolefin
HCH	Halogenated Cyclic Hydrocarbons
HDPE	High density polyethylene
HF	Hops fiber
HSD	Honestly Significant Difference
LDPE	Low density polyethylene
LFG	Landfill gas
LLDPE	Linear low-density polyethylene
MAPE	Maleated polyethylene
MAPP	Maleated polypropylene
MFR	Melt flow rate

MPW	Mixed plastic waste
MPWHF	Mixed plastic waste-Hops fiber
MSW	Municipal solid waste
PE	Polyethylene
PET	Polyethylene terephthalate
PEVA	Polyethylene-vinyl acetate
PHBV	Poly hydroxybutyrate-cohydroxyvalerate
PP	Polypropylene
PS	Polystyrene
PSW	Plastic solid waste
PVC	Polyvinyl chloride
TGA	Thermogravimetric analysis
TMA	Thermomechanical analysis
VM	Volatile matter
WA	Water absorption

Symbols

ΔHm	Melting enthalpy of peak
$\Delta H0$	Enthalpy of fusion
G' or E'	Storage modulus
G" or E'	Loss modulus
δ	Delta
η^*	Complex viscosity
X_c	Percent crystallinity
T_m	Melting temperature
T_c	Crystallization temperature

Chapter 1: Overview and Research Objectives

1.1 Overview

The term "waste" is ambiguous, as what one person considers trash may be valuable to another as a resource [1]. However, we can all agree that the creation of waste is a huge global environmental issue that affects both industrialized and developing countries. Current systems in various regions of the world are unable to handle the volume of trash produced, despite significant investment in terms of money, technical know-how, and other resources devoted to mitigating the global epidemic known as waste pollution. Humans are the primary producers of waste; they are unwanted and inevitable by-products of a variety of human activities [2] and these wastes are because of inefficient or improper use of resources and or energy [3]. Despite the fact that waste creation has been a problem since the dawn of time [1], recent economic booms as countries see a shift from low-income to middle- and ultimately high-income earners, population growth, and industrialization, urbanization began in the sixteenth century, resulting in a growing outflow of people from rural to urban areas in search of a higher quality of living as a result of industrial revolution have all been identified as some of the major contributors to the current significant increase in waste generation [4][5]. This situation forces waste management systems to be overburdened, as authorities struggle to cope with the increase with regards to collection, disposal and treatment in wastes generated [3] [6].

The world's population is continuously growing, and currently well over 7 billion people [7] and this puts a lot of strain on resources, and the wastes produced because of anthropogenic resource utilization are visible evidence that more sustainable waste management practices are not implemented at all levels or resource consumption is curtailed, the future of our world is gloomy. Because of insufficient infrastructure, ineffective, inefficient, or completely nonexistent waste management systems, limited or non-existent recycling, and unsuitable landfills and procedures, most developing countries, and regions, such as the Sub-Saharan African region, have it the worst [6], [8].

1.1.1 Waste generation and characterization

The amount of garbage produced depends on the country or region; a local economy with a larger number of industries would produce more waste than a less industrialized region. The social level of a place has a significant impact on waste composition since wealthier regions consume more packaged goods, resulting in higher volumes of plastics, paper, glass, textiles, and other materials [9]. Therefore, understanding where and what types of wastes are created in each place is critical for trash categorization as well as the implementation of appropriate mitigation programs and regulations [10]. According to the Environmental Protection Agency (EPA) [11] , Municipal solid waste (MSW) generation and management in the United States are calculated utilizing materials flow methodology, which mainly relies on production data collected from government agencies, enterprises, and industry associates by weight for materials and products that enter the waste stream. In addition to helping estimate potential material recovery and processing facility design, waste characterization also helps estimate the wastes' physical, chemical, and thermal qualities [12], [13]. Waste can be characterized by virtue of its source of origin which can include agricultural waste, construction waste and others; also, by its physical state which can be solid, liquid, or gaseous or by degree of environmental impact which can be hazardous or non-hazardous or sometimes collectively such as MSW.

1.1.2 Municipal solid waste (MSW)

EPA [11] has defined MSW to consist of common household items such as product packaging, yard trimmings, clothing, bottles and cans, food, newspaper, appliances, electronics, and batteries, but does not contain hazardous or construction and demolition debris. These wastes are commonly created in residential and commercial areas, as well as schools and other institutions such as business districts and hospitals. Season, area, feeding habits, and, of course, geography all influences the mix and features of MSW. High-income countries such as Australia, Japan, China, and Singapore generate between 1.1 and 5.0 kg per inhabitant per day [2]. Sub-Saharan Africa is expected to create almost 62 million tons of MSW, according to estimates [14]. MSW is generated in Ghana from a variety of sources, with the bulk of garbage coming from households (50 to 80%), followed by market or commercial districts (ten percent to thirty percent), and institutions and industry accounting

for varying percentages [15]. In 2018, the United States created an estimated 292 million tons of MSW (Figure 1.1), generally known as trash, which is equivalent to 2.2 kg of trash per person per day, a 23.7 million-ton increase over the previous year [16] .

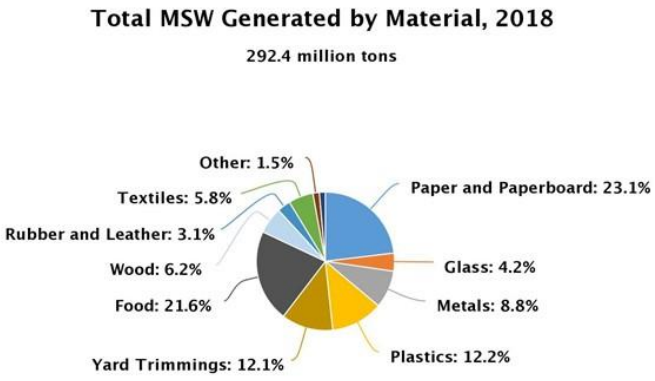

Figure 1.1 Components of MSW according to EPA [11].

1.1.3 Plastic solid waste (PSW)

Plastics a derivative of crude oil have played and continue to play an important part in human progress. Various industries use plastic thanks to their versatility which can take on many shapes, light weight, and lower production cost relative to other materials such as wood, concrete and metal. [17]. Just like other types of wastes, Because of industrialization and population growth, there has been an increase in the global need for plastics. An estimated 35.4 million metric tons of plastic waste were generated in 2017, accounting for 13.2% of all MSW. Because plastics are bulkier and more durable due to their strong molecular bond made up of hydrogen, carbon, and a couple of other elements such as chlorine, nitrogen, they take up more land space than other organic residues and only 3.1% of the plastics produced were recycled; the rest ended up in landfills [18], [19]. Plastic waste has fully disproved the three-threshold theory of pollution. According to the threshold theory, some pollution is permitted, pollution also serves as a time signal for when harm begins, and finally, harm can only be assessed and detected by laboratory procedures rather than medical ones. The chemical actions of these plastics are quite potent even at low dosage, and they have a high effect; the dangers, on the other hand, are considerable. A major problem with the threshold theory is that plastic mixes with various surroundings (sea, soil, etc.), as well as

the human system itself, making it difficult to detect. This is because their modes of operation are more correlative than causative. One thing is for certain: as plastics become increasingly popular and more expensive to produce, they will only contribute to a rise in the amount of plastic solid waste generated [17], [20]. These polymers made up of chain long single units are held together by strong molecular bond. Plasticizers (such as polychlorinated biphenyls, COCO, or commonly known as BPA) are monomer additions that are added to plastics to increase their versatility. Plasticizers rather than attach to the long plastic molecule chain, these monomers alter the properties of plastics. Over time plasticizers are only ephemerally bound in plastics and migrate out of the plastic to its surroundings, ecosystems, and even human bodies, impacting changes either directly or indirectly [21].

1.1.4 Plastics in Municipal Wastes

There are different types of plastics, and they can be classified based on method of synthesis which includes: Polycondensation, polyaddition; Based on their design: Thermoplastics and thermosets [17]. Thermoplastics are often widely found in the MSW, these plastics some time referred to polyolefins includes polyethylene (PE), polypropylene (PP), polyethylene terephthalate (PET), polystyrene (PS), and polyvinyl chloride (PVC). The thermal and mechanical properties of these plastics such as the melt temperature (T_m), glass transition temperature (T_g), tensile strength and modulus are given in Table 1.1**.**

Table 1.1 Thermal and mechanical properties of polymer

POLYMER	Thermal Properties		Mechanical Properties	
	T_g (^oC)	T_m (^oC)	Tensile strength (MPa)	Young's Modulus (MPa)
LDPE	-110	85-125	10	300
HDPE	-110	120-130	26	1,000
PP	-20 to -5	165-175	37	1,325
PET	70-78	245-265	79	2,950
PS	90-110	210-249	46-60	3,000-3,600
PVC	82-85	100-260	52-62	2,827-3,400

1.1.4.1 Polyethylene

Polyethylene (PE) is a popular plastic polymer that is both useful and affordable and used from shopping bags to milk jugs. When it comes to processing, PE's capacity to change the length, density, and crystallinity of the polymer chain is particularly useful. Because of these features, PE products can be customized for a wide range of applications [22]. PE is a polyolefin with reoccurring units of alkene monomer, ethylene (CH_2=CH_2), characterized by its semi-crystalline nature [23]. Other materials can be copolymerized with it to change or improve specific qualities. The type and quantity of comonomer or branching reacting with ethylene to produce the polymer can alter PE's density (Figure 1.2), such as low-density (LDPE) and high-density (HDPE) [24].

HDPE also known as linear PE because of its high degree of crystallinity with very low level of branching, but it can also be amorphous in some areas. The electrical insulating qualities, stiffness, and great resistance to strong acids, alcohols, and corrosion make it the most widely used grade of HDPE with density range of 950 to 956 kg/m^3 in plumbing pipes, milk bottles, rope, plastic envelopes, toys, playground equipment and automobile components. Metallocene or Ziegler-Natta catalytic reactions utilized during ionic polymerization gave it a better molecular weight distribution, which is why it has improved mechanical qualities of HDPE [23], [25], [26].

LDPE has between 5-10 long branches every 1000 carbons, and they are usually branched and composed mostly of amorphous region much unlike HDPE. It is manufactured under high temperature and pressure using peroxide initiators [27]. With a density between 910 and 940 kg/m^3, it is more flexible, and its transparent nature makes it ideal for packaging films in food industry [25].

Linear LDPE (LLDPE) is made by copolymerizing a small amount of long-chain olefin with a short branching copolymer. It is linear, however comonomers like butene-1 and octene-1 are introduced and a substantial number of branches give a density ranging from 915 to 925 kg/m^3. The strength properties of LLDPE are provided by linearity, while toughness is provided by branching [27]. LLDPE is also used in the packaging industry.

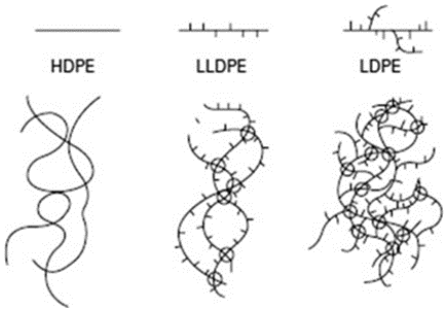

Figure 1.2 Forms of PE [24].

1.1.4.2 Polypropylene

Polypropylene (PP) is a semi-crystalline, non-polar, linear polymer made from the petroleum refining byproduct propylene (CH_2=$CHCH_3$) [23]. PP has a melting point (160-170°C) and is a thermoplastic olefin polymer. Chemical and mechanical qualities such as a high softening point, superior processability, and economic benefits make it useful in a variety of industrial applications. Though PP-based formulations are increasingly being produced, the predominant trend is toward improving impact strength [28]. Due to its excellent resistance to environmental stress cracking, sensitivity to microbial attacks, and the ability to maintain its mechanical and electrical properties at high temperatures, it finds use in the automotive industry, laboratory equipment, consumer goods (yoghurt containers, margarine tubs), and furniture market. A random copolymer or homopolymer gives it a density ranging from 904 to 908 kg/m^3 [29]. PP exists in three forms: isotactic, syndiotactic, and atactic depending on the arrangement of the propyl group. Isotactic PP (Figure 1.3) is the principal type used commercially.

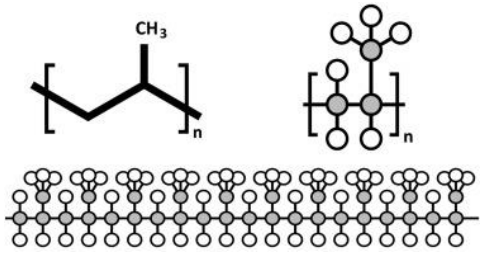

Figure 1.3 Structure of PP [30].

Because the propylene units are inserted head to tail in isotactic PP, their methyl groups are all on the same side of the polymeric backbone (Figure 1.3) making isotactic PP a

stereospecific polymer [31]. It crystallizes as a helical rod and has high stiffness and tensile strength. In the commercial world, isotactic PP is available in three main forms: homopolymer, random copolymer, and block copolymer (block copolymer is the most common) [32]. Syndiotactic PP is the stiffest and has the greatest melting point, and it's available in a wide range of melt flow rates (MFR). It is created by alternately inserting monomer units. Atactic PP is created by randomly inserting a monomer into a polymer chain. The crystallinity of atactic PP is the lowest of the PP forms and is primarily employed in the production of roofing tars and adhesives [32].

1.1.4.3 Polyethylene Terephthalate

Polyethylene Terephthalate (PET) is produced by esterification/condensation reaction of ethylene glycol and terephthalic acid or dimethyl terephthalate (DMT) with the general formula $(\text{-OOC-C}_6\text{H}_5\text{-COOCH}_2\text{-CH}_2\text{-})_n$ (Figure 1.4) [33]. Transparency, solvency, crease resistance, good barrier qualities, fatigue and chemical resistance, and high tenacity, light weight, and durability across a broad temperature range (-60 to 220 ^{o}C) are only some of the unique characteristics of PET. These attributes have led to its widespread usage in a variety of sectors especially in food packaging in form of bottles, food jar and development of artificial vascular scaffolds [34][35].

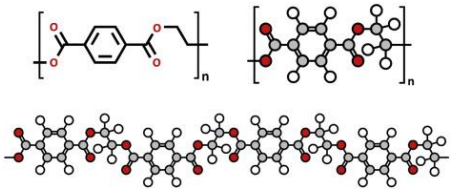

Figure 1.4 Structure of PET [35].

1.2 Environmental Impact of plastic waste

Inadequate and improper disposal and spillages from ships are some of the primary causes of plastics in our environment and their accumulation over time [36]. Single-use plastics and other environmental blights have created this problem. Plastics have been discovered in a variety of habitats, and they have a slew of negative consequences that warrant more study. Plastic pollutants can be divided into two categories based on their size: microplastics (< 5 mm), and macroplastics (> 5 mm). Primary and secondary origins of

plastics based on the mode of formation or origin can be distinguished. Primary origins are manufactured on purpose, whereas secondary origins result from the breakdown of macroplastics in the environment over time [17], [37].

1.2.1 Terrestrial Environment

Several factors contribute to land-based plastic pollution, including industrial production, poor waste management, unlawful littering and dumping, wave-washed garbage, and microplastic beads from clothes and other household items [38]. Majority of unrecyclable plastics are landfilled and in a poor constructed and managed landfill, these plastics can pose lots of effect on soil and soil biota [39]. While harvesting and plowing aided downward dispersal, soil biota also helped transfer microplastics horizontally through self-made pores and fractures in soil [40]. For instance, under laboratory conditions, Microarthropods were found to be capable of moving microplastic beads [41]. According to research, microplastics harm soil creatures like earthworms, which aid in soil preparation. There is little research on the impact of microplastics on soil creatures because the marine environment has gotten most of the attention, but the earthworm is one organism that has gotten some attention [38]. Although histopathological and immune system impairments were evident, more research on the deleterious effects of microplastic on soil organisms is needed. Ingestion of microplastics did not appear to cause mortality or affect its growth or reproduction to soil organisms [38]. Humans are not exempt, as microplastics have been discovered in food and drinking water, as well as through workers exposed to microfibers [17]. Furthermore, a higher degree of respiratory irritation, with cases of respiratory irritation are being observed and recorded.

1.2.2 Marine Environment

In the North Pacific, gyres that attract microplastics have accumulated over time, earning the appellation "The Great Pacific Garbage Patch," which is commonly interpreted as a plastic island [37], [42]. Fisheries contribute roughly 10% of all marine plastic waste, and boat pollution accounts for another 10% of marine plastic waste which is largely due to boat spills and about 80% washed into the ocean from the shoreline which are plastics used and abandoned by humans. Polymer density affects buoyancy, position in the water, and contact with aquatic life after release into the ocean. Denser plastic like PVC will sink to the ocean

floor, whereas less dense plastics (LDPE) would float; decomposition of plasticizers and/or other additives may impact plastic density and, as a result, plastic distribution in the body of water [21], [36], [37]. Plastics in the water column and on the surface entangle a great deal of marine life. If an animal becomes entangled in lost or abandoned fishing gear, it can cause laceration, sores, and infections and in extreme circumstances, if the animal is still growing, the material may cut into its flesh or impair shell formation [17]. For the introduction of new species to new coasts, marine plastics can serve as an intermediary. Sea turtles have been observed feeding on floating plastic debris and in Florida, there have been reports of manatee deaths due to plastic entanglement [43]. By diluting nutrients, displacing food, and restricting surfaces available for nutrient absorption, plastic ingestion might indirectly reduce marine life's growth [44]. Oily chemical substances such as dichlorodiphenyltrichloroethane (DDT) and Halogenated Cyclic Hydrocarbons (HCH), which are endocrine disruptors that interfere with the hormone process and accumulate in the tissue of animals when ingested are attracted plastic and upon consumption by marine life, leads to various degree of health problems [21]. DDT and HCH are also poisonous to humans. When marine life or birds eat plastic trash such as bags, containers, or plastic pellets, they may die from a clogged airway. There is evidence that loggerhead sea turtles that consume white plastic garbage lower their fat storage ability, resulting in weight gain and decreased fitness [44]. Potential damage of coral reefs due to fishing nets dragging down the seafloor and compromising gas exchange and carbon dioxide sequestration are some other impacts of plastics in the marine environment [36], [44].

1.3 MSW management

There are numerous waste streams, each with their own unique features, hence there are numerous waste management approaches to choose from. Collection of trash is a simple one step operation in the waste management process (just before they enter the MSW stream). When waste is collected it is mixed with other types of waste and the risk of cross-contamination increases, as does the amount of time and energy needed to sort it. Automated waste sorting removes impurities with the aid of scanners like X-ray based instruments [45]. Processing and finally disposing of it make up the rest of the management procedures [46].

Understanding the composition of trash necessitate different approaches to management, the EPA created a waste management hierarchy for nonhazardous waste which is as follows.

1.3.1 Reduction and Reuse

This procedure aims to stop waste from being created in the first place. Reusing or giving items, purchasing in bulk, decreasing packaging, and rethinking products are all examples of ways to reduce waste. Reduction and reuse have several advantages, including the following: decrease of pollution, energy, and resource use [47].

1.3.2 Recycling

Recycling is the process of repurposing waste materials into useful new goods by applying various processing procedures to them. To accommodate the various waste streams, a functional recycling facility, a functioning collecting and sorting system, and a market for the recycled products available to optimize recycling opportunities ought to be available [48]. In 2018, the United States recycled about 69 million tons of MSW, with paper and paperboard accounting for approximately 67% of the total and metal accounting for 13% and plastics 5% [16]. There are three types of recycling.

1.3.2.1 Primary recycling

Also known as a close loop recycling, plastic and glass are utilized to create items that are used for the same purpose prior to recycling. PET bottles used for beverages etc. are manufactured and or recycled via primary recycling processes [45].

1.3.2.2 Secondary or Mechanical recycling

Downcycling as it is also called is a type of recycling in which waste materials, such as plastic, are utilized to create a new product with a different purpose, but the new product has a lesser value. Secondary recycling is demonstrated in the manufacturing of wood plastic composites. Using an extruder, wood fiber and recycled or waste polymers are blended in various ratios, and the resulting formulation is used to mold various goods [49].

1.3.2.3 Tertiary or Chemical recycling

Tertiary or chemical recycling is a thermochemical process that degrades or changes the chemical composition of wastes; plastic wastes for instance are utilized to make chemical

compounds, fuels, biochar, and syngas, all of which are used as feedstock in various manufacturing processes [19], [50]. Some of the tertiary recycling methods includes, torrefaction, pyrolysis, gasification, liquefaction [20], [36], [51].

This work focuses mostly on the secondary and tertiary type of recycling of post-consumer plastics and fibers which constitutes a large portion of the MSW stream. The fiber component is composed mostly of paper/cardboard and hops bines and will be discussed better below. There are various advantages to recycling in general, some of which includes reducing the need for landfills, saving energy, and reducing greenhouse gas emissions.

1.3.3 Energy recovery

Combustible fuels like methane, methanol, ethanol, or synthetic fuels are derived from this process of energy recovery from landfill gas (LFG) recovery and anaerobic digestion etc. In this process, [47], [52]. Waste that are mostly non-recyclable are converted into usable energy such as heat and electricity by way of a series of processes like combustion.

1.4 Pyrolysis

The US is faced with the issue of rising plastic pollution thanks to increasing population, industrialization and changing lifestyle. Most post-consumer plastics end up in landfills and until recently, a large chunk of mixed plastic wastes (MPW) was shipped off to China for recycling [53]. The ban on the importation of wastes into China has triggered stress on the US waste management industry. Pyrolysis of plastics and or biomass has been explored as one of the ways to address the issue as it also tackles the problem of contaminants, sorting of plastics or plastic-biomass which are labor intensive and drives up the cost of waste treatment [54]. Pyrolysis is a tertiary recycling method. A thermochemical process whereby wastes are exposed to heat in the absence of oxygen, causing thermal disintegration and the formation of semisolid, liquid, solid and gaseous components, depending on the circumstance [19]. The absence of oxygen means smoke is not generated and only very minimal or no dioxins released [36], [37]. Some studies like [55]–[57] have shown plastic wastes are good raw material for pyrolysis The liquid portion typically known as pyrolysis-oil is obtained via condensation of pyrolytic vapor, the solid fraction known as

char and semi-solid known as wax. This study focuses on the pyrolysis of plastic-fiber blend often referred to as co-pyrolysis. The product yield in pyrolysis reaction can be used for several purposes. The char from the deconstruction reaction of MPW and fiber can be used as activated char through some thermal and steam activation. The char can serve as adsorbent in wastewater treatment [58], [59]. Char can be used as a soil supplement as has been observed to increase organic content of soil and its cation-exchange prowess [60]. The gaseous products which can include carbon-monoxide, hydrogen, and methane which is feedstock dependent can be used for several industrial purposes and as a heating source [18], [60].

During pyrolysis, a radical chain reaction pathway comprising hydrogen transfer steps and the gradual breaking of the polymer backbone occurs resulting in smaller molecular fragment products [19], [61]. In pyrolysis of PP and PE, this reaction begins with the random cleavage of carbon-carbon bonds, followed by intramolecular or intermolecular hydrogen transfer to form more stable radicals. This leads to the next step, which is the reaction termination, where various hydrocarbons, such as olefins, alkanes, or a mixture of radicals are formed [19]. Based on the temperature range employed during the process, it can be classified as slow (< 400 ^{o}C), fast (400-600 ^{o}C), or high/flash (> 600 ^{o}C) [62], [63]. Type of product and yield are influenced primarily by temperature. Low temperatures favor the synthesis of liquid products, whereas high temperatures favor the production of gaseous components [64]. Sharypov et al. [65] showed that wood and polymer blends at 400 ^{o}C was suitable for light liquid production. Thahir et al. pyrolyzed PP at 500 and 650 ^{o}C and found that the production of gas and liquid fuel increased from 9% to 99.9%, respectively [55]. The type of plastic (PE and PS) pyrolyzed also influences the type of products produced [64]. Combination of PE and PP led to a 71 wt% oil conversion [55]. Temperature on pyrolysis of HDPE was shown to greatly influence the degradation kinetics [66]. Furthermore, an increase in the gas fraction was recorded with reduced wax production as temperature was increased from 500 to 600 ^{o}C. Kumar and Singh [67] reported the highest pyrolysis liquid yield (79%) from HDPE at 550 ^{o}C.

1.4.1 Catalytic Pyrolysis

Catalysts are used to improve the conversion and product distribution during thermal conversion of oil, coal, and plastic feedstocks in processes like oil refining. To improve

process efficiency, catalysts target a specific reaction and reduce the process temperature as well as the overall reaction kinetics [68], [69]. When it comes to plastic pyrolysis processes, a variety of catalysts have been employed, but the most widely used are ZSM-5, zeolite, Y-zeolite, fluidized catalytic cracking (FCC), and MCM-41 [68]. Cracking, oligomerization, cyclization, aromatization, and isomerization reactions are examples of catalytic reactions that can occur during the pyrolysis of plastic waste on solid acid catalysts [69], [70]. When selecting a catalyst, parameters including homogeneity, polymer selectivity, and catalyst selectivity should be considered [61]. During catalytic pyrolysis, the degradation mechanism takes place in two stages: the initial thermolysis, also known as thermal cracking, and the subsequent catalytic cracking [19]. The pyrolysis of polyolefins yields wax as one of its components which is typically made up of long chain hydrocarbons and with catalysts, with catalyst, further reactions lead to the breakdown of these long chains into shorter chain hydrocarbon which has more desirable qualities as a fuel.

The upgrading of plastic wastes by catalytic cracking has gained interest as a way of managing waste and obtaining chemicals [61] . Plastics and mixed plastic blends in various ratios were examined by Miandad et al. [59] utilizing a modified natural zeolite (NZ) catalyst for catalytic pyrolysis. The resulting liquid possessed a heating value of 41.7-44.2 MJ/kg close to that of diesel. The liquid oil obtained had the potential to be used as an alternative energy source after being blended with conventional fuel. Uemichi et al. [71] investigated the catalytic activities and deactivation behaviors caused by coke deposition of three different zeolites: HZSM-5, HY, and H-mordenite zeolites and silica alumina in a fixed-bed flow reactor system. In the synthesis of gasoline-range fuel oils composed of primarily isoparaffins and aromatics. The HZSM-5 catalyst was found to be highly effective and showed no deactivation due to a very low yield of coke deposited on the catalyst surface. According to Aguado et al. [72], the catalytic pyrolysis of PE with HZSM-5 produced aromatics and aliphatic chemicals, but mesoporous MCM-41's poor acid catalytic activity reduced the number of aromatic compounds produced.

1.5 Factors influencing pyrolysis reaction

Various reaction parameters influence the type, amount of product gotten. The degree of degradation is also affected by these factors which includes:

1.5.1 Temperature

Temperature employed in thermal or catalytic pyrolysis has great influence on the type and quantity of yields generated. The creation of wax and incomplete degradation of MPW may result from pyrolyzing at low temperatures as observed by Lopez et al. [73]. HDPE degraded completely at heating rates between 10 and 50 ^{o}C/min between 517 and 539 ^{o}C according to Chin et al. [74]. Flash pyrolysis (> 600 ^{o}C) is characterized by a very short resident time. Fast pyrolysis (400-600 ^{o}C) has been observed to save energy because it uses a higher heating rates and shorter resident time since the quality of bio-oil is affected by longer resident time compared to slow pyrolysis (< 400 ^{o}C) also it has been argued to maximize liquid yields [60]. To help determine an ideal temperature for pyrolysis of MPW, the degradation behavior of the component elements can be measured using a thermogravimetric analyzer (TGA). Obtained thermogram gives information on the weight change as a function of temperature and or time while the derivative thermogravimetric (DTG) curve provides information on degradative steps taking place during the process [18].

1.5.2 Reactor type

The pyrolysis reactor also can influence the pyrolysis reaction. Several types of reactors have been designed (Figure 1.5) to help improve pyrolysis oil yields [60]. Batch and semi-batch reactors have a simplistic design and is major advantage. The batch system prevents reactants or products from entering or exiting while the reaction is in progress. The semi-batch system permits the addition or removal of reactants and products as required [18]. Fluidized beds are another design, Arena and Mastellone [75] argued that fluidized beds have advantages over fixed bed and rotating cylinders when it comes to gas-solid interaction.

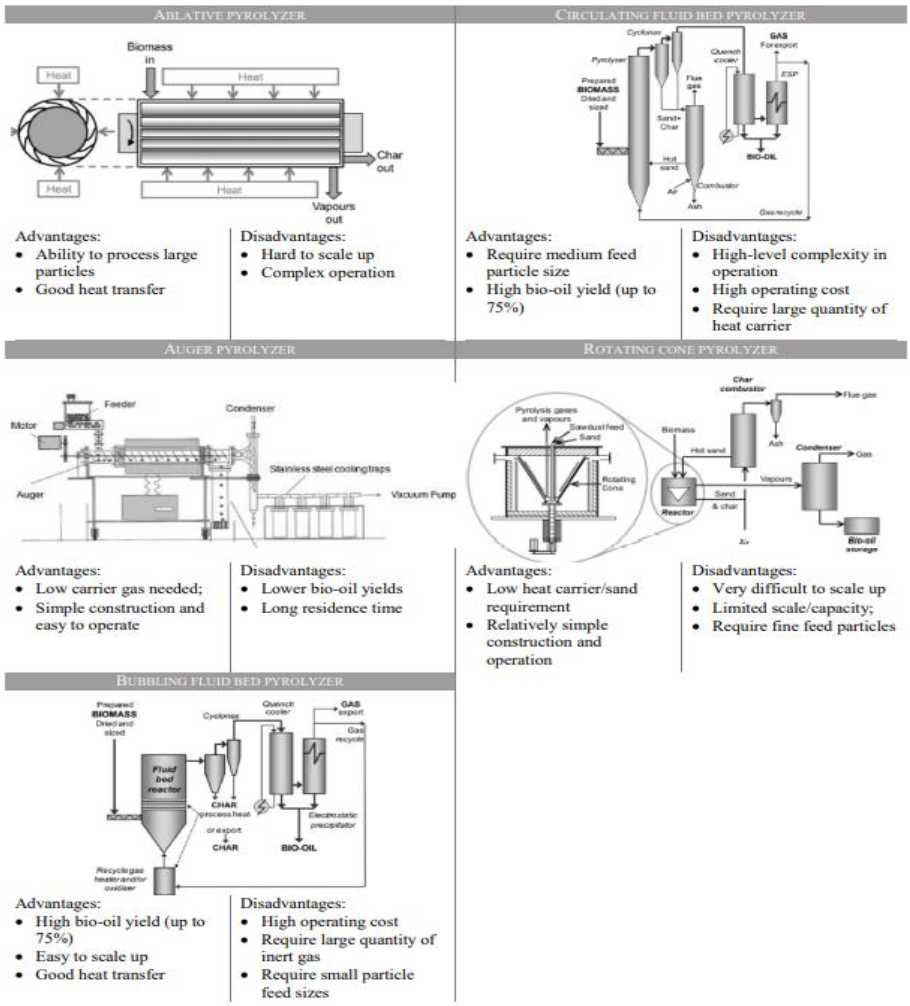

Figure 1.5 Different types of pyrolysis reactors [60].

1.5.3 Pressure and resident time

The impact of pressure (0.1 to 0.8 MPa) on PE pyrolysis increased gas yield (4 to 6%) at 440 ^{o}C [76]. Lopez et al. [73] investigated the impact of reaction time on plastic waste pyrolysis and found that reaction time of 15 to 30 min and longer had no effect on product qualities or feedstock conversion. Pressure and residence time are both affected by temperature [18], [73].

1.5.4 Presence of catalyst

Catalytic pyrolysis or fuel upgrading of the liquid and or wax fraction of the pyrolysis component uses two types of catalysts: homogeneous (one phase) and heterogeneous (more than one phase) catalysts. Heterogeneous catalysis is the most common because of its

economic advantage, however, an inorganic oxide catalyst is argued to be the most effective in improving yield [18], [77]. Zeolite type catalysts has been observed to have a positive effect on the products [78]. Benefits of the catalyst includes an increase in liquid component yield [61], [77], reduction in resident time and temperature requirement [18], [61]. and prevents the synthesis of unwanted products [19], [61].

1.6 Mechanical recycling of MPW to composite materials

A composite is a manufactured material made up of two or more different constituents, each with a particular set of attributes arising from the combination of those constituents [79]. This method of recycling falls right under secondary or mechanical recycling, and it entails the collection, sorting, washing, drying, and grinding plastics into flakes or pellets for molten state reprocessing into end products using various molding procedures like injection molding, extrusion [80]. Despite its widespread use, mechanical recycling has few challenges which includes heterogeneity when pollutant and other contaminants including other plastics are present. Separating contaminants which includes other plastics, paper, cardboard into individual constituents is often almost impossible depending on the degree of contamination and are hence dumped into landfills. The extra cost and labor for separation also makes recycling of MPW not attractive and hence the idea to make composites out of them. Fiber reinforced polymer-based materials have witnessed a growth in the last few decades [81]. They are used in different industries and for different application including but not limited to the automobile, aviation, and construction industries. The fibers added to the polymers help to increase the properties of the polymer for its intended application. Fiber reinforcement provides improved strength, modulus, viscosity, and better stress transfer in the composite material. Recently, artificial fibers like glass fiber are slowly losing their favor and being replaced with sustainably produced natural fibers. Unlike synthetic fibers, natural fibers are inexpensive, readily available, recyclable, biodegradable, better ability to withstand damage however they have lower tensile strength and moduli [82], [83]. A number of natural fibers have been explored as reinforcing fillers in plastic composite, these includes pine flour [84], [85], hemp fiber [86]–[88], wood flour [89], rice hulls [90], bamboo fiber [91], hops fiber [92], paper and cardboard [93] and other agricultural fibers [94][83]. Combining the product adaptability of polymers with the

recyclability of cellulosic resources can contribute of environmental stewardship [95][93]. Graupner et al. [96] investigated the use of recycled copy paper in polybutylene-adipate-terephthalate (PBAT) and polylactide (PLA) composites and observed improved tensile properties.

1.7 Hops fiber (HF)

Hop (*Humulus lupulus* L.) is a member of the *Cannabaceae* family and the *genus cannabis* which also contains hemp. It is native to Europe, North America and western Asia and its importance in the brewing industry has extended its cultivation to New Zealand, South Africa, and Australia as they are seen as an important condiment that enriches flavor and acts as a stabilizer [97]. Hemp plants are grown to generate fibers that have been used for millennia in textiles; Unlike in other countries, the ban on hemp cultivation was only recently (2018) lifted in the United States [98]. Hemp fibers are taken from the plant's bast fibers; therefore, it is fair to predict that hop plants, which belong to the same species, will have stems with fibers like hemp [99]. Currently, hop plant stems are considered byproducts which has seen limited use like its fiber serving as a reinforcement in composite [92]. Different sources have reported different lignin and cellulosic content of hop bines mostly due to extraction method or having varying degree of flavonoids and protein [97], [99], [100]. Hop properties are given in Table 1.2.

Table 1.2 Properties of hops stem fiber compared to cotton and hemp [99]

Fiber properties	Hop stem fibers	Cotton	Hemp
Fineness, Denier	48 ± 19	3–8	–
Length, cm	11.5 ± 2.9	1.5–5.6	–
Strength, g/den	4.1 ± 1.9	2.7–3.5	5.2–6.8
Elongation,%	3.3 ± 1.2	6.0–9.0	1.7–2.6
Modulus, g/den	161 ± 57	55–90	203–245
Moisture regain,%	8.3 ± 0.4	7.5–8.0	12
Single cell dimensions			
Length, mm	2.0 ± 1.0	15–56	5–55
Width, μm	16.5 ± 5.5	12–25	10–51
Physical structure			
Crystallinity,%	44 ± 5	65–70	81–89
MFA, deg	8 ± 0.7	20–30	–

1.8 MPW composite processing techniques

Manufacturing of MPW composites involves series of steps before the final product materializes. Some of these steps involves mixing and compounding and are important steps which foments interaction of polymers and fibers (Figure 1.6). Different parameters like temperature, volume fraction, plastic-fiber ratio, fiber types, additives amongst others are also taken into consideration as this affects useability and processing condition. Some techniques employed in MPW composite manufacturing includes extrusion, compression molding and injection molding.

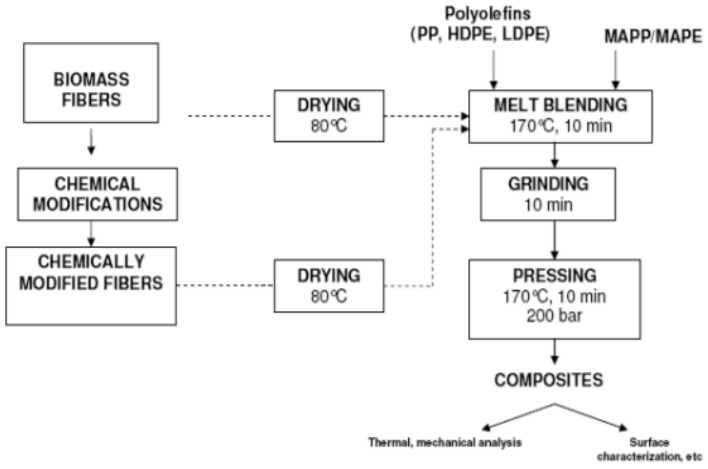

Figure 1.6 Flow diagram of MPW composite production [79].

1.8.1 Extrusion

Extruder melt process plastics typically using a single-screw extruder) to create 2-dimensional profiled shapes. To improve the mixing of composites, twin-screw extruders are typically employed, which compound the multi-component mixture into a uniform extruded composite [23][101][102]. Three types of screw configurations are available: intermeshing co-rotating, counter-rotating, and non-intermeshing counter rotating screws [103]. Extrusion is often a go to process in composite manufacturing because it is a continuous process once started and composites manufactured have greater stiffness and strength [104]. This processing technique has some advantages which includes low cost, flexibility of raw material, good compounding and mixing, range of temperature across different barrel. A typical extruder (Figure 1.7) has a feeding zone (hopper), the conveying and melting zone

which houses the barrel with screws, heaters where compounding and melting takes place and is extruded through die of different shape (rod, ribbon) and or attached to another machine for further processing [105]. Yang et el [106] reported a better tensile and modulus properties of the bio-composite fabricated using a twin screw compared to a single screw.

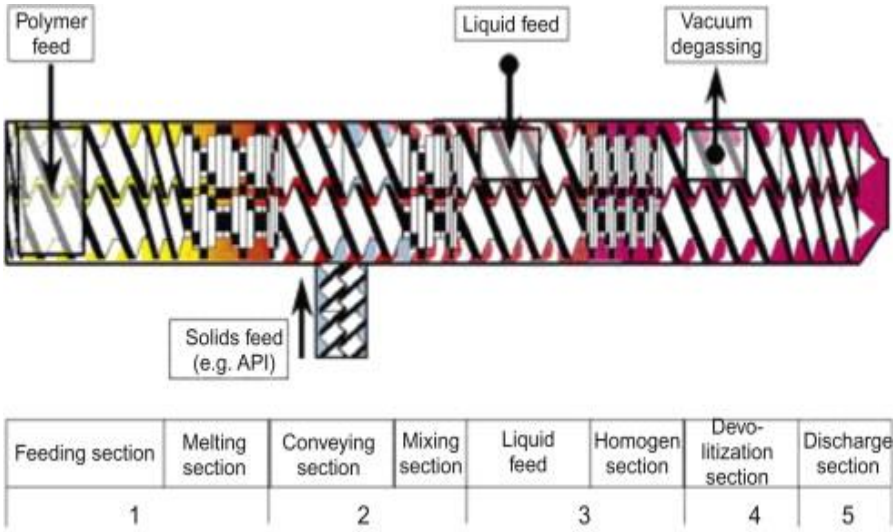

Figure 1.7 Schematics of the processing zones in a twin-screw extruder [107].

1.8.2 Injection molding

Injection molding is a melt process used to create complex 3-dimensional shaped products (Figure 1.8). The process involves plasticization/melting of the plastic resin, injection of the molten resin into a mold, cooling and solidification of the plastic in the mold, and ejection of the product (demold) from the mold [108][49], [81]. To ensure a composite with great mechanical property, the process parameters (e.g., temperature, injection speed, injection pressure, etc.) must be optimized for a particular resin/composite system. Some of the molding factors to consider are temperature: This includes the temperature of the heating zone, temperature of nozzle and mold temperatures. The temperature should be high enough to melt the polymer-fiber formulation in the barrel to encourage flow without clogging nozzle. Injection speed is another factor which is critical to achieving a void free part. Injection speed should be steady and fast to help maintain a steady pressure slope. The higher the injection speed the faster the injection pressure and low speed causes pressure drop at the nozzle, reduce material passage area as cold layers meets the mold [109]. Pressure is another important factor as high pressure is required to increase infusion of viscous composite

through a barrel into the mold. The pressure is dependent also on the temperature of the injection mold [102]. The back pressure influences homogeneity of melted materials, dispersion of material and better plasticization and care must be taken to minimize wear on the screws especially when processing glass fiber, steel fiber reinforced composites [109]. There are different variations of injection mold but the single stage screw which combines heating, mixing and injection is the most popular for its efficiency [110].

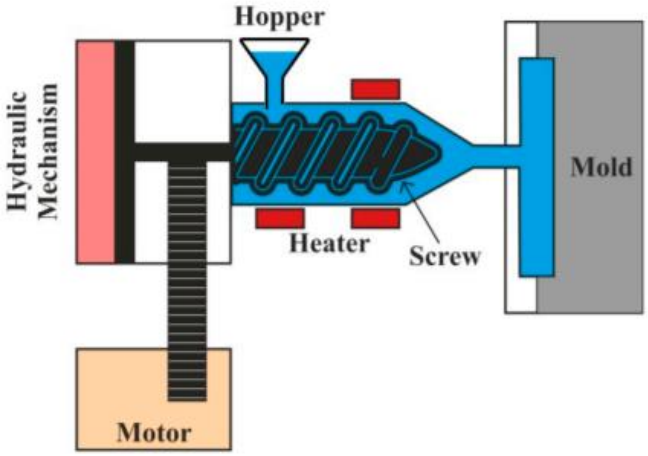

Figure 1.8 Schematics of a simple injection mold [81]

To encourage and enhance fiber-polymer interaction in the matrix and better fiber dispersion, surface treatments are often incorporated in the formulation process [111]. These additives can come in form of compatibilizers and coupling agents.

1.9 Interfacial adhesion in MPW composite

Generally different polymers are immiscible amongst themselves and with fibers. To improve the compatibilization of different polymers and/or fibers coupling agents are added to promote interfacial adhesion, good dispersion in the matrix which in turn increases the mechanical properties of MPW composites [112]. Plastics are generally hydrophobic while natural fibers are hydrophilic in nature and are incompatible and can get fiber pull-out. Coupling agents bond fibers and plastics by a combination of chemical reaction and chain entanglement [113][114].

Common coupling agents include maleic anhydride grafted polyolefins and silane coupling agents [115]. The success of maleic anhydride can be attributed to its ease of production which makes it economically feasible and their ability of creating links between polar and nonpolar substances [116]. To foment interlocking between matrix and fiber, grafted maleic anhydride on a polymer backbone will react with hydroxyl groups present on natural fibers [117]. Maleated polypropylene (MAPP) and maleated polyethylene (MAPE) are common maleated polyolefins.

Wang et al [118] showed that MAPP improved the mechanical, physical and flammability of wood fiber-PP-ammonium phosphate composites. Another study also showed that MAPP gave improvements in mechanical properties, water resistivity and surface wettability of composites [119]. Murayama et al. [120] also observed improvements in PP composites with different types of MAPP. The effects of MAPE and MAPP were compared on a rice hulls PE composites [106]. MAPE content (4 to 12%) greatly influences rubberwood based composite properties [121].

Another strategy to improve the plastic matrix properties is to cross-link the polymer chains using a of peroxide treatment. An organic peroxide is used as an initiator which generates free radicals, the radicals react with oxygen to yield peroxide radicals and via some other reactions spurs polymer chain cross-linking. Cross-linking generates a connection between polymer chains [122]. An example of an organic peroxide is dicumyl peroxide (DCP). Sari et al. [123] reported an improved mechanical performance of PE-cellulose fibers with a 4% addition of DCP. Rodi et al. observed an improvement in the fiber polymer interaction using DCP on poly hydroxybutyrate-cohydroxyvalerate (PHBV) and *Miscanthus giganteus* fibers [124].

1.10 Thermal Properties

Different plastics melt and soften at different temperatures and these properties govern how we can process these plastics into products. Differential scanning calorimetry (DSC) is a convenient tool to determine thermal properties of materials, such as melt (T_m) and glass transition temperature (T_g) and degree of crystallization (X_c) of semi-crystalline plastics [125]. An idealized DSC thermogram is shown in Figure 1.9. Thermomechanical

analysis (TMA) is another thermal technique used to determine the softening temperature (T_s) of materials [126]. Finally, thermogravimetric analysis (TGA) is employed to study the degradation behavior of materials with temperature [127]. Under very high temperature, thermal degradation sets in which can potentially affect the physical and chemical properties of fiber component of the MPW composite.

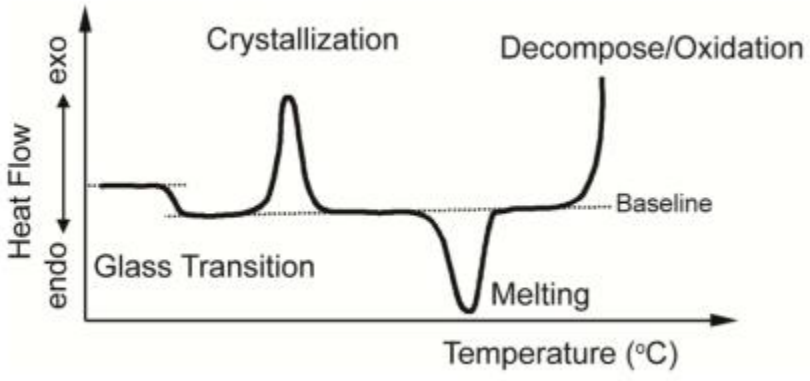

Figure 1.9 A schematic showing a DSC thermogram [128].

1.11 Rheology

The flow behavior of materials and fluids is studied by rheology. Rheology provides information on how a polymer flows as a function of shear rate at a particular temperature and this can be used to determine key processing variables [23]. The mixing of polymer blend systems can be studied by rheology [23]. The rheological behavior of polymers is heavily influenced by its molecular weight (MW) and molecular weight distribution (MWD). In the high molecular weight range, the connection between viscosity and shear rate is highly dependent on polymer polydispersity [129], [130]. Rheological measurements can be obtained on either dynamic and/or capillary rheometers.

1.11.1 Dynamic rheology

In the characterization of a polymer matrix, dynamic rheology, also known as oscillatory rheology, can be used to determine flow curves (viscosity versus shear rate or frequency) and viscoelastic behavior. This procedure is carried out under a controlled oscillation and the frequency and shear although typically low is sample dependent which also helps to prevent sample deformation during the runs [131]. Some other parameters that

can be generated from the data includes storage modulus (G'), loss modulus (G"), complex viscosity (η*) and dampening factor (tanδ). Parallel plate geometry is commonly used for samples with high viscosity to soft solids [132], [133]. A sinusoidal deformation shift is produced when a sinusoidal stress (t) is applied to the sample at a fixed angular frequency [23], [134].

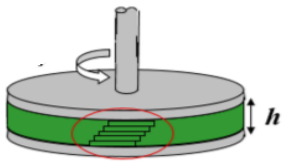

Figure 1.10 Showing parallel plate geometry [134].

1.11.2 Capillary Rheology

Capillary rheometry is used to determine polymer melt flow curves (viscosity versus shear rate) at higher shear rates than dynamic rheometry. The higher shear rates are comparable to those employed in extrusion and injection molding [135]. In a vertical setup consisting of a barrel and plunger in which the polymer melt is forced through a capillary die (of known diameter and various lengths) at a constant speed and the applied force measured at a given temperature [132]. The applied force is measured at different speeds (shear rates) (Figure 1.11) [23], [132]. Besides shear viscosity, capillary rheometer data can be used to evaluate other rheological parameters as shear rate and stress, temperature stability and wall slip, extrudate swell, and true viscosity. To account for the pressure, drop during the experiments, Bagley correction is performed as well as Weissenberg-Rabinowitsch corrections to determine apparent shear rate to true shear rate correction [90].

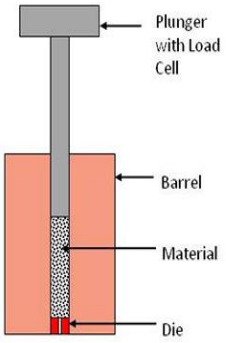

Figure 1.11 Schematic of a capillary rheometer [136].

1.12 Thesis research objectives

The overall objective of this study was to explore the chemical upgrading and mechanical recycling of MPW through the thermal deconstruction of mixed plastic wastes and fibers into wax-oil and its upgrade and evaluate the rheological and mechanical properties of mixed plastic waste-based composites and the influence of HF as a filler.

Mechanical recycling of MPW will be evaluated in Chapter 2. The addition of various additives (coupling agents, cross-linkers, and HF) will be compounded with MPW in a twin-screw extruder and the properties of the various formulations determined. HF will be isolated from hop bines after a 2-step chemical process. The tensile properties of injection molded formulations will be determined. Thermal properties will be determined by a combination of TMA, TGA, DMA and DSC. Rheological behavior of the various MPW formulations were determined by both capillary and dynamic experiments. The water absorption behavior of the MPW formulations was also evaluated.

The chemical upcycling of MPW into liquid fuels by pyrolysis will be discussed in Chapter 3. The evaluation of the calorific value and determination of the activation energy of MPW and MPW plus catalyst will be carried out. A tube reactor will be used for the pyrolytic activities at 500-600^{o}C for thermal and 600^{o}C for the catalytic pyrolysis. GCMS and will be used for the characterization of Wax-oil and liquid product from thermal and catalytic pyrolysis respectively. ESIMS is used to determine the monomer and oligomer ratio. The biochar from this reaction will be examined to determine degradation.

Chapter 4 gives the overall conclusions of chapters 2 and 3, few limitations encountered and recommendations.

Chapter 2: Mechanical recycling of MPW

2.1 Materials

The MPW containing some paper fiber was provided as shredded material (around 25 mm) by Convergen Energy (Green Bay, WI) as shown in Figure 2.1. Glycidyl methacrylate polyolefin (GMPE (Graftabond ECO-RG 00130C) and maleated polyolefin (MAPE, Graftabond ECO-RM 00325C) were provided by Savanture (Mt. Pleasant, MI). Dicumyl peroxide (DCP) and Polyethylene vinyl acetate (PEVA) (12% vinyl acetate content) were purchased from Sigma-Aldrich. Recycled LDPE (Advanced Environmental Recycling Technologies) and PP copolymer (Dow 6D83K) were provided by Dr. Karl Englund (Washington State University). Hop (*Humulus lupulus*) bines were sourced from Yakima Chief Ranches (Yakima, WA). The dried hop bines (~15 cm long pieces, 450 g x 3 batches) were boiled in 2% NaOH (15 L) for 2 h, cooled to room temperature and washed with water until neutral [137]. The softened hop bines were then treated with 1% sodium hypochlorite (bleach) solution (15 L) for 5-6 days with occasional stirring to remove lignin, washed extensively with water to form a white pulp, defibrated using a food processor, dried and yield recorded [138]. The dried hops fiber (HF) was Wiley milled to pass through a 6 mm screen.

2.2 Method

2.2.1 Hop fiber lignin and carbohydrate analysis

Total lignin content was determined, in duplicate, using acetyl bromide method [139]. Oven-dry HF (5 mg) was incubated with acetyl bromide (25% w/w, in acetic acid, 5 mL) together with perchloric acid (0.2 mL, 70%) at 70 °C for 60 min in sealed tubes. The solutions were made up to 100 mL containing 2M NaOH (10 mL) and acetic acid (25 mL). Absorbance at 280 nm was measured (Genesys 50, ThermoScientific) and lignin content determined using an absorptivity of lignin of 20.09 L g^{-1} cm^{-1}. Total carbohydrate content was determined, in duplicate, using a modified phenol-sulfuric acid colorimetric method [140]. Oven-dried HF (10 mg) and cellulose standard (Sigmacell type 101, 2 to 10 mg) were incubated in sulfuric acid (100 µL, 77%) and then aqueous phenol solution (1 mL, 5%) and subsequently concentrated sulfuric acid (5 mL) were added. Absorbance at 490 nm was measured (Genesys 50, ThermoScientific).

2.2.2 Compounding

The shredded MPW (6 kg) was manually fed into a co-rotating twin screw extruder (Leistritz, 18 mm Ø, L/D ratio of 40, 200 rpm, barrel temperature 160^{o}C, 4.7 kW motor) to form an extruded rod (Figure 2.1). The extruded rod (9 mm OD) was milled with a plastic granulator equipped with a 6 mm sized screen (Sterling BP608, New Berlin, WI, USA). To produce a homogeneous material, the milled extruded MPW was extruded a second time, fed using a K-Tron weight loss feeder (1 kg/h), to form a uniform rod, then re-granulated, as described above. The twice extruded MPW granules was subsequently blended with either MAPE (2%), GMPE (2%), DCP (0.5%), HF (10%), MAPE (2%) plus HF (10%), GMPE (2%) plus HF (10%), and DCP (0.5%) plus HF (10%) in 700 g (total) batches. For the DCP containing formulations, DCP (14 g) was dissolved in acetone (100 mL) and sprayed on MPW with continuous mixing in a Kitchen-Aid mixer, air dried overnight, and then vacuum dried for 24 h at 40^{o}C [141]. The various blended formulations and MPW control were fed into the extruder using a mass loss feeder (K-Tron) at 0.5 kg/h to form a ribbon (3.5 mm x 50 mm). The extruder screw speed was 200 rpm with extruder barrel zones 2-6 and 7-8 and die at 160^{o}C and 155^{o}C, respectively [142].

Figure 2.1 Shredded MPW to extruded rod

2.2.3 Fourier-Transform Infrared Spectroscopy (FTIR)

FTIR spectra of 100 randomly selected plastic samples were acquired on a Nicolet iS5 spectrometer (Thermo-Scientific, Madison, WI, USA) using an attenuated total reflectance (iD5, ZnSe) accessory. Data was analyzed using OMNIC v9.8 software.

2.2.4 Thermal analysis

Thermomechanical analysis (TMA) was performed on a PerkinElmer TMA-7 instrument (Shelton, CT, USA) to determine the softening temperature (T_s) of composite samples (2 x 1.5 x 1 mm^3) under nitrogen (20 mL/min), with 10 mN force applied using a penetration probe from -30 to 300°C at 5°C/min. Dynamical mechanical analysis (DMA) was performed, in duplicate, on rectangular specimens (3 x 5 x 20 mm^3) using a 3-point bending fixture using a 15 mm span, on a Perkin Elmer DMA-7 instrument at a frequency of 1 Hz, 0.2% strain, and from -50 °C to 150 °C at 3 °C/min. Data was analyzed with Pyris v13 software. Differential scanning calorimetry (DSC) was performed on composite samples (5 mg), in duplicate, using a Q200 DSC (TA instruments, New Caste, DE, USA) from 40°C (3 min) and ramped to 300°C (3 min) at 10°C/min, then cooled to -50°C (3 min) at -10°C/min and reheated to 300°C at 10°C/min.

$$Xc = \frac{\Delta H_m}{\Delta H_0 * W_f} * 100\%. \qquad \text{Eq. 1}$$

ΔH_m is the melting enthalpy derived from the area under the peak, W_f is the weight fraction of the polymer in the formulation and ΔH_0 is the enthalpy of fusion of the polymers (PP (207 J/g), HDPE (293 J/g), PET (140 J/g) and polyethylene vinyl acetate (PEVA, 293 J/g).

2.2.5 Rheology

Dynamic rheology experiments were performed using a Bohlin CVO 100 N rheometer (East Brunswick, NJ, USA) equipped with an extended temperature unit with 25mm Ø serrated parallel plates at 190°C, 0.2% strain, and from 0.01 Hz to 100 Hz. Complex viscosity (η*), elastic modulus (G'), tanδ and viscous modulus (G") were measured. High shear viscosity measurements were determined using a capillary rheometer (Instron Model 3213, Norwood, MA, USA) connected to an Instron 5500R-1137 universal testing machine (50 kN load cell) at 190°C at cross head speeds of 0.6, 2, 6, 20, 60 and 100 mm/min with a barrel diameter of 9.5504 mm, and data acquired using the BlueHill v3 software. The dies were 14 and 27 mm long with a diameter of 1.4 mm and an entrance angle of 70°. Samples (8 g) were loaded in the barrel and thermally equilibrated for 10 mins prior to testing. Each sample was run in triplicate. Since the L/D ratio was <200, Bagley correction was used to correct for the effect of drop in pressure during measurement [90].

2.2.6 Tensile Testing

Tensile dog-bone specimens (ASTM D638 type I) of LDPE, PP and MPW formulations were prepared by injection molding (Yuh-Dak Machinery Co. model Y310, 15-ton clamp) with a barrel and nozzle temperatures of 210 and 215 ^{o}C, respectively (Figure 2.2). The various MPW and plastic samples (8 replicates) were tensile tested on an Instron 5500R-1132 universal testing machine (Norwood, MA, USA) equipped with a 5 kN load cell and extensometer (model 3542, Epsilon Technology Corp) with a cross head speed of 5 mm/min according to the ASTM D638. Data was analyzed using Bluehill v3 Instron software.

Figure 2.2 Tensile dog-bone specimens

2.2.7 Water soak test

Weight gain of composite samples (25 mm Ø x 3 mm), in triplicate, were soaked continuously in a water bath for 83 d at room temperature. The diffusivity was calculated using equation 2.

$$D_f = \pi(h/4M_f)^2 (M/\sqrt{t})^2 \qquad \text{Eq. 2}$$

Where, M_f is Max moisture content at the end, *h* is sample thickness in meters, $M/\sqrt{t}$ is the initial slope from the plot MC vs $\sqrt{t}$ [90].

2.3 Results

2.3.1 Hops fiber (HF)

Hop bines had an original lignin content of 50% and this high content could be attributed to flavonoids [97], protein [100] and ash components in the bines. The hop bines were subjected to sodium hydroxide and bleaching treatments to afford a HF pulp in 45 ± 3 % yield. The HF pulp contained loose fibers and were white in color. The HF pulp had a lignin and total carbohydrate contents of 12.4 ± 0.5% and 78.3 ± 1.7%, respectively. Reddy and Yang reported lower lignin and higher cellulose values of extracted hops fibers at 6 and 84%, respectively [99] . Furthermore, these discrepancies are likely due to the harsher fiber extractions methods used (nitric and chromic acid) by Reddy and Yang [99] .

2.3.2 Mixed plastic waste analysis and compounding

The MPW was compounded by twin screw extrusion, granulated, and re-extruded to obtain a homogeneous extruded material. This extruded MPW material was then blended with either MAPE, GMPE and DCP, and with and without HF and extruded into composite ribbons.

The shredded MPW feedstock was analyzed by FTIR spectroscopy on 100 random pieces and shown to comprise (frequency basis) mainly of PE (26%), PP (3%), PET (31%), paper/cellulose (29%), PEVA (10%) and nylon (1%). A similar mix of plastics has been observed in a study by Xu et al. [142].

The extruded MPW was also analyzed by FTIR spectroscopy and an O-H stretching band was observed at the 3296 cm^{-1} which indicates the presence of a hydroxyl group of cellulosic material. The prominent C-H stretching vibrations at 2915 and 2848 cm^{-1} attributed to the methylene ($-CH_2-$) family [142] [143]. Bands at 1464, 1376 and 1161 cm^{-1} were assigned to C-H stretching bands of $-CH_2$, $-CH_3$ and CH groups, respectively and distinctive of propylene [144]. The presence of PEVA was also confirmed by the presence of absorption bands at 1464, 1019, and 719 cm^{-1} with reference to a PEVA standard. The existence of carbonyl groups (C=O) represented by bands between 1700–1750 cm^{-1} indicates the presence of ester and amide which are assigned to PET and/or PEVA and nylon, respectively [145].

2.3.3 Thermal analysis

The thermal properties of the MPW formulations were determined by a combination DSC and TMA. DSC analysis of the extruded MPW was performed (Figure 2.3) and four distinct melting points (T_m) were observed at 100 ^oC, 121 ^oC, 163 ^oC, and 242 ^oC and were assigned to PEVA, HDPE, PP and PET, respectively. In the cooling cycle, four crystallization (T_c) peaks were observed at 83, 95, 108 and 191^oC with X_c of 28% for PEVA, 9.3% for PE, 63% for PP and 6.0% for PET which were all derived from the T_m. The softening temperature (T_s), by TMA (Figure 2.4), of the MPW composite was 116 ^oC. Table 2.1 shows the data from the TMA, DSC and X_c analysis for the various MPW formulations.

The addition of coupling agents, MAPE and GMPE, to MPW didn't change the T_m (98^oC, 121^oC, 162^oC, and 239^oC) of the plastics in the matrix[146]. There was a decrease in X_c for all peaks except that assigned to PP and this phenomenon was also observed by Perez-Fonseca et al. [85]. Coupled MPW formulations were also observed to have a 1-3 ^oC increase in T_c as seen in Figure 2.3 and Table 2.1. This increase might be due to branching of MAPE, GMPE and good distribution in the matrix [147]. The T_s (Figure 2.4) were slightly reduced to 115^oC (MAPE) and 114^oC (GMPE).

DCP was added to MPW to obtain long chain branching in the material. DSC analysis (Figure 2.3 and Table 2.1) showed similar T_m's for the four T_m's at 110^oC, 120^oC, 161^oC and 235^oC. The HDPE peak at 120 ^oC showed a noticeable decrease in intensity and was broadened. T_c peaks were observed at 83, 99, 108, and 184 ^oC. The PET assigned peak (184 ^oC) decreased in temperature compared to that found in MPW control. The X_c decreased for PE, PP and PET while for PEVA showed a significant increase which could be attributed to crosslinking [146] and this X_c decrease invariably can decrease the mechanical properties [148]. In general, the X_c of HDPE in the mix was lowered after the addition of coupling agents and DCP which might indicate the compatibilization between components as seen by Lei et al. [84]. TMA showed two T_s's at 105^oC and 158^oC (Figure 2.4).

The addition of HF to MPW did not change the T_s (TMA) and T_m (DSC) of the formulations (Table 2.1). However, there was a slight decrease in X_c which might be

attributed to an increase in high surface area of fiber which spurred faster crystallization [147].

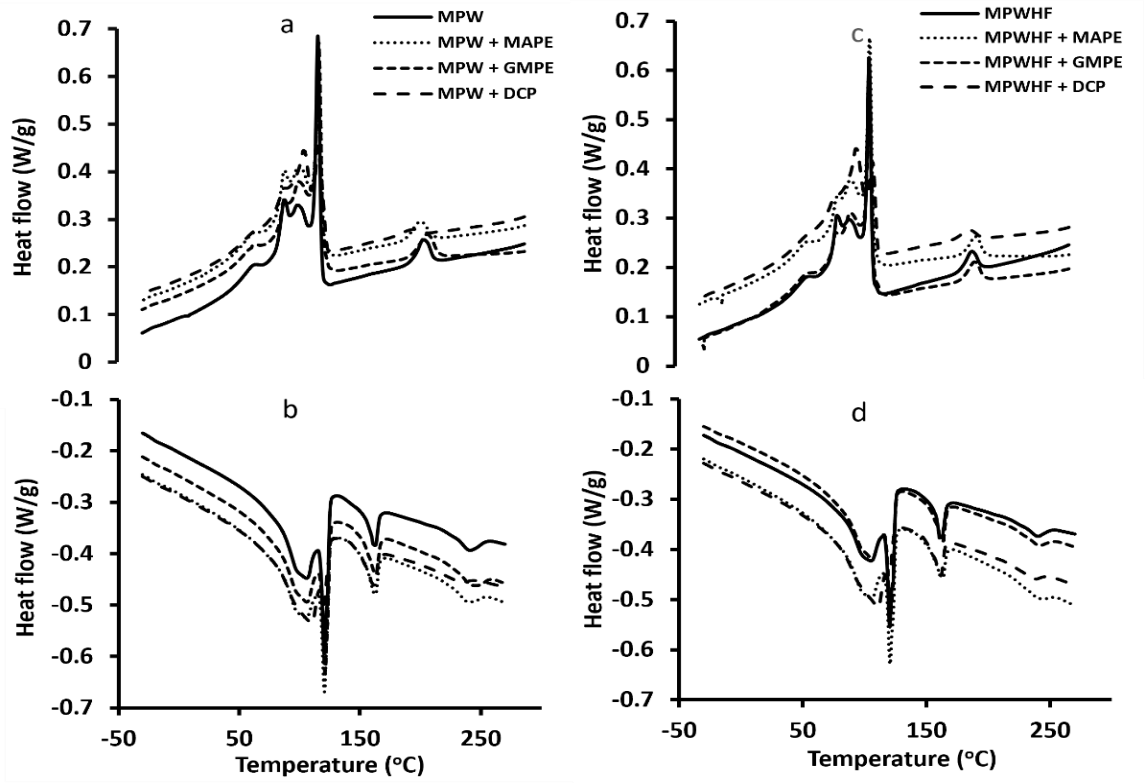

Figure 2.3 DSC thermograms showing (a) cooling and (b) heating cycle of MPW formulations with MAPE, GMPE and DCP and (c) cooling and (d) heating cycles of MPW formulations with HF and MAPE, GMPE and DCP.

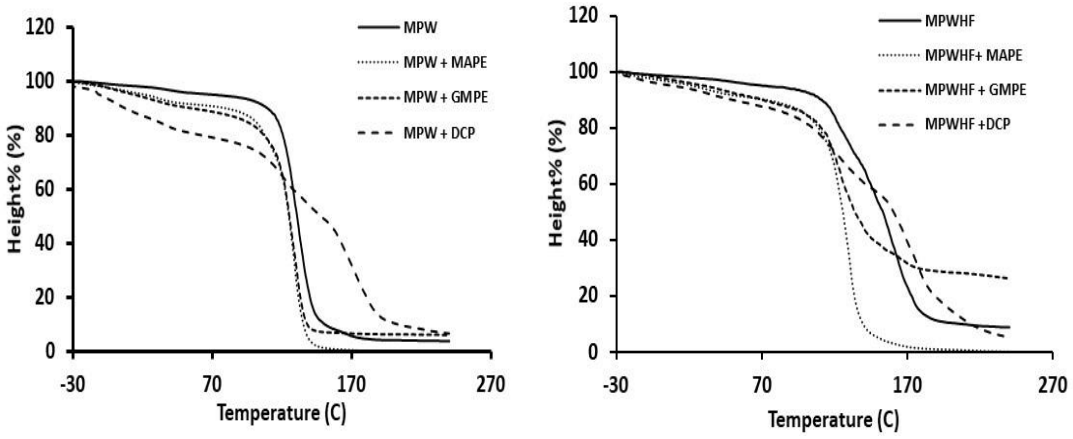

Figure 2.4 TMA thermograms of the various MPW formulations (a) without hops fiber and (b) with hops fiber

Table 2.1 Thermal data (Ts, Tm, Tc and Xc) for the various MPW formulations determined by TMA and DSC

	TMA	DSC		X_c (%) from T_m			
MPW formulations	T_s (^oC)	T_m (^oC)	T_c (^oC)	PEVA	HDPE	PP	PET
MPW	116	101, 121, 163, 240	83, 94, 107, 192	28.1	9.3	63.3	6.0
MPW + MAPE	114	98, 121, 162, 239	81, 95, 109, 193	23.7	8.3	82.8	6.0
MPW + GMPE	115	98, 121, 162, 240	81, 96, 109, 195	24.8	8.2	82.0	6.0
MPW + DCP	105, 158	110, 120, 161, 235	83, 99, 108, 184	86.5	1.8	73.9	2.6
MPWHF	112	99, 121, 161, 240	84, 95, 108, 193	25.4	8.2	63.6	4.5
MPWHF + MAPE	112	98, 121, 163, 240	81, 95, 109, 196	22.0	8.1	57.9	4.0
MPWHF + GMPE	114	101, 121, 163, 240	84, 92, 108, 196	22.7	8.3	59.7	4.6
MPWHF + DCP	101, 157	111, 121, 162, 236	81, 99, 111, 193	89.5	1.5	67.6	2.9

2.3.4 Rheology

The melt flow characteristics of the MPW composites were carried out by both dynamic and capillary rheometry. Initial studies on the effect of shear rate on the composite melts at 190^{o}C were performed on a dynamic rheometer. The rheological data obtained

shows (Figure 2.5) a general trend of decreased complex viscosity (η*) with an increase in shear rate (frequency) which indicates a shear thinning behavior [90], [149]. The power law model equations, η* at 1, 25 and 60 Hz are presented in Table 2.2. For comparisons, MPW showed a complex viscosity of 39.5 kPa.s at 1 Hz, this was higher than values reported on recycled HDPE and PP at the same frequency [90], this might be due to the low polymer degradation that possibly occurred during extrusion unlike much higher degradation for the recycled HDPE and PP [150]. Furthermore, the presence of fiber (paper/cardboard) in the MPW formulation contributed to an increase in η*. The addition of coupling agents (MAPE and GMPE) decreased the η* (at 1 Hz) to 31.6 and 36.1 kPa.s, respectively. The addition of DCP to MPW was shown to increase η* (at 1 Hz) to 67.6 kPa.s by long-chain branching resulting thus limiting polymer movement.

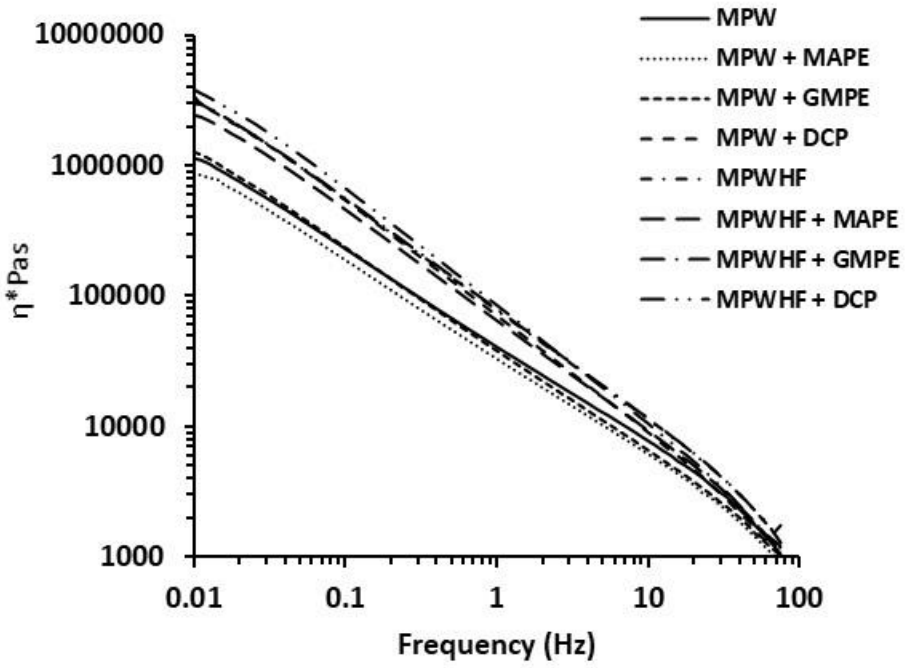

Figure 2.5 Complex viscosity with respect to frequency of MPW formulations in logarithmic scale and power law fitted

The addition of HF increased η* of MPWHF by nearly 2-fold to 74.5 kPa.s (at 1 Hz). With the hop fibers, a drop in η* occurred in the MPW melt with the addition of MAPE (62.7 kPa.s), while an increase was observed with GMPE addition (76.2 kPa.s). The general, an increase in η* with fiber addition is likely due to increased network formation and interaction

in the melt with an increase in fiber content [151]. The addition of DCP to MPWHF showed the highest change in η* and likely due long-chain branching and/or grafting of the matrix to the fibers thus restraining movement of the melt [152]. The flow curves for all the MPW formulations behaved following a power law model fit (Table 2.2).

Table 2.2 Complex viscosity (η*) of the formulations at 1, 25 and 60 Hz and power law fit model equation

Formulation	η* (kPa.s)			Power law fit model	
	1 Hz	25 Hz	60 Hz	Equation	R^2
MPW	39.5	3.7	1.5	$y = 40101x^{-0.766}$	0.997
MPW + MAPE	31.6	2.9	1.2	$y = 32427x^{-0.763}$	0.991
MPW + GMPE	36.1	3.1	1.3	$y = 37581x^{-0.79}$	0.997
MPW + DCP	67.6	3.7	1.4	$y = 67476x^{-0.888}$	0.994
MPWHF	74.5	5.1	1.8	$y = 75104x^{-0.858}$	0.994
MPWHF + MAPE	62.7	4.1	1.5	$y = 62367x^{-0.859}$	0.990
MPWHF + GMPE	76.2	5.1	1.9	$y = 75858x^{-0.861}$	0.990
MPWHF + DCP	81.8	4.4	1.5	$y = 80133x^{-0.902}$	0.988

Capillary rheological measurements were also performed to obtain flow curves (viscosity vs. shear rate) at higher shear rates. Following the ASTMD3835 standard, Bagley and Weissenberg-Rabinowitsch corrections were applied from results obtained using two die lengths [90] [153]. Figure 2.6 below shows a plot of the true shear viscosity vs. shear rate. The power law model equations and viscosity at a shear rate of 100 s^{-1} are given in Table 2.2. Shear viscosity values for all formulations were within 10^3-10^4 Pa.s, which saw a gradual decrease as true shear rate increased due to shear thinning of polymer which arises as polymer chains disentangles during flow and the degree of disentanglement is shear rate dependent [90]. The flow curves for all the MPW formulations behaved following a power

law model fit (Table 2.3). The addition of coupling agents increased the viscosity of the MPW (by improved interactions), while the addition of DCP decreased viscosity. The results from the capillary measurements (lower viscosity) contrasted with the dynamic rheological measurements for addition of DCP to MPW. This may be attributed to chain scission [154] lowering true shear viscosity due to the longer experiment time. The addition of HF to MPW increased the viscosity of the melt by 32% (at shear rate of 100 s^{-1}). A slight increase was also observed when coupling agents were added (MAPE and GMPE) to the MPWHF formulation as observed in the literature [90]. The addition of DCP to the MPWHF formulation resulted in an unexpected slight reduction in viscosity. The decrease in viscosity values could be attributed to chain scission during the extended time of testing at 190 ^{o}C. The shear viscosity values obtained from the capillary rheometer were much lower than η* obtained from the dynamic rheometer (10^6-10^7 Pa.S). This phenomenon was also observed by Mazzanti et al. [89] on PP-wood composites.

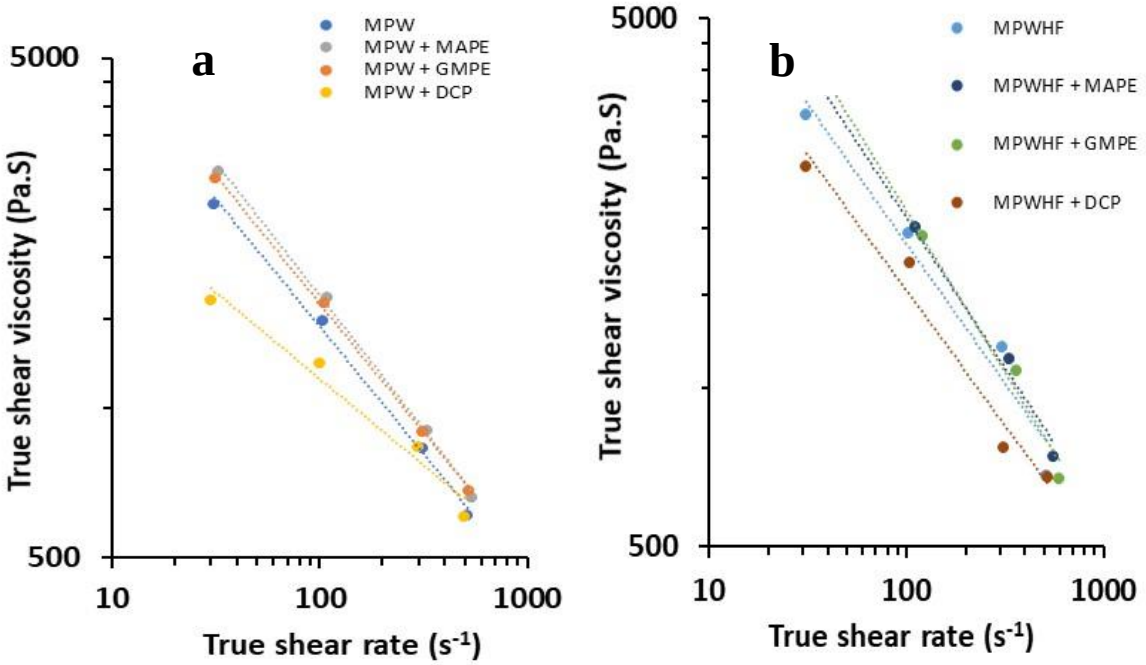

Figure 2.6 Flow curves MPW formulations with-out HF (a) and MPW formulations with HF (b) showing true shear viscosity vs true shear rate and power law fitted model.

Table 2.3 Power law fit equation and R^2 values of formulations which confirms correlation

Formulation	Power law		Viscosity at $100s^{-1}$ (Pa.S)
	Equation	R^2	
MPW	$y = 15133x^{-0.509}$	0.997	1487
MPW + MAPE	$y = 19527x^{-0.533}$	0.998	1664
MPW + GMPE	$y = 17177x^{-0.513}$	0.999	1615
MPW + DCP	$y = 5600.6x^{-0.345}$	0.974	1224
MPWHF	$y = 21309x^{-0.528}$	0.983	1961
MPWHF + MAPE	$y = 28942x^{-0.57}$	0.998	2006
MPWHF + GMPE	$y = 36034x^{-0.611}$	0.998	1940
MPWHF + DCP	$y = 16118x^{-0.511}$	0.971	1720

2.3.5 Viscoelastic properties

The viscoelastic properties (storage modulus (E′)) of the composites were determined by DMA. Thermograms of E′ for the various formulations are shown in Figure 2.7. E′ was shown to decrease with temperature. The E′ for MPW at 30 ^{o}C was 2.4 x 10^8 Pa (Table 2.4). The addition of MAPE and GMPE slightly reduced E′. The addition of DCP to MPW lowered E′ by 17% and this can be attributed to polymer chain scission which likely further reduced its resistance to deformation [155].

An increase in E′ was expected with the addition of HF, as seen in WPC [90], [156]. However, the addition of HF to MPW did not change E′ greatly. When coupling agents were introduced to MPWHF, E′ increased to 2.6 and 2.5 x 10^8 Pa (at 30 ^{o}C) for MAPE and GMPE, respectively. This increase can be attributed to better fiber-polymer matrix interaction which reduced mobility and led to better energy transfer as bending took place and thanks in part to

the coupling agents MAPE and GMPE [157]. The addition of DCP to MPWHF decreased E′ slightly.

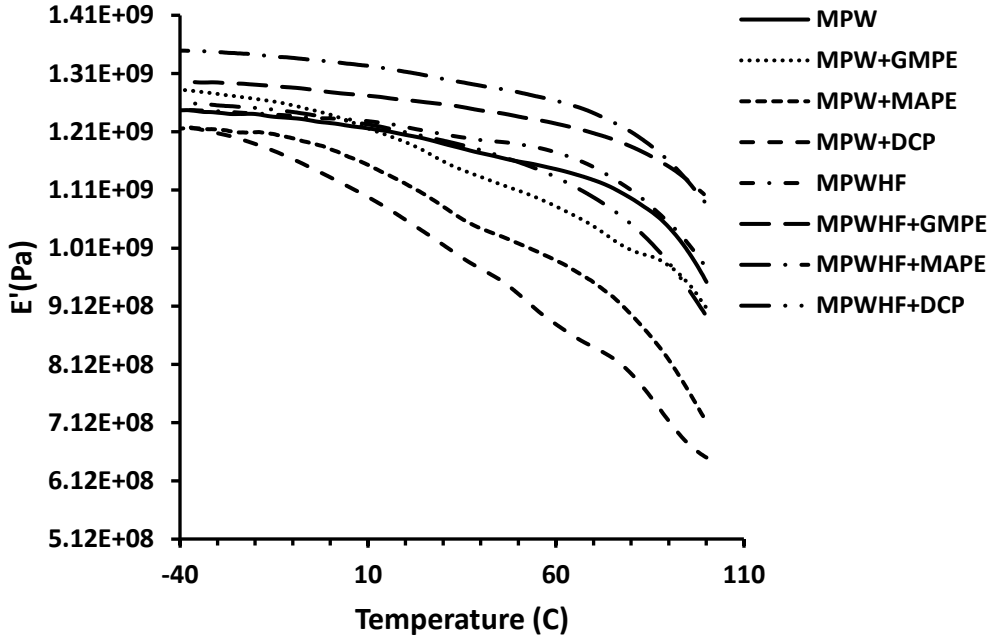

Figure 2.7 DMA thermogram of formulations showing storage modulus (E') vs Temperature.

Table 2. 4 Storage modulus of formulations at 30 ^{o}C

Formulations	E′ (MPa) at 30 ^{0}C
MPW	1192
MPW + MAPE	1084
MPW + GMPE	1160
MPW + DCP	1018
MPWHF	1208
MPWHF + MAPE	1303
MPWHF + GMPE	1260
MPWHF + DCP	1197

2.3.6 Tensile Properties

The tensile properties (strength, Young's modulus, energy at max tensile stress (EMTS) and density) of the various MPW formulations are given in Table 2.5. Composite composition (additives and fiber) greatly influences properties and thus its usability and application [158][159]. The tensile strength of MPW was 11.9 MPa which is lower than recycled LDPE (15.3 MPa) and PP copolymer (25.6 MPa). The addition of MAPE and DCP did not change MPW tensile strength. GMPE addition resulted in a significant increase (11%) in tensile strength. It was expected that coupling agents and DCP would improve the adhesion and interaction in the MPW [124] [155]. The addition of 10% HF to the MPW formulations improved its tensile strength by 8% which was further increased with addition of MAPE (Table 2.5).

Table 2.5 Tensile properties of MPW formulations

Formulation	Strength (MPa)	Young's modulus (MPa)	EMTS (J)	Density (kg/m^3)
MPW	11.9 (0.8)^{a,b}	1,405 (157)^{b}	0.37 (0.05)^{c}	1217
MPW + MAPE	12.9 (0.3)^{a,d}	1,361 (120)^{a}	0.71 (0.07)^{a}	1150
MPW + GMPE	13.2 (0.2)^{c}	1,391 (97)^{c}	0.70 (0.05)^{b}	1295
MPW + DCP	11.0 (0.4)^{b}	1,088 (153)^{a}	0.61 (0.06)^{a,b}	1279
Hop Fiber (HF)	-	-	-	1383
MPWHF	12.9 (0.5)^{e}	1,965 (119)^{e}	0.36 (0.03)^{d}	1193
MPWHF + MAPE	13.6 (0.4)^{f}	1,808 (146)^{d}	0.40 (0.06)^{e}	1268
MPWHF + GMPE	12.4 (0.2)^{c}	1,665 (201)^{b,c}	0.37(0.03)^{f}	1262
MPWHF + DCP	12.0 (0.7)^{d}	1,525 (192)^{d}	0.41 (0.05)^{g}	1318

Note: Standard deviation in parentheses and same superscript letters ($^{a, b, c, d, e, f, g}$) are statistically different via Tukey's HSD pairwise comparison test.

The Young's modulus of MPW was 1,405 MPa (Table 2.5) and was higher than that of recycled LDPE (612 MPa) and PP copolymer (1034 MPa). The addition of coupling agents and DCP gave a significantly decrease in Young's modulus. The addition of HF to MPW significantly increased its Young's modulus by 40%. This improvement in modulus by adding reinforcing fibers has also been observed in wood plastic composite [160] [91] due to the fiber contributing to better stress transfer [161]. The addition of coupling agent (MAPE and GMPE) to MPWHF formulation significantly decreased the Young's moduli and was counter to what was expected. DCP addition resulted a 22% decrease in Young's modulus for MPWHF and again this could be attributed to plastic chain scission rather than cross-linking [141]. It was observed also that the mechanism of failure changed from ductile to brittle failure possibly due to DCP content [162], and a similar drop in tensile strength of composite coupled with 0.2% DCP was observed by Gu and Kokta [163].

EMTS, a measure of a materials toughness, was 0.37 J for the MPW and was shown to significantly increase (65-92%) with the addition of coupling agents (MAPE and GMPE) and DCP (Table 2.5). The addition of HF to MPW did not improve EMTS. Also, the addition of coupling agents and DCP to MPWHF did not improve the EMTS. In general, HF in the composites created stress points for crack propagation and thus resulted in lower tensile strength and EMTS values [164]–[166]. HF reinforcement fell short of expectations in improving the properties of MPW formulations as compared to other natural fibers [167]. The slight increase in tensile strength of the MPWHF than MPW formulations is likely due to cellulosic content [99], [168].

2.3.7 Water absorption tests

Water soak tests was carried out to determine the water absorption behavior of the various MPW formulations with respect to time based on Fick's diffusion behavior [90] as shown in Figure 2.8 and Table 2.6. In general, a positive relationship between fiber content and WA was observed. At day 83, the WA of MPW was 10.6%, and the introduction of MAPE and GMPE did not significantly change WA values. Coupling agents generally retard WA in plastics and MPW [169]. The addition of DCP to MPW resulted in a significant 50% increase in water uptake relative to MPW after 83 d.

The addition of HF to MPW did not significantly change the WA either. Addition of coupling agents unexpectedly did not change the WA values significantly [170] [171]. MPWHF with DCP composite had a significantly lower WA than MPW + DCP. The formulation without HF has a higher diffusion coefficient and are expected to consume less water following equal amount of exposure with the HF reinforced counterpart because the formal having higher diffusion coefficient will require just a short time to reach equilibrium absorption [172] .

Table 2.6 WA (%) and diffusion coefficient of composite formulations

Formulations	WA (%)		Diffusion Coefficient
	5 Days	83 Days	m^2/s
MPW	2.9 (0.3)^{af}	10.6 (0.3)^{a}	8.6 x 10^{-11}
MPW + MAPE	2.3 (0.6)^{bdg}	10.0 (0.6)^{b}	8.1 x 10^{-11}
MPW + GMAPE	2.8 (0.4)^{ch}	9.7 (0.5)^{c}	7.8 x 10^{-11}
MPW + DCP	10.3 (0.6)^{acde}	15.9 (0.7)^{abcde}	5.6 x 10^{-11}
MPWHF	3.6 (0.4)^{bci}	11.5 (0.8)^{bcf}	9.2 x 10^{-11}
MPWHF + MAPE	3.1 (0.6)^{dj}	10.4 (0.7)^{d}	1.1 x 10^{-10}
MPWHF + GMPE	3.0 (0.2)^{ek}	10.4 (0.6)^{ef}	4.1 x 10^{-10}
MPWHF + DCP	10.1 (0.4)^{fghijk}	13.7 (0.5)^{abcde}	4.6 x 10^{-11}

Note: Standard deviation in parentheses and same superscript letters ($^{a, b, c, d, e, f, g, h, I, j, k}$) are statistically different via Scheffe's test.

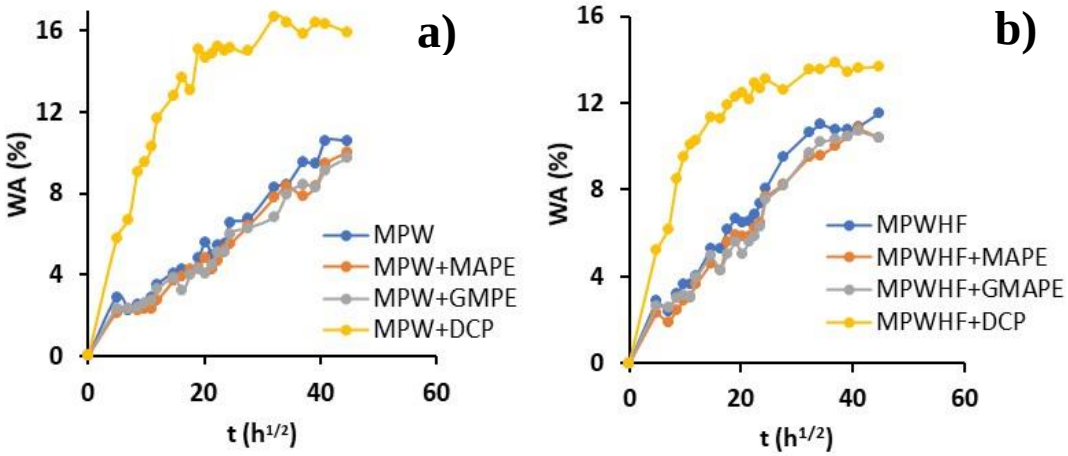

Figure 2.8 Water soak of formulations with respect to time. a): without HF, b): with HF

Chapter 3: Chemical upcycling through thermal deconstruction of MPW and fiber into wax-oil and its upgrading: pilot-scale investigation.

3.1 Characterization of the MPW

The calorific value of the extruded MPW (1.0 g) was determined by bomb calorimetry (Parr oxygen bomb calorimeter, model number: 1261) in duplicate following the ASTM D5865-04 standard. The ash content (600^{o}C for 16 h), fixed carbon (FC), and volatile matter (VM) (900^{o}C for 7 min) on extruded MPW were determined according to ASTM E870-82 in duplicate.

Thermogravimetric analysis (TGA) was used to determine the activation energy and degradation behavior and mass yield [173] of MPW and the effects of catalyst on MPW samples using a PerkinElmer TGA-7 instrument from 35 to 800 ^{0}C at heating rates of 5, 15, 25, 35, and 50 ^{0}C/min under 30 mL/min nitrogen flow. Runs with catalysts were a 1:1 mix of granulated MPW and zeolite Y (H form) catalyst (Si:Al = 30:1, 780 m^2/g, Alfa Aesar). To determine the mass yield of MPW and MPW+catalyst at specific isothermal temperatures, the temperature was ramped up from 35 ^{0}C to either 500, 550, or 600 ^{0}C at 200 ^{0}C /min and then held isothermally for 60 min. Pyris v13.3.1 software was used to analyze the data.

3.2 Thermal and catalytic pyrolysis experiments

MPW samples (1.0 g, inserted in a small tube between glass wool) were pyrolyzed at different temperatures ranging from 500-600^{0}C in a small quartz tube (20 mm ID x 300 mm) reactor with a nitrogen purge of 100 mL/min using a mass flow controller (Dakota instruments) [173]. The tube reactor was connected to a U-tube condenser (immersed in liquid N_2) to capture any hydrocarbon products. A schematic of the reactor is given in Figure 3.1 The condenser was weighed before and after each experiment.

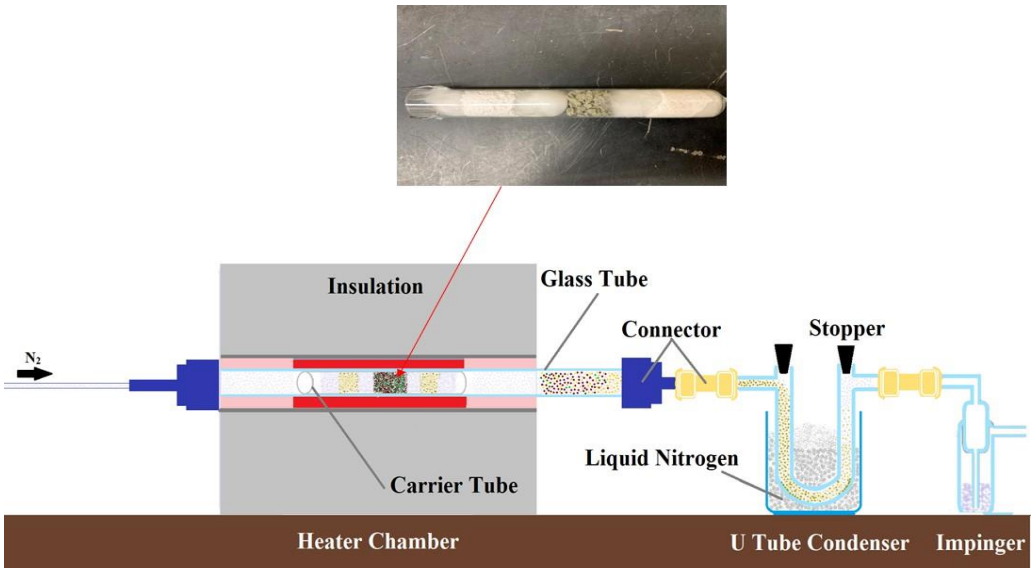

Figure 3.1 Schematic of the pyrolysis tube reactor [173]

For the catalytic pyrolysis experiments, a similar system setup as described above (Figure 3.1) was used except that the MPW sample (0.5 g) was inserted between glass wool and catalyst (1.0 g comprising of Zeolite Y + sand mix (1:1)) on each end of the small tube which was inserted into a heated zone with a nitrogen purge of 60 mL/min by [173].

3.3 Characterization of pyrolysis products

The wax-oil products (1.0 mg in CH_2Cl_2 (1 mL) containing 1,2,4-trichlorobenzene as internal standard (0.05 mg/mL)) from pyrolysis and catalytic pyrolysis experiments were analyzed in duplicate by gas chromatography-mass spectrometry (GC-MS, Trace 1300-ISQ, Thermo Scientific). Separation was achieved using a temperature ramp of 40^0C (1 min) to 320^0C at 5^0C/min on a ZB-5 capillary column (30 m x 0.25 mm Ø, 0.25 µm coating, Phenomenex).

Positive ion electrospray ionization mass spectrometry (ESI-MS) on a Finnigan LCQ-Deca instrument (Thermo-Quest) was used to determine the molar mass of the of pyrolysis products (1 mg mL^{-1} in CH_2Cl_2:methanol:acetic acid (50:49:1) at 20 µL min^{-1}). The ESI-MS scan range was m/z 100 to 2000 using a capillary e and ion source voltages of 50 and 4.5 kV, respectively. The capillary temperature was 275 ^{0}C. The number average (M_n) and weight average (M_w) molar masses were calculated from M_i (mass after accounting for charge) and N_i (ion intensity) using equations 3.1 and 3.2.

$$M_n = \frac{\sum N_i M_i}{\sum N_i} \quad \text{Eq. 3.1}$$

$$M_w = \frac{\sum N_i M_i^2}{\sum N_i M_i} \quad \text{Eq. 3.2}$$

Fourier Transform Infrared Spectroscopy (FTIR) was used to analyze the MPW and pyrolysis char samples (in triplicate) using a Thermo-Nicolet iS5 spectrometer with a ZnSe or Ge attenuated total reflection (iD5 ATR) probe. Each spectra obtained were averaged and baseline corrected using Omnic v9.8 software.

3.4 Results and Discussion

3.4.1 MPW characterization

The compounded MPW was shown to have an ash content of 2.4% and attributed to inorganic additives (e.g., metal foil, talc) used during polymer formulation [174]. The calorific value of compounded MPW was 35 KJ/g which is consistent with mixed plastics [175] but lower than that of PE, PP, and gasoline [176]. The fix carbon (FC) content was 6.1% and with a volatile matter (VM) content of 91.5%. This is within the range reported for PET [177], PP [178] and waste plastics [179].

TGA was used to investigate the kinetics and thermal degradation of MPW and MPW+catalyst. Figure 3.2 shows the TGA and DTG thermograms of MPW and MPW+catalyst at various heating rates (5-50^{o}C/min). In the TGA thermograms of the MPW, a small weight loss was observed <80^{o}C which can be attributed to water loss. The DTG of MPW (at 5^{0}C/min) showed a minor degradation peak at 347^{0}C which can be attributed to the cellulosic component [180] of the waste which is estimated at about 29% of the mix. Furthermore, a peak signifying a major weight loss occurred at 480^{0}C and a final degradation step at 520^{0}C.

TGA analysis was also performed on MPW+catalyst (Figure 3.2b), which showed a small peak below <70^{0}C which is due to water. A minor peak at 345^{0}C (at 5^{0}C/min) was designated to cellulose degradation. The major degradation occurred at 440^{0}C and with a final degradation at 498^{0}C. The TGA peaks for the MPW+catalyst occurred at a lower temperature than MPW suggesting that the catalyst assisted in the catalytic breakdown of

MPW. This shift to lower temperature with the addition of catalyst to hydrocarbon substrate has been observed by Sotoudehnia et al. [173]. There was a modest shift in decomposition temperature (T_d) and onsets (T_{onset}) with increasing heating rates. Also, the higher heating rates broadened peak intensity in the DTG thermograms [181]. Based on TGA results, MPW pyrolysis and catalytic pyrolysis experiments were performed at 500-600^{0}C and 600^{0}C, respectively.

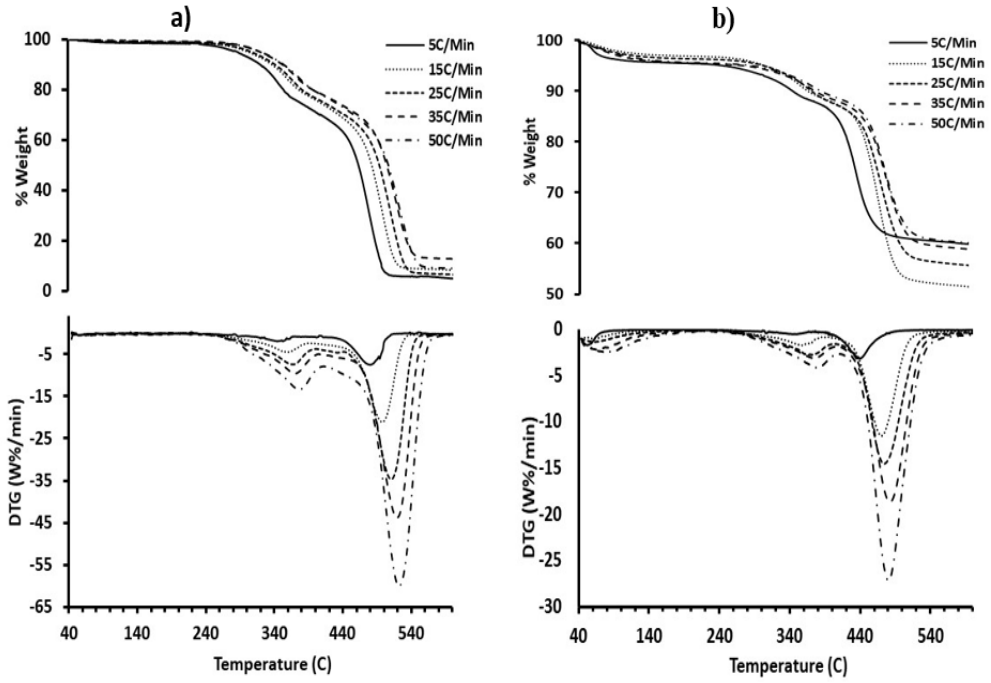

Figure 3.2 TGA and DTG thermogram of (a) MPW and (b) MPW+catalyst at different heating rates

The apparent activation energy (*E*) was determined for the MPW and MPW+catalyst at a conversion range of 10% to 90% using the iso-conversional approach based on linear regression of the FWO method (Table 3.1) [173], [174]. These results fall within the range of those reported for plastics [182]. It is apparent from the kinetic data that the use of catalyst decreased (for example 30% decrease at 50% conversion) the *E* of MPW degradation.

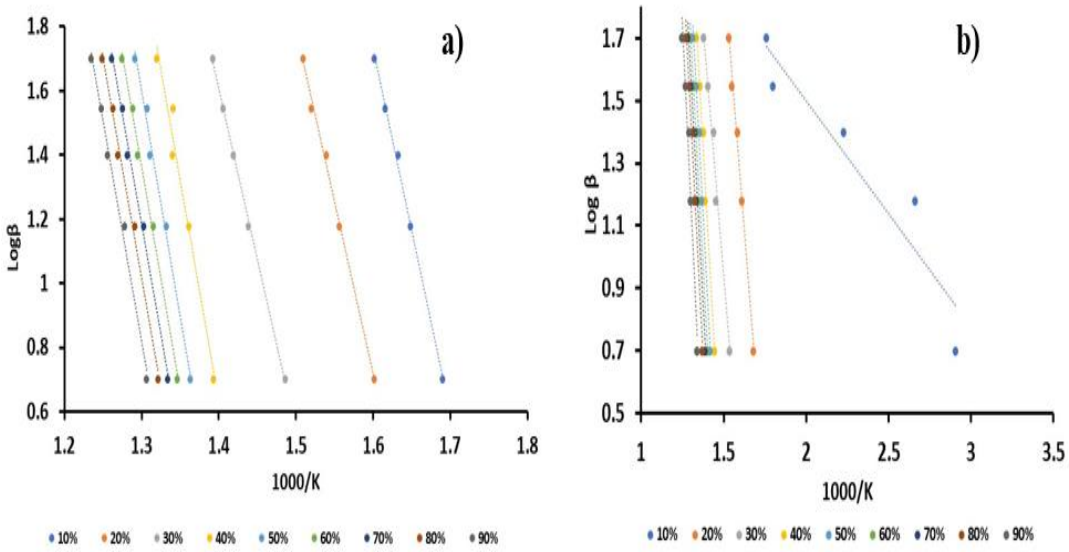

Figure 3.3 Plots of log heating rate (β) versus 1/K of a) MPW, b) MPW+catalyst

Table 3.1 Activation energy (*E*) and R^2 values of MPW and MPW+catalyst at various conversion factors (10-90%)

Conversion	***E* (J/mol)**		**R^2**	
(%)	MPW	MPW+catalyst	MPW	MPW+catalyst
10	206	13	0.997	0.902
20	196	123	0.996	0.992
30	193	117	0.999	0.983
40	251	168	0.973	0.981
50	254	176	0.991	0.981
60	251	179	0.993	0.983
70	251	179	0.994	0.981
80	250	186	0.993	0.978
90	248	206	0.991	0.969

Isothermal TGA was used to simulate temporal pyrolysis reaction and the experiment showed a biochar yield of 7% at 500^0C, 6.5% at 550^0C, and 5% at 600^0C which confirms an increase in temperature leads to a decrease in char yield [174].

3.4.2 Pyrolysis experiments

TGA analysis showed complete degradation occurs just below 550 ^{0}C and therefore, 3 temperatures (500, 550 and 600^{0}C) were selected for pyrolysis experiments. MPW was pyrolyzed at the various temperatures in a small tube reactor to generate solid (char), a wax-oil and gaseous products and their yields determined (Figure 3.4) [183]. Gas yield was determined by weight difference (original (MPW) – oil – char). The waxy material contained some oil which the 2-phases could not be separated.

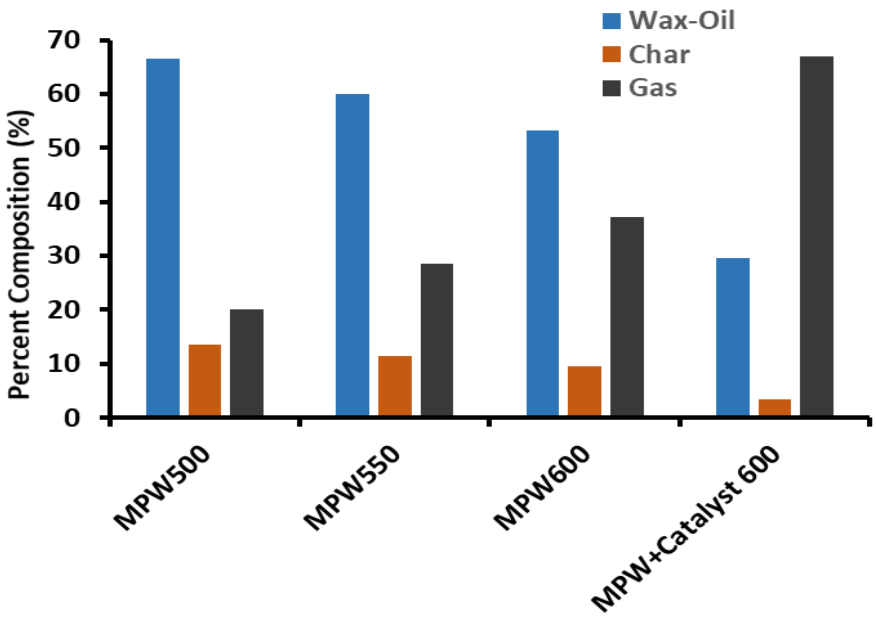

Figure 3.4 Products yield of thermal and catalytic pyrolysis

The char and wax-oil yields decreased with temperature. The wax product was cream-colored which was different to that observed by [184]. The highest wax-oil yield was 67% and achieved at 500 ^{0}C (Figure 3.4), which was higher than that obtained for plastic waste using a batch reactor at the same temperature [54]. The wax-oil yield was also higher than that obtained by co-pyrolysis of a biomass-plastic blend (1:3 ratio) in a fixed bed reactor [185]. However, the yield was lower than that achieved on plastic material using a two-stage fixed bed reactor at 500 ^{0}C [183]. An increase in the gaseous yield with temperature was also observed with the highest yield of 37% at 600 ^{0}C. This is due to more thermal cracking at the higher temperature which invariably leads to lower char and oil yields. LDPE has been

claimed to contribute to gas yield [186][187]. The char is likely derived from wood fibers within the MPW [188].

Catalytic pyrolysis was performed on MPW at only 600 ^{0}C to ensure that a good chemical conversion was achieved. The use of zeolite Y catalyst resulted in a decrease in liquid yield (30%) (Figure 3.4) with a concomitant increase in gas yield. The liquid yield was lower than that reported by other researchers [189][19],[186]. The acidic nature of Zeolite Y catalyst often leads to the cracking of lighter hydrocarbon thereby reducing liquid yield and increasing the gas fraction [190]. In addition, the presence of impurities in the MPW and char buildup could also contribute reducing catalyst activity towards liquid products [186]. The gas fraction yield was high (67%) which was an 82% increase compared to the normal pyrolysis of MPW at 600^{0}C. This increase in gas yield has also been reported by Muhammad et al. [191][192]. The light hydrocarbons were most likely not fully trapped in the liquid nitrogen cooled condenser. Finally, a char yield of 2.5% was obtained.

3.4.3 Characterization of pyrolysis products

The MPW pyrolysis liquid products trapped in the condenser were analyzed by GC-MS (Figure 3.5). The pyrolysis products were made up of mixtures of long-chain (C_7-C_{33}) alkanes, alkenes, dienes, aromatics (6-17%), and oxygenated compounds (6-12%) (Table 3.2). A detailed list and quantity of these compounds are given in Table 3.3. The chromatograms showed a series of peaks, based on chain length, which appeared as triplet peaks especially in pyrolysis experiments performed at 550 and 600 ^{o}C. This triplet pattern was also reported by [193], [194] and were identified to be alkadiene, alkene, and alkane compounds for a particular carbon chain length [193]. The most predominant compounds found in the wax-oil were long-chain alkanes and alkenes (C_{25}-C_{38}) derived from chain scission of PE and PP. The hydrocarbons chain length appeared to decrease with pyrolysis temperature (Figure 3.5 and Table 3.3). The appearance of the pyrolysis products changed from a wax product to an oily product (shorter chain length) as pyrolysis temperature increased and this has been previously observed [195]. Aromatic compounds, such as naphthalene and substituted benzenes and naphthalenes were also observed. Naphthalene can be produced from pyrolysis of PVC that is present in the MPW [196]. Water was observed in the wax-oil product which is likely a result of dehydration reactions of cellulosic components

presents in the MPW during pyrolysis [197]. The presence of oxygenated compounds like vanillin, furfuryl, methyl catechol, etc. are from lignocellulosic components and can reduce the quality of the liquid hydrocarbon product [185].

Catalytic pyrolysis of MPW afforded a completely different product profile than that of MPW pyrolysis (Figure 3.5). A list of products identified, and quantity are given in Table 3.4. The catalytic MPW products were a mixture of shorter chain (C_{16}-C_{18}) alkanes and alkenes plus aromatic compounds (C_6-C_{13}). The aromatics make up about 60% of the liquid products detected (Tables 3.2) and this has also been observed with Zeolite Y catalyst in the literature [189]. The presence of compounds such as toluene, xylene, ethylbenzene, propylbenzene, hexane, amongst others was also found in gasoline [198]. Zeolite Y is known to convert hydrocarbons into aromatic compounds due to the porous and acidic nature of this catalyst [199]. An absence of oxygenated compounds in the catalytic pyrolysis products was observed. The MPW catalytic pyrolysis GCMS profile had similarities to that of regular gasoline (Figure 3.5).

Table 3.2 Percentage composition of compounds found in thermal and catalytic pyrolysis

Pyrolysis	Sample Name	Alkane (%)	Olefins (%)	Aromatic (%)	Oxygenated (%)	Diene (%)	Unknown (%)
Thermal	MPW500	38.8	23.5	12.9	11.8	10.6	2.4
	MPW550	37.8	26.8	8.5	9.8	15.9	1.2
	MPW600	38.1	26.2	11.9	5.6	16.7	1.2
Catalytic	MPWCat600	15.5	22.5	60.6	-	-	1.4
Reference	Gasoline	47.4	4.0	48.6	-	-	-

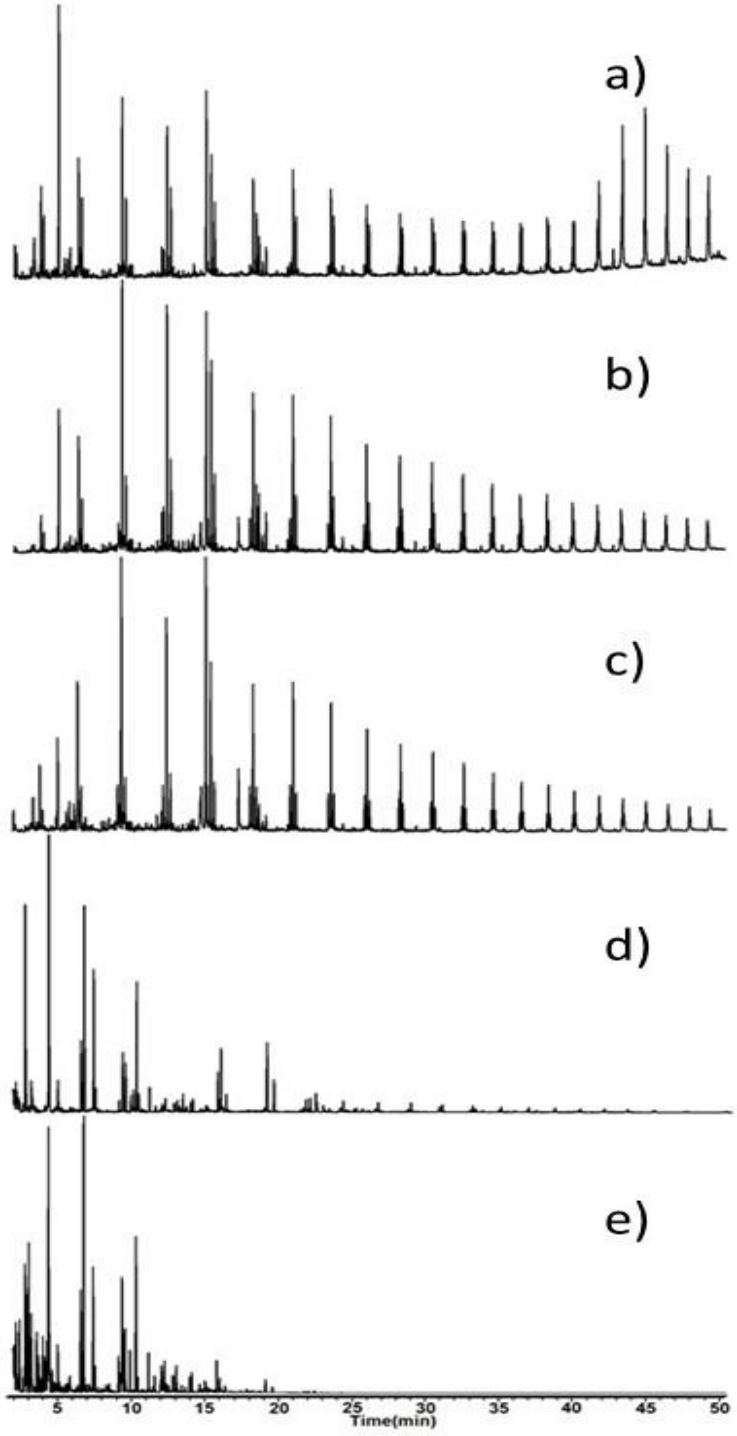

Figure 3.5 GCMS chromatograms of thermal pyrolysis of MPW at (a) 500^0C, (b) 550^0C, (c) 600^0C, (d) catalytic pyrolysis of MPW at 600^0C, and (e) regular gasoline

Table 3.3 Identified compounds and amount in the wax-oil product of thermal pyrolysis of MPW at 500, 550 and 600^{0}C

Compounds Name	**Formula**	**MW**	**RT**	**MPW5OO mg/g wax-oil**	**MPW55O mg/g wax-oil**	**MPW60O mg/g wax-oil**
1-Heptene	C_7H_{14}	98	3.05	2.80	0.75	3.25
Heptane	C_7H_{16}	100	3.16	2.17	0.55	0.71
Toluene	C_7H_8	92	4.33	3.20	0.88	6.41
1-Octene	C_8H_{16}	112	4.78	7.55	5.10	9.96
Octane	C_8H_{18}	114	4.96	4.99	2.36	2.99
2,4-Dimethyl-1-heptene	C_9H_{18}	126	5.96	23.12	18.14	12.99
Heptane, 2,3-dimethyl-	C_9H_{20}	128	6.34	1.46	-	-
Ethylbenzene	C_8H_{10}	106	6.52	1.57	-	3.32
p-Xylene	C_8H_{10}	106	6.73	2.47	2.39	5.40
2-Furfuryl alcohol	$C_5H_6O_2$	126	7.27	9.93	15.52	
o-Xylene	C_8H_{10}	106	7.35	2.37	3.51	29.19
Nonane	C_9H_{20}	128	7.51	6.83	7.08	7.01
Cyclodecane	$C_{10}H_{20}$	140	9.94	-	-	7.29
1-Decene	$C_{10}H_{20}$	140	10.17	14.99	34.21	37.95
Decane	$C_{10}H_{22}$	142	10.42	6.50	9.32	7.07
cis-4-Decene	$C_{10}H_{20}$	140	10.6	0.99	-	-
Isobutyl-benzene	$C_{10}H_{14}$	134	10.69	1.06	-	-
5-Ethyl-2-methyloctane	$C_{11}H_{24}$	156	10.83	1.03	-	-
4-ethyl-1,2-dimethyl- Benzene	$C_{10}H_{14}$	134	12.81	2.53	5.00	2.26
Naphthalene	$C_{10}H_8$	128	12.93	2.41	7.37	6.25
Vanillin	$C_8H_8O_3$	152	13.16	12.78	31.74	30.37
Undecane	$C_{11}H_{24}$	156	13.41	7.38	12.05	8.38
1-Ethyl-3,5-dimethyl-benzene	$C_{10}H_{14}$	134	13.57	0.92	-	1.38
3-Methylundecane	$C_{12}H_{26}$	170	15.48	-	-	16.58
Benzene, 1-methyl-4-(1-methyl-2-propenyl)-	$C_{11}H_{14}$	146	15.86	-	-	4.92
1-Dodecene	$C_{12}H_{24}$	168	16.08	10.24	26.84	24.62

Dodecane	$C_{12}H_{26}$	170	16.31	6.14	10.53	6.90
4-Methyl-catechol	$C_7H_8O_2$	124	17.92	-	5.66	13.47
8-Dodecenol	$C_{12}H_{24}O$	184	18.68	-	5.08	7.14
1-Tridecene	$C_{13}H_{26}$	182	18.87	7.99	21.64	21.87
Tridecane	$C_{13}H_{28}$	184	19.1	5.19	8.61	6.13
2-methyl-Naphthalene	$C_{11}H_{10}$	142	19.27	3.34	9.06	4.17
1-methyl Naphthalene-	$C_{11}H_{10}$	142	19.5	1.18	2.79	1.83
3-ethyl-3-methyl Decane,	$C_{13}H_{28}$	184	19.73	2.41	5.86	2.49
1,14-Tetradecanediol	$C_{14}H_{30}O_2$	230	21.16	0.86	1.79	1.71
1,13-Tetradecadiene	$C_{14}H_{26}$	194	21.32	1.19	5.64	7.47
1-Tetradecene	$C_{14}H_{28}$	196	21.53	9.02	22.84	22.21
Tetradecane	$C_{14}H_{30}$	198	21.72	4.98	7.80	5.26
10-Pentadecenol	$C_{15}H_{30}O$	226	23.86	0.86	5.22	7.37
1-Pentadecene	$C_{15}H_{30}$	210	24.03	7.24	19.38	19.30
Pentadecane	$C_{15}H_{32}$	212	24.22	4.91	7.63	5.30
2-Hexadecanol	$C_{16}H_{34}O$	242	24.83	0.78	1.83	1.22
1,4,5-trimethyl-Naphthalene	$C_{13}H_{14}$	170	25.48	0.55	-	-
Hexadecadiene	$C_{16}H_{30}$	222	26.25	0.90	4.38	5.91
1-Hexadecene	$C_{16}H_{32}$	224	26.41	5.85	15.14	15.28
Hexadecane	$C_{16}H_{34}$	226	26.58	4.19	8.34	5.26
10-Heptadecenoic acid	$C_{17}H_{32}O_2$	268	26.7	0.43	-	-
n-Heptadecadiene	$C_{17}H_{32}$	236	28.52	0.75	3.96	5.38
1-Heptadecene	$C_{17}H_{34}$	238	28.67	5.13	14.10	13.43
Heptadecane	$C_{17}H_{36}$	240	28.82	3.93	6.70	4.49
13-Octadecenoic acid	$C_{18}H_{34}O_2$	282	28.93	0.43	-	
2-methyl-1-Hexadecanol	$C_{17}H_{36}O$	256	29.7	0.63	-	
9,12-Octadecadiene	$C_{18}H_{34}$	250	30.67	0.59	3.33	4.48
1-Octadecene	$C_{18}H_{36}$	252	30.81	4.81	12.97	12.76
Octadecane	$C_{18}H_{38}$	254	30.95	3.59	5.55	3.97
8,11-Nonadecadiene	$C_{19}H_{36}$	264	32.73	0.77	3.57	4.45
1-Nonadecene	$C_{19}H_{38}$	266	32.85	4.38	11.88	11.09
Nonadecane	$C_{19}H_{40}$	268	32.98	3.65	5.84	3.69

1-Eicosanol	$C_{20}H_{42}O$	298	34.06	0.39	-	-
1,19-Eicosadiene	$C_{20}H_{38}$	278	34.69	0.56	3.03	3.47
1-Eicosene	$C_{20}H_{40}$	280	34.8	4.23	10.10	9.20
Eicosane	$C_{20}H_{42}$	282	34.92	3.47	5.09	3.37
Heneicosadiene	$C_{21}H_{40}$	292	36.56	0.74	2.61	3.37
1-Heneicosene	$C_{21}H_{42}$	294	36.67	4.15	9.03	8.58
Heneicosane	$C_{21}H_{44}$	296	36.77	3.88	4.39	2.94
Erucic acid	$C_{22}H_{42}O_2$	338	38.03	0.43	0.74	
Docosadiene	$C_{22}H_{42}$	306	38.34	0.69	2.34	2.73
1-Docosene	$C_{22}H_{44}$	308	38.44	4.51	8.23	7.13
Docosane	$C_{22}H_{46}$	310	38.54	3.85	4.37	2.84
Tricosadiene	$C_{23}H_{44}$	320	40.08	-	2.08	2.68
1-Tricosene	$C_{23}H_{46}$	322	40.15	4.15	7.51	6.34
Tricosane	$C_{23}H_{48}$	324	40.24	4.25	5.63	2.62
Tetracosadiene	$C_{24}H_{46}$	334	41.73	-	1.86	2.11
1-Tetracosene	$C_{24}H_{48}$	336	41.8	4.21	6.11	5.27
Tetracosane	$C_{24}H_{50}$	338	41.88	7.44	5.02	2.75
6,9-Pentacosadiene	$C_{25}H_{48}$	348	42.83	1.68	1.75	2.12
9-Pentacosene	$C_{25}H_{50}$	350	43.45	11.90	4.91	5.27
Pentacosane	$C_{25}H_{52}$	352	43.46	-	3.40	2.28
Hexacosa-1,3-diene	$C_{26}H_{50}$	362	44.84	-	1.50	1.78
1-Hexacosene	$C_{26}H_{52}$	364	44.91	-	4.65	5.27
Hexacosane	$C_{26}H_{54}$	366	44.96	13.49	4.61	2.59
Heptacosadiene	$C_{27}H_{52}$	376	46.31	-	1.26	1.27
1-Heptacosene	$C_{27}H_{54}$	378	46.37	-	3.41	3.78
Heptacosane	$C_{27}H_{56}$	380	46.41	10.10	3.41	1.74
Octacosane	$C_{28}H_{58}$	394	47.81	7.94	-	-
1-Nonacosene	$C_{29}H_{58}$	406	47.78	-	12.2	8.40
Nonacosane	$C_{29}H_{60}$	408	49.16	7.02	11.96	7.63
Triacontane	$C_{30}H_{62}$	422	50.48	6.22	10.80	6.90
Hentriacontane	$C_{31}H_{64}$	436	51.74	5.41	10.28	6.90
Dotriacontane	$C_{32}H_{66}$	450	52.98	4.97	8.88	6.06
1-Tritriacontene	$C_{33}H_{66}$	462	54.17	4.52	6.99	4.87

Tetratriacontane	$C_{34}H_{70}$	478	55.33	4.86	7.05	3.97
Pentatriacontane	$C_{35}H_{72}$	492	56.46	4.22	6.43	3.81
Hexatriacontane	$C_{36}H_{74}$	507	57.56	3.49	4.81	2.74
Heptatriacontane	$C_{37}H_{76}$	521	58.79	2.62	3.96	2.02
Octatriacontane	$C_{38}H_{78}$	535	60.2	2.39	3.36	-

Table 3.4 Identified compounds and amounts in gasoline and the liquid product of catalytic pyrolysis of MPW

Compound Name	**M+**	**Formula**	**RT**	**Gasoline mg/g**	**MPWCat600^{0}C mg/g**
3-Methylpentane	86	C_6H_{14}	1.99	19.71	1.84
3-methylene-pentane	84	C_6H_{12}	2.1	29.60	3.38
methyl-cyclopentane	84	C_6H_{12}	2.35	32.38	1.52
2,3-dimethyl-pentane	100	C_7H_{16}	2.71	73.92	61.90
3-ethyl-Pentane	100	C_7H_{16}	2.81	32.31	-
2,2,3,3-Tetramethylbutane	114	C_8H_{18}	2.97	65.80	-
3-methyl-Hexane	100	C_7H_{16}	3.13	25.18	6.17
3,3-dimethyl-1,4-Pentadiene	96	C_7H_{12}	3.2	6.79	3.42
methyl-Cyclohexane	95	C_7H_{14}	3.5	23.12	-
2,5-dimethyl-Hexane	114	C_8H_{18}	3.59	6.46	-
2,4-dimethyl-Hexane	114	C_8H_{18}	3.63	11.61	-
1,2,4-trimethyl-Cyclopentane	112	C_8H_{18}	3.77	4.72	-
3-Ethylpentane	100	C_7H_{16}	3.92	19.68	-
2,3,3-Trimethylpentane	114	C_8H_{18}	4.02	14.22	-
2,3-Dimethylhexane	114	C_8H_{18}	4.11	9.73	-
2-Methylheptane	114	C_8H_{18}	4.22	21.50	-
Toluene	92	C_7H_8	4.31	103.69	138.22
3-Methylheptane	114	C_8H_{18}	4.37	21.92	-
cis-1,3-Dimethylcyclohexane	112	C_8H_{16}	4.49	6.27	-
2,2,4-Trimethylhexane	128	C_9H_{20}	4.55	7.25	-
Ethylcyclohexane	112	C_8H_{16}	4.69	3.27	-
Octane	114	C_8H_{18}	4.93	17.64	-
1,4-Dimethylcyclohexane	112	C_8H_{16}	5.07	4.13	0.83
1,2,3-Trimethylcyclopentene	110	C_8H_{14}	5.18	3.21	1.02

2,3-Dimethylheptane	128	C_9H_{20}	5.28	1.85	0.60
3-Ethylhexane	114	C_8H_{18}	5.45	3.39	6.51
2-Methyloctane	128	C_9H_{20}	5.6	4.00	-
3,5-Dimethylheptane	128	C_9H_{20}	5.76	9.34	1.07
1,2,4-Trimethylcyclohexane	126	C_9H_{18}	6.18	1.68	-
3-Ethyl-2,4-dimethylpentane	128	C_9H_{20}	6.3	2.66	-
Ethylbenzene	106	C_8H_{10}	6.49	48.49	18.11
p-Xylene	106	C_8H_{10}	6.71	129.08	91.79
2,2,3-Trimethyldecane	184	$C_{13}H_{28}$	6.86	3.11	-
2,2-Dimethyloctane	142	$C_{10}H_{22}$	7.05	4.00	-
Cis-1-ethyl-2-methyl-Cyclohexane,	126	C_9H_{18}	7.14	2.54	-
o-Xylene	106	C_8H_{10}	7.34	49.38	34.56
Nonane	128	C_9H_{20}	7.47	9.35	4.61
1-ethyl-2-methyl-Cyclohexane	128	C_9H_{20}	7.67	2.19	-
2,3-Dimethyloctane	142	$C_{10}H_{22}$	7.91	1.70	-
2,4,6-Trimethylheptane	142	$C_{10}H_{22}$	7.96	1.33	-
4-Methylnonane	142	$C_{10}H_{22}$	8.18	2.14	-
Cumene	120	C_9H_{12}	8.22	3.41	-
2,6-Dimethyloctane	142	$C_{10}H_{22}$	8.43	3.73	-
2-Butyloctanol	186	$C_{12}H_{26}O$	8.6	1.63	-
3-Ethyl-2-methylheptane	142	$C_{10}H_{22}$	8.65	0.91	
Propylbenzene	120	C_9H_{12}	9.07	15.00	2.84
2,2,6-Trimethyloctane	156	$C_{11}H_{24}$	9.21	9.50	-
1-ethyl-3-methyl-Benzene	120	C_9H_{12}	9.3	64.52	18.83
1-ethyl-4-methyl- Benzene	120	C_9H_{12}	9.5	26.55	11.26
1-ethyl-2-methyl- Benzene	120	C_9H_{12}	9.84	16.27	3.92
5-Decene	140	$C_{10}H_{20}$	10.04	-	4.62
Mesitylene	120	C_9H_{12}	10.25	63.98	28.58
Decane	142	$C_{10}H_{22}$	10.39	6.14	3.56
Isobutylbenzene	134	$C_{10}H_{14}$	10.65	1.25	-
Sec-butylbenzene	134	$C_{10}H_{14}$	10.75	1.84	-
1,2,4-Trimethylbenzene	120	C_9H_{12}	11.11	17.86	5.40
Allylbenzene	118	C_9H_{10}	11.42	2.02	-
Indane	118	C_9H_{10}	11.52	7.15	1.41
1,3-Diethylbenzene	134	$C_{10}H_{14}$	11.92	3.75	0.99

1-Methyl-3-propylbenzene	134	$C_{10}H_{14}$	11.97	12.38	1.69
4-methylene-1-(1-methylethyl)-Bicyclo[3.1.0]hex-2-ene	134	$C_{10}H_{14}$	12.11	9.98	1.96
2-Ethyl-p-xylene	134	$C_{10}H_{14}$	12.19	12.22	3.29
2-Methyldecane	156	$C_{11}H_{24}$	12.3	4.04	-
1-Methyl-2-propylbenzene	134	$C_{10}H_{14}$	12.44	3.05	0.53
3-Methyldecane	156	$C_{11}H_{24}$	12.5	1.90	0.43
1-Ethyl-2,4-dimethylbenzene	134	$C_{10}H_{14}$	12.75	6.58	1.83
4-ethyl-1,2-dimethyl-Benzene	134	$C_{10}H_{14}$	12.8	5.60	1.54
4-Allyltoluene	132	$C_{10}H_{12}$	12.87	0.99	-
p-Cymene	134	$C_{10}H_{14}$	12.99	13.78	2.85
O-Cymene	134	$C_{10}H_{14}$	13.2	0.70	0.69
Undecane	156	$C_{11}H_{24}$	13.38	3.15	3.59
1-methyl-4-(2-methylpropyl)-Benzene	148	$C_{11}H_{16}$	13.46	0.86	-
(1,1-dimethylpropyl)- Benzene	148	$C_{11}H_{16}$	13.55	0.91	0.52
1-Ethyl-3,5-dimethylbenzene	134	$C_{10}H_{14}$	13.63	2.30	1.43
trans-4a-Methyl-decahydronaphthalene	152	$C_{11}H_{20}$	13.72	0.52	-
1,2,3,4-Tetramethylbenzene,	134	$C_{10}H_{14}$	13.90	-	2.29
1,2,4,5-Tetramethylbenzene	134	$C_{10}H_{14}$	14.04	9.34	2.90
3,7-Dimethyldecane	170	$C_{12}H_{26}$	14.18	0.69	-
1-Methyl-4-(1-methylpropyl)-benzene	148	$C_{11}H_{16}$	14.52	1.71	-
5-Methylindan	132	$C_{10}H_{12}$	14.60	4.01	-
1,3-Diethyl-4-methylbenzene	148	$C_{11}H_{16}$	14.71	1.52	-
3,5-Diethyltoluene	148	$C_{11}H_{16}$	14.75	2.18	-
1-Methylindan	132	$C_{10}H_{12}$	14.93	5.06	1.39
1,4-Diethylbenzene	132	$C_{10}H_{12}$	14.98	4.55	1.65
Isopentylbenzene	148	$C_{11}H_{16}$	15.12	2.20	-
2,4-dimethyl-1-(1-methylethyl)-Benzene	148	$C_{11}H_{16}$	15.28	3.08	-
1,4-Diethyl-2-methylbenzene	148	$C_{11}H_{16}$	15.36	0.76	-
3-Methylundecane	170	$C_{12}H_{26}$	15.45	0.98	-

1-methyl-4-(1-methyl-2-propenyl)-Benzene	146	$C_{11}H_{14}$	15.87	0.59	-
1-methylene-1H-Indene	128	$C_{10}H_{8}$	15.94	6.45	14.79
1,1-Dimethylindan	146	$C_{11}H_{14}$	16.00	1.79	-
2,3-dihydro-2,2-Dimethylindene	146	$C_{11}H_{14}$	16.07	0.95	0.87
3,4-Dimethylcumene	148	$C_{11}H_{16}$	16.30	3.68	3.67
4,7-Dimethylindan	146	$C_{11}H_{14}$	17.78	2.42	0.97
1,6-Dimethylindan	146	$C_{11}H_{14}$	18.17	1.04	-
2-methyl- Naphthalene	142	$C_{11}H_{10}$	19.05	6.92	8.17
1-methyl-Naphthalene	142	$C_{11}H_{10}$	19.51	2.94	19.09
1,13-Tetradecadiene	194	$C_{14}H_{26}$	21.32	-	0.42
1-Tetradecene	196	$C_{14}H_{28}$	21.50	-	0.96
2-ethyl-Naphthalene	156	$C_{12}H_{12}$	21.71	0.68	3.34
2,6-dimethyl-Naphthalene	156	$C_{12}H_{12}$	21.97	0.84	4.634
1,7-dimethyl-Naphthalene	156	$C_{12}H_{12}$	22.35	0.91	4.84
1,5-dimethyl-Naphthalene	156	$C_{12}H_{12}$	22.44	0.45	2.21
1,3-dimethyl-Naphthalene	156	$C_{12}H_{12}$	22.84	-	1.98
2,7-dimethyl-Naphthalene	156	$C_{12}H_{12}$	22.93	-	0.53
1-Pentadecyne	208	$C_{15}H_{28}$	23.24	-	0.82
1-Pentadecene	210	$C_{15}H_{30}$	24.01	-	1.16
Pentadecane	212	$C_{15}H_{32}$	24.20	-	2.35
2-(1-methylethyl)-Naphthalene	170	$C_{13}H_{14}$	24.44	-	0.48
2,3,6-trimethyl-Naphthalene	170	$C_{13}H_{14}$	25.09	-	0.84
1,4,5-trimethyl-Naphthalene	170	$C_{13}H_{14}$	25.47	-	0.72
1,6,7-trimethyl-Naphthalene	170	$C_{13}H_{14}$	25.55	-	0.58
1,4,6-trimethyl-Naphthalene	170	$C_{13}H_{14}$	25.88	-	0.73
1-Hexadecene	224	$C_{16}H_{32}$	26.39	-	0.83
Hexadecane	226	$C_{16}H_{34}$	26.56	-	1.96
1-Heptadecene	238	$C_{17}H_{34}$	28.65	-	0.76
Heptadecane	240	$C_{17}H_{36}$	28.8	-	1.95
1-Octadecene	252	$C_{18}H_{36}$	30.74	-	1.29
Octadecane	254	$C_{18}H_{38}$	30.94	-	1.58

Positive ion ESI-MS was performed on the MPW pyrolysis products (Figure 3.6) to determine the M_n and M_w distribution of compounds (Table 3.5). ESI-MS would allow the

observation of products (higher chain length) than that obtained by GCMS. For pyrolysis of MPW, $[M+H]^+$ peaks for alkanes were found at C_8 (m/z= 115) to C_{40} (m/z = 563), as well as hydrocarbon dienes from C_8 (m/z= 111) to C_{40} (m/z = 559) and alkenes from C_8 (m/z= 113) to C_{40} (m/z = 561). Due to the complexity of the MS full analysis was not performed. The M_w of MPW decreased from 1000 to 768 g/mol as pyrolysis temperature increased from 500 to 600 ^oC, as expected. An arbitrary range of (Σ *m/z* 100-300) for monomers and (Σ *m/z* 301-2000) for oligomers was chosen arbitrarily to show low and high molar mass which were used in calculating ion intensities [174]. At 500^oC, pyrolyzed MPW had a monomer/oligomer ratio of 0.19 and increased to 0.34 at 600^oC due to the scission of longer molecules into smaller fragments.

For catalytic pyrolysis, $M+H]^+$ peaks were observed for substituted benzene (e.g., *m/z*=107 (xylene, C_8)) alkanes (e.g., *m/z*=115 (octane, C_8), m/*z*=255 (octadecane, C_{18})) and alkenes (e.g. *m/z*=113 (octene, C_8), and m/*z*=253 (octadecene, C_{18})). There was a sharp decrease in M_w (355 g/mol) and M_n (690 g/mol) after the use of zeolite Y to pyrolyze MPW which was similar to that reported by Sotodehnia et al. [173].

Table 3.5 Weight (M_w) and number average molar mass (M_n) and monomer/oligomer ratio of MPW pyrolysis oil

Temperature	M_n (g/mol)	M_w (g/mol)	Monomer/Oligomer
pyrolysis 500^0C	728	1000	0.19
pyrolysis 550^0C	685	971	0.23
pyrolysis 600^0C	534	768	0.34
Catalytic pyrolysis 600^0C	355	690	1.94

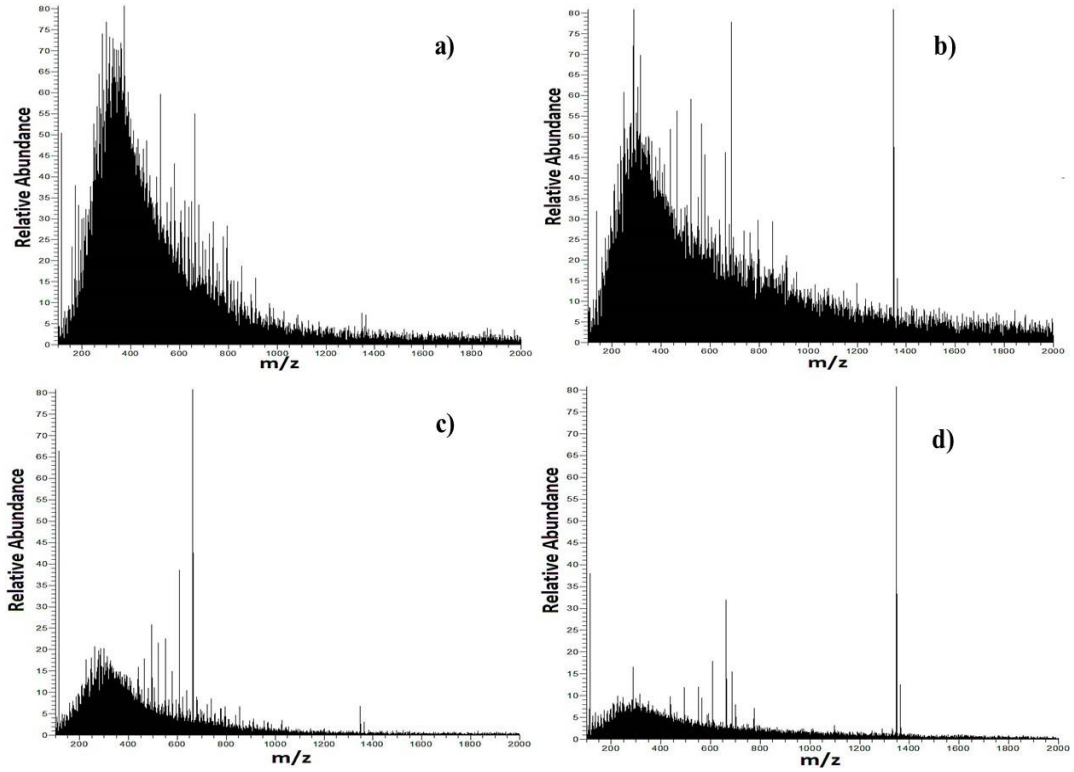

Figure 3.6 Positive-ion ESI-MS spectra of products of MPW pyrolysis at (a) 500°C, (b) 550°C, (c) 600°C, and (d) catalytic pyrolysis at 600°C.

3.4.4 Char characterization

The MPW and char products from the pyrolysis and catalytic pyrolysis of MPW were analyzed for chemical groups by FTIR spectroscopy (Figure 3.7). The extruded MPW exhibits an O-H stretching band at 3296 cm^{-1} which indicates the presence of a hydroxyl group in cellulosic material. After pyrolysis the O-H band was absent indicating dehydration reactions occurred as seen by Xu et al. in torrefaction of MPW [200]. Bands at 1464, 1376, and 1161 cm^{-1} were assigned to C-H stretching bands of $-CH_2$, $-CH_3$, and CH groups, respectively, and distinctive of propylene [144]. The prominent C-H stretching vibrations at 2915 and 2848 cm^{-1} of MPW can be attributed to the methylene family in PE, PP and PEVA [142][143]. The presence of PEVA was confirmed by the presence of absorption bands at 1464, 1019, and 719 cm^{-1}. The existence of carbonyl groups (C=O) represented by bands

between 1700–1750 cm^{-1} indicates the presence of ester and amide which are associated to PET/PEVA and nylon, respectively [145].

There was a clear difference between char obtained from pyrolysis at 500^0C versus 550 and 600°C. The absorbance band at 1022 cm^{-1} in char (500°C) was assigned to C-O stretching in cellulose [201] and its intensity creased at higher pyrolysis temperatures. The bands at 1601 and 1503 cm^{-1} for char produced at 500°C were assigned to aromatic skeletal stretching associated with PET [173] and lignin [202] and these decreased as pyrolysis temperature increased. The most dominant band for the chars was at 1435 cm^{-1}, which is associated with aromatic C=C ring stretching [201]. This char band shifted to 1445 cm^{-1} from catalytic pyrolysis. The band at 874 cm^{-1} (C-H) was assigned to an aromatic hydrogen and its intensity increased with pyrolysis temperature which is associated with the formation of polyaromatic structures. The bands at 1371, 1307 (C-C stretching), 1149, and 1098 cm^{-1} (C-C stretching) found in the 500°C char were absent at the higher pyrolysis temperatures probably suggesting further thermal decomposition of MPW to a condensed structure.

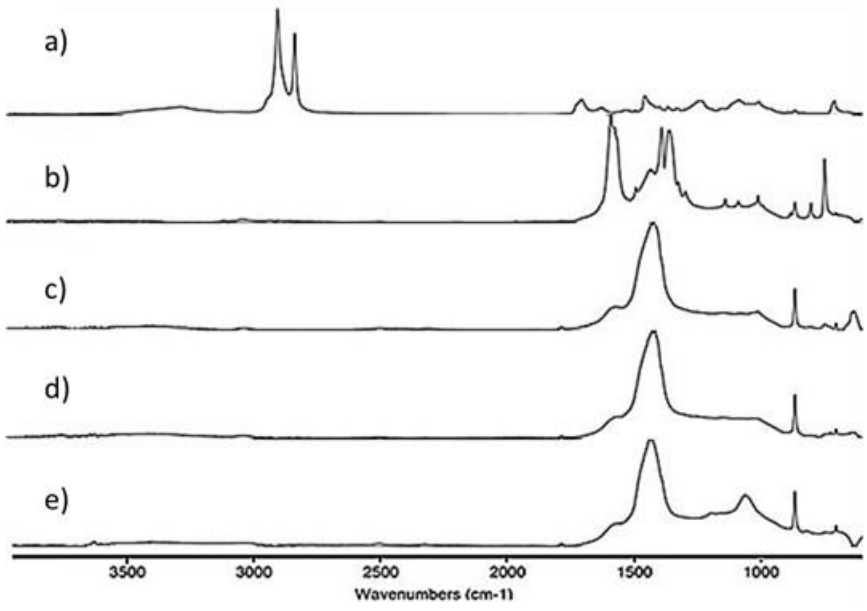

Figure 3.7 FTIR spectra of (a) extruded MPW, MPW pyrolysis char at (b) 500^0C, (c) 550^0C, (d) 600^0C, and (e) catalytic pyrolysis at 600^0C

Chapter 4: Conclusion and future recommendation

4.1 Conclusion

This research has demonstrated different ways to upcycle MPW and fiber into value added products. This process began with successfully compounding MPW and its fiber components into a homogeneous mixture, followed by its characterization. The predominant plastics in the extruded MPW were identified to be PP, PET, PEVA and PE through FTIR analysis and DSC.

For mechanical recycling, MPW was used in the formulation of composite and the influence of different coupling agents and hops fiber on the composite were investigated. Coupling agents did not significantly increase the interaction between these various polymers and fibers. The use of 0.5% DCP cross-linking was shown to decrease the performance of MPW due to chain scission. The use of lower concentration of DCP could limit the extent of chain scission versus long chain branching reactions. On the other hand, the addition of 10% HF improved the tensile properties of MPW by enhanced fiber-polymer interactions hence better mechanical properties.

The rheology data from the experiments generally showed a decrease in complex viscosity with an increase in frequent. Compared to HDPE and PP, MPW had a higher complex viscosity. This increase was further amplified following the addition of HF. MPWHF+DCP showed the highest change in complex viscosity probably due to chain branching. The use of coupling agents increased the viscosity of MPW because of increased fiber-matrix interaction however DCP reduced viscosity. A 32% increase in viscosity was observed upon HF addition into the MPW melt. Hops fiber alone did not increase the storage modulus of MPW however using MAPE and GMPE led to a better energy transfer between the fibers and matrix as bending took place hence the observed increase in storage modulus.

The water absorption experiment as expected showed a positive relationship between fiber content and water absorption (WA). The use of MAPE and GMPE did not change WA values significantly at day 83. Formulations without Hops fiber are expected to consume less water compared to formulations with hops following same amount of exposure. Formulations with DCP had the highest water absorption.

The chemical recycling of MPW via pyrolysis in a tube reactor (500-600^{0}C) was successful in obtaining a liquid/wax product. The highest wax-oil yield produced was at 500^{0}C, while the highest gas yield was achieved at 600^{0}C. The wax-oil pyrolysis product was comprised mainly of a series of alkanes, alkenes, and dienes because of thermal chain scission of the polyolefin plastics. the hydrocarbon chain length was shown to decrease with pyrolysis temperature. The wax-oil products also contained oxygenated compounds and aromatics. The pyrolysis oil obtained from MPW pyrolysis could be a useful feedstock for use in a petrochemical refinery to produce fuels and chemicals.

Catalytic pyrolysis of MPW at 600^{0}C with zeolite Y was successful in producing a liquid product containing mainly aromatics and some light hydrocarbons. The liquid product contained some essential compounds found in gasoline like methyl benzenes, propylbenzene, hexane, etc. Catalytic pyrolysis of MPW is a potentially viable approach to produce transportation fuels in small-distributed facilities.

4.2 Future recommendation

Following the use of 0.5% DCP as a cross linker, the issue of scission experienced might be addressed using lower amount of DCP. The use of other chain extenders will be explored. For pyrolysis of MPW, to obtain a better fuel quality through catalytic pyrolysis, an increase in reaction temperature or amount of catalyst might be necessary to further breakdown the few long chain hydrocarbon that was still present in the liquid product after thermolysis at 600^{0}C. Catalyst reuse will be explored to help reduce cost involved in catalytic pyrolysis.

Chapter 5: References

[1] E. Amasuomo and J. Baird, "The Concept of Waste and Waste Management," *Journal of Management and Sustainability*, vol. 6, no. 4, p. 88, 2016, doi: 10.5539/jms.v6n4p88.

[2] United Nations Economic and Social Commission for Asia and the Pacific, "Chapter 8 Types of wastes," *United Nations ESCAP Library*, pp. 170–194, 2002, [Online]. Available: http://www.unescap.org/sites/default/files/CH08.PDF.

[3] K. D. Sharma and S. Jain, "Municipal solid waste generation, composition, and management: the global scenario," *Social Responsibility Journal*, vol. 16, no. 6, pp. 917–948, 2020, doi: 10.1108/SRJ-06-2019-0210.

[4] D. C. Wilson, "Development drivers for waste management," *Waste Management and Research*, vol. 25, no. 3, pp. 198–207, 2007, doi: 10.1177/0734242X07079149.

[5] K. Laohalidanond, P. Chaiyawong, and S. Kerdsuwan, *Municipal Solid Waste Characteristics and Green and Clean Energy Recovery in Asian Megacities*, vol. 79. Elsevier B.V., 2015. doi: 10.1016/j.egypro.2015.11.508.

[6] C. C. Nnaji, "Status of municipal solid waste generation and disposal in Nigeria," *Management of Environmental Quality: An International Journal*, vol. 26, no. 1, pp. 53–71, 2015, doi: 10.1108/MEQ-08-2013-0092.

[7] "Population Clock." https://www.census.gov/popclock/ (accessed Sep. 27, 2021).

[8] E. K. Orhorhoro and O. Oghoghorie, "Review on Solid Waste Generation and Management in Sub-Saharan Africa: A Case Study of Nigeria," *Journal of Applied Sciences and Environmental Management*, vol. 23, no. 9, p. 1729, 2019, doi: 10.4314/jasem.v23i9.19.

[9] S. Kumar *et al.*, "Challenges and opportunities associated with waste management in India," *Royal Society Open Science*, vol. 4, no. 3, 2017, doi: 10.1098/rsos.160764.

[10] L. Lebreton and A. Andrady, "Future scenarios of global plastic waste generation and disposal," *Palgrave Communications*, vol. 5, no. 1, pp. 1–11, 2019, doi: 10.1057/s41599-018-0212-7.

[11] "Report on the Environment (ROE) | US EPA." https://cfpub.epa.gov/roe/indicator.cfm?i=53 (accessed Dec. 07, 2020).

[12] A. E. Adeniran, A. T. Nubi, and A. O. Adelopo, "Solid waste generation and characterization in the University of Lagos for a sustainable waste management," *Waste Management*, vol. 67, pp. 3–10, 2017, doi: 10.1016/j.wasman.2017.05.002.

[13] O. O. Ayeleru, F. N. Okonta, and F. Ntuli, "Municipal solid waste generation and characterization in the City of Johannesburg: A pathway for the implementation of zero waste," *Waste Management*, vol. 79, pp. 87–97, 2018, doi: 10.1016/j.wasman.2018.07.026.

[14] N. Scarlat, V. Motola, J. F. Dallemand, F. Monforti-Ferrario, and L. Mofor, "Evaluation of energy potential of Municipal Solid Waste from African urban areas," *Renewable and Sustainable Energy Reviews*, vol. 50, pp. 1269–1286, 2015, doi: 10.1016/j.rser.2015.05.067.

[15] P. J. Sachi and E. A. Mensah, "Household characteristics and waste generation paradox: what influences solid waste generation in Bolgatanga," *International Journal of Environment and Waste Management*, vol. 26, no. 2, p. 212, 2020, doi: 10.1504/ijewm.2020.108815.

[16] "National Overview: Facts and Figures on Materials, Wastes and Recycling | US EPA." https://www.epa.gov/facts-and-figures-about-materials-waste-and-recycling/national-overview-facts-and-figures-materials (accessed Sep. 28, 2021).

[17] C. J. Rhodes, "Plastic pollution and potential solutions," *Science progress*, vol. 101, no. 3, pp. 207–260, 2018, doi: 10.3184/003685018X15294876706211.

[18] S. D. Anuar Sharuddin, F. Abnisa, W. M. A. Wan Daud, and M. K. Aroua, "A review on pyrolysis of plastic wastes," *Energy Conversion and Management*, vol. 115, pp. 308–326, 2016, doi: 10.1016/j.enconman.2016.02.037.

[19] D. Almeida and M. de Fátima Marques, "Thermal and catalytic pyrolysis of plastic waste," *Polimeros*, vol. 26, no. 1, pp. 44–51, 2016, doi: 10.1590/0104-1428.2100.

[20] S. M. Al-Salem, A. Antelava, A. Constantinou, G. Manos, and A. Dutta, "A review on thermal and catalytic pyrolysis of plastic solid waste (PSW)," *Journal of Environmental Management*, vol. 197, no. 1408, pp. 177–198, 2017, doi: 10.1016/j.jenvman.2017.03.084.

[21] M. Liboiron, "Redefining pollution and action: The matter of plastics," *Journal of Material Culture*, vol. 21, no. 1, pp. 87–110, 2016, doi: 10.1177/1359183515622966.

[22] H. N. Dhakal and S. O. Ismail, “Introduction to composite materials,” *Sustainable Composites for Lightweight Applications*, pp. 1–16, Jan. 2021, doi: 10.1016/B978-0-12-818316-8.00001-3.

[23] B. O. Orji, A. G. Mcdonald, D. E. Committee, M. Aston, and P. E. Maughan, “EVALUATION OF THE THERMAL, MECHANICAL AND RHEOLOGICAL PROPERTIES OF RECYCLED POLYOLEFINS RICE HULL COMPOSITES”.

[24] S. R. Malkan, “Improving the use of polyolefins in nonwovens,” *Polyolefin Fibres: Structure, Properties and Industrial Applications: Second Edition*, pp. 285–311, Jan. 2017, doi: 10.1016/B978-0-08-101132-4.00009-6.

[25] J. B. P. (João B. P.) Soares and T. F. (Timothy F.) McKenna, “Polyolefin reaction engineering,” p. 328, 2012.

[26] A. J. Peacock and A. Calhoun, “[Allison Calhoun Andrew J Peacock_Polymer Chemistry_Properties and Applications (Bookos.org).pdf.” p. 422, 2012.

[27] O. Agboola, R. Sadiku, T. Mokrani, I. Amer, and O. Imoru, “Polyolefins and the environment,” *Polyolefin Fibres: Structure, Properties and Industrial Applications: Second Edition*, pp. 89–133, Jan. 2017, doi: 10.1016/B978-0-08-101132-4.00004-7.

[28] N. Z. Tomić and A. D. Marinković, “Compatibilization of polymer blends by the addition of graft copolymers,” *Compatibilization of Polymer Blends: Micro and Nano Scale Phase Morphologies, Interphase Characterization, and Properties*, pp. 103–144, Jan. 2020, doi: 10.1016/B978-0-12-816006-0.00004-9.

[29] Clive. Maier and Teresa. Calafut, “Polypropylene : the definitive user’s guide and databook,” p. 432, 1998.

[30] C. B. Crawford and B. Quinn, “Physiochemical properties and degradation,” *Microplastic Pollutants*, pp. 57–100, Jan. 2017, doi: 10.1016/B978-0-12-809406-8.00004-9.

[31] Y. K. Kim, “5 - The use of polyolefins in industrial and medical applications A2 - Ugbolue, Samuel C.O. BT - Polyolefin Fibres (Second Edition),” *The Textile Institute Book Series*, pp. 135–155, 2017, Accessed: Oct. 19, 2021. [Online]. Available: https://www.sciencedirect.com/science/article/pii/B9780081011324000059

[32] S. R. Malkan, “Improving the use of polyolefins in nonwovens,” *Polyolefin Fibres: Structure, Properties and Industrial Applications: Second Edition*, pp. 285–311, Jan. 2017, doi: 10.1016/B978-0-08-101132-4.00009-6.

[33] G. L. Robertson, “Food Packaging,” *Encyclopedia of Agriculture and Food Systems*, pp. 232–249, Jan. 2014, doi: 10.1016/B978-0-444-52512-3.00063-2.

[34] W. Zeng, Y. Li, Y. Wang, and Y. Cao, “Tissue Engineering of Blood Vessels,” *Encyclopedia of Tissue Engineering and Regenerative Medicine*, vol. 1–3, pp. 413–424, Jan. 2019, doi: 10.1016/B978-0-12-801238-3.65848-8.

[35] C. B. Crawford and B. Quinn, “Physiochemical properties and degradation,” *Microplastic Pollutants*, pp. 57–100, Jan. 2017, doi: 10.1016/B978-0-12-809406-8.00004-9.

[36] M. Sigler, “The effects of plastic pollution on aquatic wildlife: Current situations and future solutions,” *Water, Air, and Soil Pollution*, vol. 225, no. 11, 2014, doi: 10.1007/s11270-014-2184-6.

[37] S. L. Wright, R. C. Thompson, and T. S. Galloway, “The physical impacts of microplastics on marine organisms: a review.,” *Environmental pollution (Barking, Essex : 1987)*, vol. 178, pp. 483–492, 2013, doi: 10.1016/j.envpol.2013.02.031.

[38] Y. Chae and Y. J. An, “Current research trends on plastic pollution and ecological impacts on the soil ecosystem: A review,” *Environmental Pollution*, vol. 240, pp. 387–395, 2018, doi: 10.1016/j.envpol.2018.05.008.

[39] S. I. Pathan, P. Arfaioli, T. Bardelli, M. T. Ceccherini, P. Nannipieri, and G. Pietramellara, “Soil pollution from micro-and nanoplastic debris: A hidden and unknown biohazard,” *Sustainability (Switzerland)*, vol. 12, no. 18, pp. 1–31, 2020, doi: 10.3390/su12187255.

[40] M. C. Rillig, R. Ingraffia, and A. A. de Souza Machado, “Microplastic incorporation into soil in agroecosystems,” *Frontiers in Plant Science*, vol. 8, no. October, pp. 8–11, 2017, doi: 10.3389/fpls.2017.01805.

[41] S. Maaß, D. Daphi, A. Lehmann, and M. C. Rillig, “Transport of microplastics by two collembolan species,” *Environmental Pollution*, vol. 225, pp. 456–459, 2017, doi: 10.1016/j.envpol.2017.03.009.

[42] "Where Are the Pacific Garbage Patches? | response.restoration.noaa.gov." https://response.restoration.noaa.gov/about/media/where-are-pacific-garbage-patches.html (accessed Oct. 27, 2020).

[43] N. A. Welden, *The environmental impacts of plastic pollution*. Elsevier Inc., 2020. doi: 10.1016/b978-0-12-817880-5.00008-6.

[44] K. L. Law, "Plastics in the Marine Environment," *Annual Review of Marine Science*, vol. 9, no. 1, pp. 205–229, 2017, doi: 10.1146/annurev-marine-010816-060409.

[45] A. R. Rahimi and J. M. Garciá, "Chemical recycling of waste plastics for new materials production," *Nature Reviews Chemistry*, vol. 1, pp. 1–11, 2017, doi: 10.1038/s41570-017-0046.

[46] R. Siddique, J. Khatib, and I. Kaur, "Use of recycled plastic in concrete: A review," *Waste Management*, vol. 28, no. 10, pp. 1835–1852, 2008, doi: 10.1016/j.wasman.2007.09.011.

[47] "Sustainable Materials Management: Non-Hazardous Materials and Waste Management Hierarchy | Sustainable Materials Management | US EPA." https://www.epa.gov/smm/sustainable-materials-management-non-hazardous-materials-and-waste-management-hierarchy (accessed Dec. 08, 2020).

[48] "Waste Management Hierarchy and Homeland Security Incidents | Managing Materials and Wastes for Homeland Security Incidents | US EPA." https://www.epa.gov/homeland-security-waste/waste-management-hierarchy-and-homeland-security-incidents (accessed Dec. 08, 2020).

[49] D. J. Gardner, Y. Han, and L. Wang, "Wood–Plastic composite technology," *Current Forestry Reports*, vol. 1, no. 3, pp. 139–150, 2015, doi: 10.1007/s40725-015-0016-6.

[50] PlasticsEurope AISBL, "Plastics convert iron ore to steel Feedstock recycling in blast furnaces," *Plastics Europe*, pp. 1–8, 2009.

[51] U. Arena, "Process and technological aspects of municipal solid waste gasification. A review," *Waste Management*, vol. 32, no. 4, pp. 625–639, 2012, doi: 10.1016/j.wasman.2011.09.025.

[52] M. V. Reddy, "Municipal solid waste -waste to energy conversion in India: An overview," *International Journal of Environmental Technology and Management*, vol. 17, no. 2–4, pp. 283–292, 2014, doi: 10.1504/IJETM.2014.061799.

[53] “Climate change: China bans import of foreign waste to stop pollution.” https://www.cnbc.com/2018/04/16/climate-change-china-bans-import-of-foreign-waste-to-stop-pollution.html (accessed Sep. 30, 2021).

[54] S. Kolapkar, “Digital Commons @ Michigan Tech Pyrolysis of Fiber-Plastic Waste Blends,” no. January 2018, 2018, [Online]. Available: https://digitalcommons.mtu.edu/cgi/viewcontent.cgi?article=1777&context=etdr

[55] R. Thahir, A. Altway, S. R. Juliastuti, and Susianto, “Production of liquid fuel from plastic waste using integrated pyrolysis method with refinery distillation bubble cap plate column,” *Energy Reports*, vol. 5, pp. 70–77, 2019, doi: 10.1016/j.egyr.2018.11.004.

[56] H. Bockhorn, J. Hentschel, A. Hornung, and U. Hornung, “Environmental engineering: Stepwise pyrolysis of plastic waste,” *Chemical Engineering Science*, vol. 54, no. 15–16, pp. 3043–3051, 1999, doi: 10.1016/S0009-2509(98)00385-6.

[57] H. Bockhorn, A. Hornung, and U. Hornung, “Stepwise pyrolysis for raw material recovery from plastic waste,” *Journal of Analytical and Applied Pyrolysis*, vol. 46, no. 1, pp. 1–13, 1998, doi: 10.1016/S0165-2370(98)00066-7.

[58] G. López, M. Olazar, M. Artetxe, M. Amutio, G. Elordi, and J. Bilbao, “Steam activation of pyrolytic tyre char at different temperatures,” *Journal of Analytical and Applied Pyrolysis*, vol. 85, no. 1–2, pp. 539–543, 2009, doi: 10.1016/j.jaap.2008.11.002.

[59] R. Miandad *et al.*, “Catalytic pyrolysis of plastic waste: Moving toward pyrolysis based biorefineries,” *Frontiers in Energy Research*, vol. 7, no. MAR, pp. 1–17, 2019, doi: 10.3389/fenrg.2019.00027.

[60] F. Sotoudehniakarani and A. G. Mcdonald, “Production and Characterization of Bio-Oil and Biochar from Fast Pyrolysis of Micro-Algae Chlorella vulgaris,” 2017.

[61] J. Aguado, D. P. Serrano, and J. M. Escola, *Catalytic Upgrading of Plastic Wastes*. 2006. doi: 10.1002/0470021543.ch3.

[62] A. Buekens, *Introduction to Feedstock Recycling of Plastics*. 2006. doi: 10.1002/0470021543.ch1.

[63] T. Itoh *et al.*, “Effects of pyrolysis temperature and feedstock type on particulate matter emission characteristics during biochar combustion,” *Fuel Processing Technology*, vol. 204, no. February, p. 106408, 2020, doi: 10.1016/j.fuproc.2020.106408.

[64] N. Kiran, E. Ekinci, and C. E. Snape, “00/03732 Recycling of plastic wastes via pyrolysis,” *Fuel and Energy Abstracts*, vol. 41, no. 6, pp. 417–418, 2000, doi: 10.1016/s0140-6701(00)94792-1.

[65] V. I. Sharypov *et al.*, “Co-pyrolysis of wood biomass and synthetic polymer mixtures. Part I: Influence of experimental conditions on the evolution of solids, liquids and gases,” *Journal of Analytical and Applied Pyrolysis*, vol. 64, no. 1, pp. 15–28, 2002, doi: 10.1016/S0165-2370(01)00167-X.

[66] S. M. Al-Salem and P. Lettieri, “Kinetic study of high density polyethylene (HDPE) pyrolysis,” *Chemical Engineering Research and Design*, vol. 88, no. 12, pp. 1599–1606, 2010, doi: 10.1016/j.cherd.2010.03.012.

[67] S. Kumar and R. K. Singh, “Recovery of hydrocarbon liquid from waste high density polyethylene by thermal pyrolysis,” *Brazilian Journal of Chemical Engineering*, vol. 28, no. 4, pp. 659–667, 2011, doi: 10.1590/S0104-66322011000400011.

[68] D. K. Ratnasari, M. A. Nahil, and P. T. Williams, “Catalytic pyrolysis of waste plastics using staged catalysis for production of gasoline range hydrocarbon oils,” *Journal of Analytical and Applied Pyrolysis*, vol. 124, pp. 631–637, Mar. 2017, doi: 10.1016/J.JAAP.2016.12.027.

[69] D. P. Serrano, J. Aguado, and J. M. Escola, “Developing Advanced Catalysts for the Conversion of Polyolefinic Waste Plastics into Fuels and Chemicals,” *ACS Catalysis*, vol. 2, no. 9, pp. 1924–1941, Sep. 2012, doi: 10.1021/CS3003403.

[70] R. Miandad *et al.*, “Catalytic Pyrolysis of Plastic Waste: Moving Toward Pyrolysis Based Biorefineries,” *Frontiers in Energy Research*, vol. 0, no. MAR, p. 27, 2019, doi: 10.3389/FENRG.2019.00027.

[71] * Yoshio Uemichi, Masahiko Hattori, Toshihiro Itoh, and Junko Nakamura, and M. Sugioka, “Deactivation Behaviors of Zeolite and Silica−Alumina Catalysts in the Degradation of Polyethylene,” *Industrial and Engineering Chemistry Research*, vol. 37, no. 3, pp. 867–872, 1998, doi: 10.1021/IE970605C.

[72] * J. Aguado, J. L. Sotelo, D. P. Serrano, and J. A. Calles, and J. M. Escola, “Catalytic Conversion of Polyolefins into Liquid Fuels over MCM-41: Comparison with ZSM-5 and Amorphous SiO2−Al2O3,” *Energy and Fuels*, vol. 11, no. 6, pp. 1225–1230, 1997, doi: 10.1021/EF970055V.

[73] A. López, I. de Marco, B. M. Caballero, M. F. Laresgoiti, and A. Adrados, “Influence of time and temperature on pyrolysis of plastic wastes in a semi-batch reactor,” *Chemical Engineering Journal*, vol. 173, no. 1, pp. 62–71, 2011, doi: 10.1016/j.cej.2011.07.037.

[74] B. L. F. Chin, S. Yusup, A. al Shoaibi, P. Kannan, C. Srinivasakannan, and S. A. Sulaiman, “Kinetic studies of co-pyrolysis of rubber seed shell with high density polyethylene,” *Energy Conversion and Management*, vol. 87, pp. 746–753, 2014, doi: 10.1016/j.enconman.2014.07.043.

[75] U. Arena and M. L. Mastellone, *Fluidized Bed Pyrolysis of Plastic Wastes*. 2006. doi: 10.1002/0470021543.ch16.

[76] K. Murata, K. Sato, and Y. Sakata, “Effect of pressure on thermal degradation of polyethylene,” *Journal of Analytical and Applied Pyrolysis*, vol. 71, no. 2, pp. 569–589, 2004, doi: 10.1016/j.jaap.2003.08.010.

[77] M. J. Mclntosh, G. G. Arzoumanidis, and F. E. Brockmeier, “Environmental Progress & Sustainable Energy Volume 17 issue 1 1998 [doi 10.1002%2Fep.670170114] Michael J. McIntosh; Gregory G. Arzoumanidis; Frederick E. Brock -- Recovery of fuels and chemicals thro.pdf,” no. 1, pp. 19–23, 1998.

[78] Y. H. Seo, K. H. Lee, and D. H. Shin, “Investigation of catalytic degradation of high-density polyethylene by hydrocarbon group type analysis,” *Journal of Analytical and Applied Pyrolysis*, vol. 70, no. 2, pp. 383–398, 2003, doi: 10.1016/S0165-2370(02)00186-9.

[79] C. Chemistry, “I. natural fiber-polyolefin composites. mini-review,” vol. 48, pp. 599–611, 2014.

[80] S. Yin, R. Tuladhar, F. Shi, M. Combe, T. Collister, and N. Sivakugan, “Use of macro plastic fibres in concrete: A review,” *Construction and Building Materials*, vol. 93, pp. 180–188, May 2015, doi: 10.1016/J.CONBUILDMAT.2015.05.105.

[81] D. K. Rajak, D. D. Pagar, P. L. Menezes, and E. Linul, “Fiber-reinforced polymer composites: Manufacturing, properties, and applications,” *Polymers*, vol. 11, no. 10, 2019, doi: 10.3390/polym11101667.

[82] K. Jayaraman and D. Bhattacharyya, “Mechanical performance of woodfibre-waste plastic composite materials,” *Resources, Conservation and Recycling*, vol. 41, no. 4, pp. 307–319, 2004, doi: 10.1016/j.resconrec.2003.12.001.

[83] R. Badrinath and T. Senthilvelan, “Comparative Investigation on Mechanical Properties of Banana and Sisal Reinforced Polymer based Composites,” *Procedia Materials Science*, vol. 5, pp. 2263–2272, 2014, doi: 10.1016/j.mspro.2014.07.444.

[84] Y. Lei and Q. Wu, “Wood plastic composites based on microfibrillar blends of high density polyethylene/poly(ethylene terephthalate),” *Bioresource Technology*, vol. 101, pp. 3665–3671, 2010, doi: 10.1016/j.biortech.2009.12.069.

[85] A. A. Pérez-Fonseca, J. R. Robledo-Ortíz, F. J. Moscoso-Sánchez, F. J. Fuentes-Talavera, D. Rodrigue, and R. González-Núñez, “Self-hybridization and Coupling Agent Effect on the Properties of Natural Fiber/HDPE Composites,” *Journal of Polymers and the Environment*, vol. 23, no. 1, pp. 126–136, Mar. 2015, doi: 10.1007/s10924-014-0706-3.

[86] A. Shahzad, “Hemp fiber and its composites-a review”, doi: 10.1177/0021998311413623.

[87] S. Musio, J. Müssig, and S. Amaducci, “Optimizing Hemp Fiber Production for High Performance Composite Applications,” *Frontiers in Plant Science*, vol. 9, p. 1702, Nov. 2018, doi: 10.3389/FPLS.2018.01702.

[88] N. Shah, J. Fehrenbach, and C. A. Ulven, “Hybridization of hemp fiber and recycled-carbon fiber in polypropylene composites,” *Sustainability (Switzerland)*, vol. 11, no. 11, 2019, doi: 10.3390/su11113163.

[89] V. Mazzanti, F. Mollica, and N. el Kissi, “Rheological and mechanical characterization of polypropylene-based wood plastic composites,” *Polymer Composites*, vol. 37, no. 12, pp. 3460–3473, Dec. 2016, doi: 10.1002/pc.23546.

[90] B. O. Orji and A. G. McDonald, “Evaluation of the mechanical, thermal and rheological properties of recycled polyolefins rice-hull composites,” *Materials*, vol. 13, no. 3, 2020, doi: 10.3390/ma13030667.

[91] O. O. Adefisan and A. G. McDonald, “Evaluation of the strength, sorption and thermal properties of bamboo plastic composites,” *Maderas: Ciencia y Tecnologia*, vol. 21, no. 1, pp. 3–14, 2019, doi: 10.4067/S0718-221X2019005000101.

[92] Y. Zou, N. Reddy, and Y. Yang, “Using hop bines as reinforcements for lightweight polypropylene composites,” *Journal of Applied Polymer Science*, vol. 116, no. 4, pp. 2366–2373, May 2010, doi: 10.1002/APP.31770.

[93] D. TechConnect World Innovation Conference and Expo 11. 2017 Washington *et al.*, “TechConnect briefs 2017. Vol. 2 Materials for energy, efficiency and sustainability”.

[94] A. O. Ogah, J. N. Afiukwa, and A. A. Nduji, “Characterization and Comparison of Rheological Properties of Agro Fiber Filled High-Density Polyethylene Bio-Composites,” *Open Journal of Polymer Chemistry*, vol. 04, no. 01, pp. 12–19, 2014, doi: 10.4236/ojpchem.2014.41002.

[95] R. Santi, A. Piselli, C. Dastoli, A. Cigada, B. del Curto, and P. Milano, “AN INNOVATIVE THERMOPLASTIC ECO-COMPOSITE MATERIAL RECYCLABLE WITH PAPER AND CARDBOARD National Interuniversity Consortium of Materials Science and Technology (INSTM), Florence , Italy Department of Chemistry , Materials and Chemical Engineering , Polit,” no. March 2020, pp. 235–238, 2018.

[96] N. Graupner *et al.*, “Copy paper as a source of reinforcement for biodegradable composites – Influence of fibre loading, processing method and layer arrangement – An overview,” *Composites Part A: Applied Science and Manufacturing*, vol. 120, pp. 161–171, May 2019, doi: 10.1016/J.COMPOSITESA.2019.02.016.

[97] U. Kunej, M. Mikulič-Petkovšek, S. Radišek, and N. Štajner, “Changes in the phenolic compounds of hop (Humulus lupulus l.) induced by infection with verticillium nonalfalfae, the causal agent of hop verticillium wilt,” *Plants*, vol. 9, no. 7, pp. 1–16, Jul. 2020, doi: 10.3390/plants9070841.

[98] “Hemp | USDA.” https://www.usda.gov/topics/hemp (accessed Nov. 16, 2021).

[99] N. Reddy and Y. Yang, “Properties of natural cellulose fibers from hop stems,” *Carbohydrate Polymers*, vol. 77, no. 4, pp. 898–902, 2009, doi: 10.1016/j.carbpol.2009.03.013.

[100] E. Detmann, M. de Oliveira Franco, D. Í. Gomes, M. M. Barbosa, and S. de Campos Valadares Filho, “Notas Científicas: Protein contamination on klason lignin contents in tropical grasses and legumes,” *Pesquisa Agropecuaria Brasileira*, vol. 49, no. 12, pp. 994–997, 2014, doi: 10.1590/S0100-204X2014001200010.

[101] Kehinde Adedeji Adekola, “Engineering Review Food Extrusion Technology and Its Applications,” *Journal of Food Science and Engineering*, vol. 6, no. 3, Jun. 2016, doi: 10.17265/2159-5828/2016.03.005.

[102] “Handbook of Polypropylene and Polypropylene Composites”, Accessed: Oct. 04, 2021. [Online]. Available: http://bit.ly/1dHAD9Y

[103] P. Nygård, B. S. Tanem, T. Karlsen, P. Brachet, and B. Leinsvang, “Extrusion-based wood fibre–PP composites: Wood powder and pelletized wood fibres – a comparative study,” *Composites Science and Technology*, vol. 15–16, no. 68, pp. 3418–3424, Dec. 2008, doi: 10.1016/J.COMPSCITECH.2008.09.029.

[104] “Handbook of Polyolefins,” *Handbook of Polyolefins*, Jun. 2000, doi: 10.1201/9780203908716/HANDBOOK-POLYOLEFINS-CORNELIA-VASILE.

[105] B. Vergnes, G. della Valle, and L. Delamare, “A global computer software for polymer flows in corotating twin screw extruders,” *Polymer Engineering & Science*, vol. 38, no. 11, pp. 1781–1792, Nov. 1998, doi: 10.1002/PEN.10348.

[106] H. S. Yang, M. P. Wolcott, H. S. Kim, S. Kim, and H. J. Kim, “Properties of lignocellulosic material filled polypropylene bio-composites made with different manufacturing processes,” *Polymer Testing*, vol. 25, no. 5, pp. 668–676, 2006, doi: 10.1016/j.polymertesting.2006.03.013.

[107] S. A. Ashter, “Other Processing Approaches,” *Thermoforming of Single and Multilayer Laminates*, pp. 229–260, Jan. 2014, doi: 10.1016/B978-1-4557-3172-5.00010-4.

[108] J. P. Greene, “Injection Molding,” *Automotive Plastics and Composites*, pp. 241–254, 2021, doi: 10.1016/B978-0-12-818008-2.00019-2.

[109] J. R. Lerma Valero, “Key Parameters for Setting the Injection Molding Process,” *Plastics Injection Molding*, pp. 178–192, 2020, doi: 10.3139/9781569906903.014.

[110] C. Maier and T. Calafut, “14 - Injection molding BT - Polypropylene,” pp. 159–188, 1998, Accessed: Oct. 04, 2021. [Online]. Available: http://www.sciencedirect.com/science/article/pii/B9781884207587500199

[111] M. E. González-López, A. A. Pérez-Fonseca, R. Manríquez-González, M. Arellano, D. Rodrigue, and J. R. Robledo-Ortíz, “Effect of surface treatment on the physical and mechanical properties of injection molded poly(lactic acid)-coir fiber biocomposites,” *Polymer Composites*, vol. 40, no. 6, pp. 2132–2141, Jun. 2019, doi: 10.1002/PC.24997.

[112] V. Subramanian and D. Varade, “Thermoelectric Properties of Biopolymer Composites,” *Biopolymer Composites in Electronics*, pp. 155–183, Jan. 2017, doi: 10.1016/B978-0-12-809261-3.00005-X.

[113] N. M. Stark and D. J. Gardner, “Outdoor durability of wood-polymer composites,” *Wood-Polymer Composites*, pp. 142–165, 2008, doi: 10.1533/9781845694579.142.

[114] E. A. Coleman, “Plastics Additives,” *Applied Plastics Engineering Handbook*, pp. 419–428, 2011, doi: 10.1016/B978-1-4377-3514-7.10023-6.

[115] J. W. Kaczmar, J. Pach, and C. Burgstaller, “The chemically treated hemp fibres to reinforce polymers,” *Polimery/Polymers*, vol. 56, no. 11–12, pp. 817–822, 2011.

[116] T. J. Keener, R. K. Stuart, and T. K. Brown, “Maleated coupling agents for natural fibre composites,” *Composites Part A: Applied Science and Manufacturing*, vol. 35, no. 3, pp. 357–362, 2004, doi: 10.1016/j.compositesa.2003.09.014.

[117] I. Aranberri-Askargorta, T. Lampke, and A. Bismarck, “Wetting behavior of flax fibers as reinforcement for polypropylene,” *Journal of Colloid and Interface Science*, vol. 263, no. 2, pp. 580–589, 2003, doi: 10.1016/S0021-9797(03)00294-7.

[118] W. Wang, H. Chen, and J. Li, “Effects of Maleic Anhydride Grafted Polypropylene on the Physical, Mechanical and Flammability Properties of Wood-flour/Polypropylene/Ammonium Polyphosphate Composites,” *Fibers and Polymers*, vol. 22, no. 4, pp. 1137–1144, 2021, doi: 10.1007/s12221-021-0202-z.

[119] X. Zhou, Y. Yu, Q. Lin, and L. Chen, “Effects of maleic anhydride-grafted polypropylene (MAPP) on the physico-mechanical properties and rheological behavior of bamboo powder-

polypropylene foamed composites," *BioResources*, vol. 8, no. 4, pp. 6263–6279, 2013, doi: 10.15376/biores.8.4.6263-6279.

[120] K. Murayama *et al.*, "The Effects of Different Types of Maleic Anhydride-Modified Polypropylene on the Physical and Mechanical Properties of Polypropylene-based Wood/Plastic Composites," *Journal of Wood Chemistry and Technology*, vol. 38, no. 3, pp. 224–232, 2018, doi: 10.1080/02773813.2018.1432655.

[121] J. K. Sameni, S. H. Ahmad, and S. Zakaria, "Effect of MAPE on the mechanical properties of rubber wood fiber/thermoplastic natural rubber composites," *Advances in Polymer Technology*, vol. 23, no. 1, pp. 18–23, 2004, doi: 10.1002/adv.10070.

[122] S. Kurtz and M. Manley, "Cross-Linked Polyethylene," *Surgical Treatment of Hip Arthritis: Reconstruction, Replacement, and Revision*, no. December, pp. 456–467, 2009, doi: 10.1016/B978-1-4160-5898-4.00061-6.

[123] N. H. Sari, M. R. Sanjay, G. R. Arpitha, C. I. Pruncu, and S. Siengchin, "Synthesis and properties of pandanwangi fiber reinforced polyethylene composites: Evaluation of dicumyl peroxide (DCP) effect," *Composites Communications*, vol. 15, pp. 53–57, Oct. 2019, doi: 10.1016/J.COCO.2019.06.007.

[124] E. G. Rodi, V. Langlois, E. Renard, V. Sansalone, and T. Lemaire, "Biocomposites Based on Poly(3-Hydroxybutyrate-co-3-Hydroxyvalerate) (PHBHV) and Miscanthus giganteus Fibers with Improved Fiber/Matrix Interface," *Polymers*, vol. 10, no. 5, May 2018, doi: 10.3390/POLYM10050509.

[125] J. D. Menczel, L. Judovits, R. B. Prime, H. E. Bair, M. Reading, and S. Swier, "Differential Scanning Calorimetry (DSC)," in *Thermal Analysis of Polymers: Fundamentals and Applications*, 2008, pp. 7–239. doi: 10.1002/9780470423837.ch2.

[126] J. Duncan and D. Price, "Thermomechanical, Dynamic Mechanical and Dielectric Methods," *Principles of Thermal Analysis and Calorimetry*, no. February, pp. 164–213, 2016.

[127] H. Ishida, "Overview and Historical Background of Polybenzoxazine Research," *Handbook of Benzoxazine Resins*, pp. 3–81, Jan. 2011, doi: 10.1016/B978-0-444-53790-4.00046-1.

[128] G. W. (Gottfried W. Ehrenstein, Gabriela. Riedel, and Pia. Trawiel, "Thermal analysis of plastics : theory and practice," p. 368.

[129] D. Nichetti and I. Manas-Zloczower, “Viscosity model for polydisperse polymer melts,” *Journal of Rheology*, vol. 42, no. 4, pp. 951–969, Jul. 1998, doi: 10.1122/1.550908.

[130] L. A. Utracki and M. M. Dumoulin, “Polypropylene alloys and blends with thermoplastics,” *Polypropylene Structure, blends and composites*, pp. 50–94, 1995, doi: 10.1007/978-94-011-0521-7_3.

[131] S. Ikeda and E. A. Foegeding, “Measurement of Gel Rheology: Dynamic Tests,” *Current Protocols in Food Analytical Chemistry*, vol. 7, no. 1, p. H3.2.1-H3.2.9, Feb. 2003, doi: 10.1002/0471142913.FAH0302S07.

[132] R. K. Gupta, “Polymer and Composite Rheology,” *Polymer and Composite Rheology*, Jun. 2000, doi: 10.1201/9781482273700/POLYMER-COMPOSITE-RHEOLOGY-RAKESH-GUPTA.

[133] “Rheology of Thermosets Part 2: Rheometers - Polymer Innovation Blog.” https://polymerinnovationblog.com/rheology-thermosets-part-2-rheometers/ (accessed Oct. 10, 2021).

[134] “WHITEPAPER 2 A Basic Introduction to Rheology Shear Flow”.

[135] “What is Capillary Rheometer - Instron.” https://www.instron.com/en/our-company/library/glossary/c/capillary-rheometer?region=Global%20Site&lang=en (accessed Oct. 10, 2021).

[136] “Polymers and Plastics - Resources for Scientific Molding and Scientific Processing.” https://fimmtech.com/knowledgebase-2/polymers-and-plastics/ (accessed Oct. 10, 2021).

[137] S. Amaducci, J. Müssig, A. Zatta, and G. Venturi, “An Innovative Production System for Hemp Fibre for Textile Destinations : From Laboratory Results to Industrial Validation,” *International Conference on Flax and Other Bast Plants*, no. February, pp. 104–117, 2008.

[138] C. Aurelia, A. Murdiati, . S., and A. Ningrum, “Effect of Sodium Hydroxide and Sodium Hypochlorite on the Physicochemical Characteristics of Jack Bean Skin (Canavalia ensiformis),” *Pakistan Journal of Nutrition*, vol. 18, no. 2, pp. 193–200, Jan. 2019, doi: 10.3923/pjn.2019.193.200.

[139] K. Iiyama and A. F. A. Wallis, “An improved acetyl bromide procedure for determining lignin in woods and wood pulps,” *Wood Science and Technology*, vol. 22, no. 3, pp. 271–280, Sep. 1988, doi: 10.1007/BF00386022.

[140] T. R. Green and R. Popa, “A Simple Assay for Monitoring Cellulose in Paper-Spiked Soil,” *Journal of Polymers and the Environment*, vol. 18, no. 4, pp. 634–637, Dec. 2010, doi: 10.1007/s10924-010-0239-3.

[141] E. G. Rodi, V. Langlois, E. Renard, V. Sansalone, and T. Lemaire, “Biocomposites based on poly(3-hydroxybutyrate-co-3-hydroxyvalerate) (PHBHV) and Miscanthus giganteus fibers with improved fiber/matrix interface,” *Polymers*, vol. 10, no. 5, 2018, doi: 10.3390/polym10050509.

[142] Z. Xu *et al.*, “Bypassing Energy Barriers in Fiber-Polymer Torrefaction,” *Frontiers in Energy Research*, vol. 9, Mar. 2021, doi: 10.3389/fenrg.2021.643371.

[143] R. Chércoles Asensio, M. San Andrés Moya, J. M. de La Roja, and M. Gómez, “Analytical characterization of polymers used in conservation and restoration by ATR-FTIR spectroscopy,” in *Analytical and Bioanalytical Chemistry*, Dec. 2009, vol. 395, no. 7, pp. 2081–2096. doi: 10.1007/s00216-009-3201-2.

[144] M. R. Jung *et al.*, “Validation of ATR FT-IR to identify polymers of plastic marine debris, including those ingested by marine organisms,” 2018, doi: 10.1016/j.marpolbul.2017.12.061.

[145] D. W. Mayo, F. A. Miller, and R. W. Hannah, Eds., *Course Notes on the Interpretation of Infrared and Raman Spectra*. Hoboken, NJ, USA: John Wiley & Sons, Inc., 2004. doi: 10.1002/0471690082.

[146] E. E. M. Ahmad and A. S. Luyt, “Effects of organic peroxide and polymer chain structure on morphology and thermal properties of sisal fibre reinforced polyethylene composites,” *Composites Part A: Applied Science and Manufacturing*, vol. 43, no. 4, pp. 703–710, Apr. 2012, doi: 10.1016/j.compositesa.2011.12.011.

[147] D. Ndiaye and A. Tidjani, “Effects of coupling agents on thermal behavior and mechanical properties of wood flour/polypropylene composites:,” *http://dx.doi.org/10.1177/0021998311435675*, vol. 46, no. 24, pp. 3067–3075, Feb. 2012, doi: 10.1177/0021998311435675.

[148] M. Aljnaid and R. Banat, “Effect of coupling agents on the olive pomace-filled polypropylene composite,” *e-Polymers*, vol. 21, no. 1, pp. 377–390, May 2021, doi: 10.1515/epoly-2021-0038.

[149] X. Wang, Z. Yu, and A. G. McDonald, “Effect of Different Reinforcing Fillers on Properties, Interfacial Compatibility and Weatherability of Wood-plastic Composites,” *Journal of Bionic Engineering*, vol. 16, no. 2, pp. 337–353, 2019, doi: 10.1007/s42235-019-0029-0.

[150] H. M. da Costa, V. D. Ramos, and M. C. G. Rocha, “Rheological properties of polypropylene during multiple extrusion,” *Polymer Testing*, vol. 24, no. 1, pp. 86–93, Feb. 2005, doi: 10.1016/J.POLYMERTESTING.2004.06.006.

[151] R. Ou, Y. Xie, M. P. Wolcott, F. Yuan, and Q. Wang, “Effect of wood cell wall composition on the rheological properties of wood particle/high density polyethylene composites,” *Composites Science and Technology*, vol. 93, pp. 68–75, Mar. 2014, doi: 10.1016/j.compscitech.2014.01.001.

[152] L. Wei, N. M. Stark, and A. G. McDonald, “Interfacial improvements in biocomposites based on poly(3-hydroxybutyrate) and poly(3-hydroxybutyrate-co-3-hydroxyvalerate) bioplastics reinforced and grafted with α-cellulose fibers,” *Green Chemistry*, vol. 17, no. 10, pp. 4800–4814, 2015, doi: 10.1039/c5gc01568e.

[153] J. M. Dealy and K. F. Wissbrun, “Melt Rheology and Its Role in Plastics Processing,” *Melt Rheology and Its Role in Plastics Processing*, 1990, doi: 10.1007/978-94-009-2163-4.

[154] P. Rytlewski, M. Zenkiewicz, and R. Malinowski, “Influence of dicumyl peroxide content on thermal and mechanical properties of polylactide,” *International Polymer Processing*, vol. 26, no. 5, pp. 580–586, 2011, doi: 10.3139/217.2521.

[155] H. Akil and M. H. Zamri, “Performance of natural fiber composites under dynamic loading,” *Natural Fibre Composites: Materials, Processes and Applications*, pp. 323–344, 2013, doi: 10.1533/9780857099228.3.323.

[156] S. Mohanty, S. K. Verma, and S. K. Nayak, “Dynamic mechanical and thermal properties of MAPE treated jute/HDPE composites,” *Composites Science and Technology*, vol. 66, no. 3–4, pp. 538–547, Mar. 2006, doi: 10.1016/j.compscitech.2005.06.014.

[157] H. L. Ornaghi, A. S. Bolner, R. Fiorio, A. J. Zattera, and S. C. Amico, “Mechanical and dynamic mechanical analysis of hybrid composites molded by resin transfer molding,” *Journal of Applied Polymer Science*, vol. 118, no. 2, p. n/a-n/a, Oct. 2010, doi: 10.1002/app.32388.

[158] M. F. M. Alkbir, S. M. Sapuan, A. A. Nuraini, and M. R. Ishak, “Fibre properties and crashworthiness parameters of natural fibre-reinforced composite structure: A literature review,” *Composite Structures*, vol. 148, pp. 59–73, 2016, doi: 10.1016/j.compstruct.2016.01.098.

[159] S. Ochi, “Mechanical properties of kenaf fibers and kenaf/PLA composites,” *Mechanics of Materials*, vol. 40, no. 4–5, pp. 446–452, 2008, doi: 10.1016/j.mechmat.2007.10.006.

[160] J. S. Fabiyi and A. G. McDonald, “Effect of wood species on property and weathering performance of wood plastic composites,” *Composites Part A: Applied Science and Manufacturing*, vol. 41, no. 10, pp. 1434–1440, 2010, doi: 10.1016/j.compositesa.2010.06.004.

[161] E. O. Cisneros-López, M. E. González-López, A. A. Pérez-Fonseca, R. González-Núñez, D. Rodrigue, and J. R. Robledo-Ortíz, “Effect of fiber content and surface treatment on the mechanical properties of natural fiber composites produced by rotomolding,” *Composite Interfaces*, vol. 24, no. 1, pp. 35–53, 2017, doi: 10.1080/09276440.2016.1184556.

[162] H. Azizi and I. Ghasemi, “Reactive extrusion of polypropylene: Production of controlled-rheology polypropylene (CRPP) by peroxide-promoted degradation,” *Polymer Testing*, vol. 23, no. 2, pp. 137–143, 2004, doi: 10.1016/S0142-9418(03)00072-2.

[163] R. Gu and B. v. Kokta, “Mechanical properties of pp composites reinforced with BCTMP aspen fiber,” *Journal of Thermoplastic Composite Materials*, vol. 23, no. 4, pp. 513–542, 2010, doi: 10.1177/0892705709355232.

[164] N. M. Stark and M. J. Berger, “Effect of particle size on properties of wood-flour reinforced polypropylene composites,” *Fourth International Conference on Woodfiber-Plastic Composites*, pp. 134-143\r324, 1997.

[165] Y. H. Liu, J. Q. Xu, and H. J. Ding, “Mechanical behavior of a fiber end in short fiber reinforced composites,” *International Journal of Engineering Science*, vol. 37, no. 6, pp. 753–770, 1999, doi: 10.1016/S0020-7225(98)00096-2.

[166] H. Bouafif, A. Koubaa, P. Perré, and A. Cloutier, “Effects of fiber characteristics on the physical and mechanical properties of wood plastic composites,” *Composites Part A: Applied Science and Manufacturing*, vol. 40, no. 12, pp. 1975–1981, 2009, doi: 10.1016/j.compositesa.2009.06.003.

[167] J. Holbery and D. Houston, “Natural-fiber-reinforced polymer composites in automotive applications,” *Jom*, vol. 58, no. 11, pp. 80–86, 2006, doi: 10.1007/s11837-006-0234-2.

[168] M. Sfiligoj, S. Hribernik, K. Stana, and T. Kree, “Plant Fibres for Textile and Technical Applications,” *Advances in Agrophysical Research*, 2013, doi: 10.5772/52372.

[169] P. v. Joseph, M. S. Rabello, L. H. C. Mattoso, K. Joseph, and S. Thomas, “Environmental effects on the degradation behaviour of sisal fibre reinforced polypropylene composites,” *Composites Science and Technology*, vol. 62, no. 10–11, pp. 1357–1372, Aug. 2002, doi: 10.1016/S0266-3538(02)00080-5.

[170] H. Bouafif, A. Koubaa, P. Perré, A. Cloutier, and B. Riedl, “Wood particle/high-density polyethylene composites: thermal sensitivity and nucleating ability of wood particles,” *Journal of Applied Polymer Science*, vol. 113, no. 1, pp. 593–600, 2009, doi: 10.1002/app.30129.

[171] A. A. Pérez-Fonseca, M. Arellano, D. Rodrigue, R. González-Núñez, and J. R. Robledo-Ortíz, “Effect of coupling agent content and water absorption on the mechanical properties of coir-agave fibers reinforced polyethylene hybrid composites,” *Polymer Composites*, vol. 37, no. 10, pp. 3015–3024, Oct. 2016, doi: 10.1002/PC.23498.

[172] S. Luo, J. Cao, and A. G. McDonald, “Esterification of industrial lignin and its effect on the resulting poly(3-hydroxybutyrate-co-3-hydroxyvalerate) or polypropylene blends,” *Industrial Crops and Products*, vol. 97, pp. 281–291, Mar. 2017, doi: 10.1016/j.indcrop.2016.12.024.

[173] F. Sotoudehnia, B. Orji, E. Mengistie, A. M. Alayat, and A. G. McDonald, “Catalytic Upgrading of Pyrolysis Wax Oil Obtained from Waxed Corrugated Cardboard Using Zeolite Y Catalyst,” *Energy & Fuels*, vol. 35, no. 11, pp. 9450–9461, 2021, doi: 10.1021/acs.energyfuels.1c00767.

[174] F. Sotoudehnia, E. Mengistie, A. Alayat, and A. G. McDonald, “Valorization of waste waxed corrugated cardboard via pyrolysis for recovering wax,” *Environmental Progress and Sustainable Energy*, vol. 40, no. 3, 2021, doi: 10.1002/ep.13566.

[175] A. K. Panda, R. K. Singh, and D. K. Mishra, “Thermolysis of waste plastics to liquid fuel. A suitable method for plastic waste management and manufacture of value added products-A world prospective,” *Renewable and Sustainable Energy Reviews*, vol. 14, no. 1, pp. 233–248, 2010, doi: 10.1016/j.rser.2009.07.005.

[176] U. S. A. Pa, “The 27th International Conference on Solid Waste Technology and Management,” no. June 2014, 2012.

[177] F. Zannikos, S. Kalligeros, G. Anastopoulos, and E. Lois, “Converting Biomass and Waste Plastic to Solid Fuel Briquettes,” *Journal of Renewable Energy*, vol. 2013, pp. 1–9, 2013, doi: 10.1155/2013/360368.

[178] S. H. Jung, M. H. Cho, B. S. Kang, and J. S. Kim, “Pyrolysis of a fraction of waste polypropylene and polyethylene for the recovery of BTX aromatics using a fluidized bed reactor,” *Fuel Processing Technology*, vol. 91, no. 3, pp. 277–284, Mar. 2010, doi: 10.1016/J.FUPROC.2009.10.009.

[179] M. N. Islam, M. N. Islam, M. N. Islam, and M. R. A. Beg, “Fixed Bed Pyrolysis of Waste Plastic for Alternative Fuel Production,” 2004, Accessed: Oct. 29, 2021. [Online]. Available: http://citeseerx.ist.psu.edu/viewdoc/summary?doi=10.1.1.610.1568

[180] C. Zhou, W. Yang, and W. Blasiak, “Characteristics of waste printing paper and cardboard in a reactor pyrolyzed by preheated agents,” *Fuel Processing Technology*, vol. 116, pp. 63–71, 2013, doi: 10.1016/j.fuproc.2013.04.023.

[181] I. Kremer, T. Tomić, Z. Katančić, Z. Hrnjak-Murgić, M. Erceg, and D. R. Schneider, “Catalytic decomposition and kinetic study of mixed plastic waste,” *Clean Technologies and Environmental Policy*, vol. 23, no. 3, pp. 811–827, 2021, doi: 10.1007/s10098-020-01930-y.

[182] A. Aboulkas, K. el harfi, and A. el Bouadili, “Thermal degradation behaviors of polyethylene and polypropylene. Part I: Pyrolysis kinetics and mechanisms,” *Energy Conversion and Management*, vol. 51, no. 7, pp. 1363–1369, 2010, doi: 10.1016/J.ENCONMAN.2009.12.017.

[183] R. K. Singh, B. Ruj, A. K. Sadhukhan, and P. Gupta, “Thermal degradation of waste plastics under non-sweeping atmosphere: Part 1: Effect of temperature, product optimization, and degradation mechanism,” *Journal of Environmental Management*, vol. 239, no. December 2018, pp. 395–406, 2019, doi: 10.1016/j.jenvman.2019.03.067.

[184] R. K. Singh and B. Ruj, “Time and temperature depended fuel gas generation from pyrolysis of real world municipal plastic waste,” *Fuel*, vol. 174, pp. 164–171, 2016, doi: 10.1016/j.fuel.2016.01.049.

[185] J. Chattopadhyay, T. S. Pathak, R. Srivastava, and A. C. Singh, “Catalytic co-pyrolysis of paper biomass and plastic mixtures (HDPE (high density polyethylene), PP (polypropylene) and PET (polyethylene terephthalate)) and product analysis,” *Energy*, vol. 103, pp. 513–521, 2016, doi: 10.1016/j.energy.2016.03.015.

[186] M. Syamsiro *et al.*, “Fuel oil production from municipal plastic wastes in sequential pyrolysis and catalytic reforming reactors,” *Energy Procedia*, vol. 47, no. December, pp. 180–188, 2014, doi: 10.1016/j.egypro.2014.01.212.

[187] B. K. Sharma, B. R. Moser, K. E. Vermillion, K. M. Doll, and N. Rajagopalan, “Production, characterization and fuel properties of alternative diesel fuel from pyrolysis of waste plastic grocery bags,” *Fuel Processing Technology*, vol. 122, no. September 2018, pp. 79–90, 2014, doi: 10.1016/j.fuproc.2014.01.019.

[188] P. T. Williams and E. Slaney, “Analysis of products from the pyrolysis and liquefaction of single plastics and waste plastic mixtures,” *Resources, Conservation and Recycling*, vol. 51, no. 4, pp. 754–769, 2007, doi: 10.1016/j.resconrec.2006.12.002.

[189] R. Miandad, M. A. Barakat, M. Rehan, A. S. Aburiazaiza, I. M. I. Ismail, and A. S. Nizami, “Plastic waste to liquid oil through catalytic pyrolysis using natural and synthetic zeolite catalysts,” *Waste Management*, vol. 69, pp. 66–78, 2017, doi: 10.1016/j.wasman.2017.08.032.

[190] N. S. Akpanudoh, K. Gobin, and G. Manos, “Catalytic degradation of plastic waste to liquid fuel over commercial cracking catalysts: Effect of polymer to catalyst ratio/acidity content,” *Journal of Molecular Catalysis A: Chemical*, vol. 235, no. 1–2, pp. 67–73, Jul. 2005, doi: 10.1016/J.MOLCATA.2005.03.009.

[191] C. Muhammad, J. A. Onwudili, and P. T. Williams, “Thermal degradation of real-world waste plastics and simulated mixed plastics in a two-stage pyrolysis-catalysis reactor for fuel production,” *Energy and Fuels*, vol. 29, no. 4, pp. 2601–2609, 2015, doi: 10.1021/ef502749h.

[192] E. T. Aisien, I. C. Otuya, and F. A. Aisien, “Thermal and catalytic pyrolysis of waste polypropylene plastic using spent FCC catalyst,” *Environmental Technology and Innovation*, vol. 22, p. 101455, 2021, doi: 10.1016/j.eti.2021.101455.

[193] P. T. Williams and E. A. Williams, “Fluidised bed pyrolysis of low density polyethylene to produce petrochemical feedstock,” *Journal of Analytical and Applied Pyrolysis*, vol. 51, no. 1, pp. 107–126, 1999, doi: 10.1016/S0165-2370(99)00011-X.

[194] R. Bagri and P. T. Williams, “Catalytic pyrolysis of polyethylene,” *Journal of Analytical and Applied Pyrolysis*, vol. 63, no. 1, pp. 29–41, 2002, doi: 10.1016/S0165-2370(01)00139-5.

[195] S. Papari, H. Bamdad, and F. Berruti, “Pyrolytic conversion of plastic waste to value-added products and fuels: A review,” *Materials*, vol. 14, no. 10, 2021, doi: 10.3390/ma14102586.

[196] Z. Xu, S. S. Kolapkar, S. Zinchik, E. Bar-Ziv, and A. G. McDonald, “Comprehensive kinetic study of thermal degradation of polyvinylchloride (PVC),” *Polymer Degradation and Stability*, vol. 176, Jun. 2020, doi: 10.1016/J.POLYMDEGRADSTAB.2020.109148.

[197] V. Dhyani and T. Bhaskar, “A comprehensive review on the pyrolysis of lignocellulosic biomass,” *Renewable Energy*, vol. 129, pp. 695–716, Dec. 2018, doi: 10.1016/J.RENENE.2017.04.035.

[198] S. Ito, “Analysis of Aromatic Hydrocarbons in Gasoline and Naphtha with the Agilent 6820 Series Gas Chromatograph and a Single Polar Capillary Column Application,” *Agilent Technologies*, 2003, [Online]. Available: https://www.agilent.com/cs/library/applications/5988-9261EN.pdf

[199] K. H. Lee, “Effects of the types of zeolites on catalytic upgrading of pyrolysis wax oil,” *Journal of Analytical and Applied Pyrolysis*, vol. 94, pp. 209–214, 2012, doi: 10.1016/j.jaap.2011.12.015.

[200] Z. Xu *et al.*, “Properties of Torrefied U.S. Waste Blends,” *Frontiers in Energy Research*, vol. 6, Jul. 2018, doi: 10.3389/FENRG.2018.00065.

[201] W. Chen, M. Chen, and X. Zhou, “Characterization of Biochar Obtained by Co-Pyrolysis of Waste Newspaper with High-Density Polyethylene,” *BioResources*, vol. 10, no. 4, pp. 8253–8267, 2015, doi: 10.15376/biores.10.4.8253-8267.

[202] H. Li and A. G. McDonald, “Fractionation and characterization of industrial lignins,” *Industrial Crops and Products*, vol. 62, pp. 67–76, 2014, doi: 10.1016/J.INDCROP.2014.08.013.